# Transfer of Tracers and Pesticides in lab-scale Wetland Systems

Master Thesis at IHF, Institute of Hydrology Freiburg - Germany
in cooperation with LHyGeS, Laboratory of Hydrology and Geochemistry of Strasbourg, France

**30th November 2011**

**Master of Science in Hydrology**

**Romy Durst**

**Master Thesis supervised by Dr. Gwenael Imfeld (LHyGeS) Strasbourg (FR)**
**and Dr. Jens Lange (IHF) Freiburg im Breisgau (GER)**
**November 2011**

Master Thesis at IHF, Institute of Hydrology Freiburg – Germany
in cooperation with
LHyGeS, Laboratory of Hydrology and Geochemistry
of Strasbourg - France

# Transfer of Tracers and Pesticides in Lab – scale Wetland Systems

**30th November 2011**

**Master of Science in Hydrology**

**Romy Durst**

**Master Thesis supervised by Dr. Gwenael Imfeld (LHyGeS) Strasbourg (FR)**
**and Dr. Jens Lange (IHF) Freiburg im Breisgau (GER)**
**November 201**

Freiburg, November 30, 2011

I, Romy Durst, (Master Student in the Hydrology Master Program of the Institute of Hydrology at the University in Freiburg), hereby declare that I have written the presented study independently, without using any other resource than the ones declared. The work has never been presented in this or similar form to any other examination commission.

# Acknowledgements

First of all, I would like to thank my supervisors, Jens Lange at the Institute of Hydrology in Freiburg and Gwenäel Imfeld at the Institute if Hydrology and Geochemistry of Strasbourg for proposition of this topic and for making this binational collaboration possible.

Sincere tanks goes to Gwenael Imfeld for his constant support and scientific advice, especially in the fields of biogeochemistry and organic contaminants and for helpful reviews on my work. I also acknowledge the expertise of Jens Lange supporting me in the fields of tracer hydrology and experimental design.

Special thanks go to the PhytoRet working groups in Freiburg and Strasbourg, to Robin Steudten for constant exchange of questions and ideas, to Tobias Schütz and Benjamin Gralher for being open to any question at any time and Barbara Herbstritt for her support in hydrochemistry. I want to thank Marie Lefrancq, Elodie Maillard, Omneia Elsayed Azzam, Nicolas Tissot and Pablo Alvarez for supporting me during my experimental work in Strasbourg and for their company and hospitality.

I am also grateful to all technical and laboratory experts involved in field sampling and hydrochemical sample analysis at LHyGeS and IHF.

# I Contents

# II List of Abbreviations

### *Symbols*

| | | |
|---|---|---|
| $A_C$ | Column surface Area | $cm^2$ |
| Ar | Argon | |
| $Br^-$ | Bromide | |
| BTC | Break through curve | |
| C | Concentration | mg/L, µg/L |
| $C_b$ | background concentration | mg/L, µg/L |
| $C_i$ | Measured concentration | mg/L, µg/L |
| $C_P$ | peak concentration | mg/L, µg/L |
| CaO | Calcium oxide | |
| C1, C2, C3, C4 | mesocosm setups recieving CW Alteckendorf influent | |
| CDE | Convection Dispersion Equation | |
| CW | Constructed wetland | |
| CXTFIT | Code for estimating transport parameters (Toride et al. 1999) | |
| D | Hydrodynamic dispersion | $cm^2/h$, $m^2/h$ |
| $D_L$ | Longitudinal hydrodynamic dispersion coefficient | $Cm^2/h$, $m^2/d$ |
| DIC | Dissolved inorganic carbon | mg/L |
| DO | Dissolved oxygen | mg/L |
| DOC | Dissolved organic carbon content | mg/L |
| $DT_{50}$ | Half life time of parent compound | h |
| $DT_{50Soil}$ | Half life time of parent compound in soil | h |
| EC | Electric conductivity | µS/cm |
| EIC | Estimated injection concentration | µg/L |
| E(t) | Hydraulic residence time distribution function | µg/L |
| FT | Fluorescent tracer | |
| h | height | m |
| HDPE | High density Polyethylene | |
| HRT | Hydraulic residence time | h |
| IC | Ion chromatography | |
| ICP | Inductively coupled plasma mass spectrometry | |
| IHF | Institute of Hydrology Freiburg | |
| IPU | Isoproturon | |

| | | |
|---|---|---|
| $K_d$ | Partitioning coefficient liquid- solid phase | $cm^3/g$ |
| $k_f$ | Hydraulic conductivity | m/s |
| $K_{OC}$ | Organic carbon-water partitioning coefficient | ml/g |
| l | length | m |
| $L_{diss}$ | Dissolved load | µg/h |
| $L_P$ | Normalized particle associated load | µg/h |
| $L_S$ | Sediment associated load | µg/g |
| LHyGeS | Laboratory of Hydrology and Geochemistry of Strasbourg | |
| $Log_{Pow}$ | Partitioning coefficient octanol/ water | (-) |
| m | masse | g |
| $m_{Sat}$ | Saturated sediment mass | g |
| $m_{105°C}$ | dried mass (105°C) | g |
| $m_{375°C}$ | dried mass (105°C) | g |
| max | Subscript: maximum | |
| mean | Subscript: mean | |
| min | Subscript: minimum | |
| M | Injection mass | mg, µg |
| MTX | Metalaxyl | |
| n | Statistical number of individuals | |
| nRT | Nominal residence time | hours |
| NV | Non-vegetated mesocosm setup | |
| OC | Organic carbon | |
| P | Total porosity | % volume |
| $P_{eff}$ | Effective porosity | % volume |
| POC | Particulate organic carbon | mg/L |
| PTFE | Polytetrafluorethylen | |
| Q | Discharge | L/h |
| R | Solute recovery | % |
| Rd | Retardation factor | (-) |
| RFI | Relative fluorescence intensity (FIx / FIUR) | (-) |
| RTD | Residence time distribution | h |
| $R^2$ | Coefficient of determination | (-) |
| SRB | Sulphorhodamine B | |
| SFW | Surface flow wetland | |
| SSFW | Sub surface flow wetland | |

| | | |
|---|---|---|
| t | Time | H |
| $t_P$ | Time of peak arrival | h |
| $t_1$ | Time of first target compound detection | h |
| $t_{50}$ | Time of detection of 50 % of compound in effluent | h |
| T | Temperature | °C |
| TIC | Total inorganic carbon | mg/L |
| TOC | Total organic carbon | mg/L |
| TSS | total suspended solids | mg/L |
| PPDB | Pesticide Properties Database Herfordshire | |
| PTFE | Polytetrafluorethylen | |
| UR | Uranine | |
| VEG | Vegetated mesocosm setup | |
| v | Pore water velocity | m/s |
| V | Volume | L, $cm^3$ |
| $V_F$ | filtrate volume | L, $cm^3$ |
| $V_S$ | Sediment volume | L, $cm^3$ |
| $V_T$ | Total sample volume | L, $cm^3$ |
| $V_W$ | Water volume | L, $cm^3$ |
| WS | Wetland sediment | |
| x | Flow length | cm, m |

## *Greek symbols*

| | | |
|---|---|---|
| Δ | Difference operator | (-) |
| β | partitioning variable in non-equilibrium transport | (-) |
| μ | First-order decay coefficient | $h^{-1}$ |
| $\mu_1$ | First-order decay coefficient for equilibrium sites | (-) |
| $\mu_2$ | First-order decay coefficient non-equilibrium sites | (-) |
| ρ | Bulk density(dry) | $g/cm^3$ |
| $\rho_{sat}$ | Saturated bulk density | $g/cm^3$ |
| τ | Mean detention time | h |
| σ | Standard deviation | |
| $\sigma^2$ | Spread of RTD around τ, first moment of E(t) | |
| ω | Mass transfer coefficient | (-) |
| θ | Relative pore water volume | (-) |

# II List of figures in the text

# III List of tables in the text

# IV List of figures in the appendix

# V List of tables in the appendix

# Summary

Wetland systems offer natural pesticide mitigation services that may result in retardation and retention of contaminants. The prediction of pesticide fate in wetlands receiving pesticide contaminated runoff is crucial for the evaluation of contamination risks for connected surface (streams, lakes) and subsurface flow systems (groundwater ground water). The transport behaviour of the fluorescent dye Sulphorhodamine B (SRB) was found to simulate that of the commonly applied herbicide Isoproturon (IPU) in SF constructed wetlands. Yet, the feasibility of SRB as a model for IPU transport in SSF wetland systems is unknown so far. We compared the transport behaviour of two fluorescent dyes, the photo-sensitive, conservative tracer Uranine (UR) and the sorptive tracer SRB as models for pesticide transport and transfer in vegetated (VEG) and non-vegetated (NV) SSF wetland mesocosms to that of the herbicide Isoproturon (IPU) and the fungicide Metalaxyl (MTX). We show that both dyes are affected by irreversible sorption processes in the presence of naturally inoculated wetland sediments and that macrophytes (*P. australis*) significantly affected the transport of SRB by macropore flow along root channels. Plant uptake of the dye tracers was not observed. In the case of SRB, our results highlight the significance of the interaction between tracer and mesocosm matrix in terms of peak attenuation and tracer velocity. Partitioning of SRB between dissolved and particle associated fractions was observed. The $K_{OC}$ for SRB was calculated based on fitting the non-equilibrium CDE. Values were under estimated by the model and went significantly below the ones reported in literature. The presented study underlines the interest of comparative investigations of dye tracer and pesticide tracking and sorption kinetics in wetland systems to draw patterns of feasibility of dey tracers as tools for pesticide fate estmation.

***Keywords:*** *Wetland, mesocosm, transport, subsurface flow, tracers, pesticides, Bromide, Sulphorodamine B, Uranine, Phragmites australis, reference tracer.*

# Zusammenfassung

In Feuchtflächen finden biogeochemische Prozesse statt, die sich mindernd und verzögernd auf Pestizidkontaminationen auswirken können. Die Bewertung des Transportverhaltens von Pestiziden in Feuchtflächen, die landwirtschaftliche Nutzflächen drainieren, ist essentiell für die Beurteilung von Kontaminationsrisiken für angrenzende ober- und unterirdische Fließsysteme (Grundwasser, Fleißgewässer, Stillgewässer). Mit dem Fluoreszenztracer Sulphorhodamin B (SRB) ließ sich der Transport des oft angewendeten Herbizids Isoproturon (IPU) in künstlichen oberirdisch fließenden Feuchtflächen simulieren. Allerdings ist die Anwendbarkeit von SRB als Modell für IPU in unteririsch fließenden Feuchtflächen bisher nicht bekannt. In diesem Zusammenhang wurde die Anwendbarkeit des photo-sensitiven, konservativen Fluoreszenztracers Uranine (UR) und des sorbtions-sensitiven Tracers SRB als Indikatoren für den Transport von Pestiziden in unteririsch fließenden Modellfeuchtflächen auf Laborskale untersucht. Der Transport beider Tracer wurde in natürlichem Feuchtflächensediment von irreversiblen Sorptionsprozessen beeinflusst. Makrophytenvegetation (*P. australis*) hatte großen Einfluss auf den Transport von sorbtivem SRB durch Makroporenfluss entlang von Wurzelkanälen. Die Assimilation der Fluoreszenztracer durch *P. australis* wurde nicht beobachtet. Gegenüber UR wurde SRB um den Retardationsfaktor $R = 1.9$ verzögert. Der durch Anpassung der Durchgänge an die non-equilibrium Konvektions-Dispersions-Gleichung ermittelte $K_{OC}$ Wert für SRB wurde durch das Modell unterschätzt und lag deutlich unterhalb entsprechenden Refernzwerten aus der Literatur. Für SRB konnte die Auftrennung zwischen gelöster und partikulär assoziierter Phase im Mesokosmenabfluss beobachtet werden. Die vorgelegte Arbeit unterstreicht das bereits bestehende Interesse an komparativen Untersuchungen zu Transport und Sorptionskinetik von Fluoreszenztracern und Pestiziden im Hinblick auf eine genauere Beschreibung der Anwendbarkeit von Fluoreszenztracern zur Modellierung des Pestizidtransports in Feuchtflächen.

**Schlüsselworte:** *Feuchtfläche, Mesokosmen, Transport, Matrixfluss, Tracer, Pestizide, Bromid, Sulphorodamine B, Uranine, Phragmites australis, reference tracer.*

# 1. Introduction

***Pesticides Hazardous Potential***. Agricultural cultivation practices have been notably intensified during so-called Green Revolution. A key element of intensively managed monocultures has since then been the application of pesticides (Matson et al., 1997). Intensification of agricultural practices has not yet reached its climax and global pesticides usage is expected to further increase until 2050 (Tilman et al., 2001). However, in many European countries pesticides have already become a source of contamination for both, surface and groundwater systems (Barth et al., 2009; Rodriguez-Cruz et al., 2011). During the last decades, detected pesticide concentrations in ground water often exceeded the threshold value for drinking water defined by the European Commission of Health and Consumer Protection of 0. 1 µg/L for individual pesticide compounds (Larsen & Aamand, 2000, Sorensen et al., 2003, Si et al., 2011). The evidence of such ground water contamination lead to intensified scientific interest supported by the European Union aiming on determination of mobility, turnover and storage of various pollutants including pesticides in soils, sediments, water and biomass, such as Aqua Terra (Barth et al., 2009), the EU integrated LIFE project ArtWet (2006 – 2010) (Gregoire et al., 2008; Lange et al., 2011; Maillard et al., 2011, Stehle et al., 2011) and the follow-up INTERREG IV project PhytoRET (2011 – 2013). Among the pesticides detected in European surface and ground water systems, many compounds were found to be persistent for decades or even centuries (Barth et al., 2009). While some compound groups may persist in the field for days only, other may be highly persistent and mobile (Stehle et al., 2011). A combination of long half-life and high mobility (e.g. less hydrophobic herbicides) may cause long term contamination risks of aquifer waters in those vulnerable areas, where pesticides are not exceeding threshold concentrations by now (Barth et al., 2009; De Wilde et al., 2009; Stehle et al., 2011). The evidence of widespread pesticide contamination of water resources provoked a new scientific interest in wetlands as bioremediation systems and treatment plants for pesticides contaminated agricultural runoff (Imfeld et al., 2009).

***Wetlands for Bioremediation***. As demonstrated by Stehle et al. (2011) the number of scientific publications on pesticide transfer and pesticide fate in wetland systems was constant before the 1990s. 2009, a literature research on Web of Knowledge[SM] on publications dealing with fate and transfer of organic pollutants in wetlands in general was conducted by Imfeld et al. and showed that the big majority of publications on this topic were related to efficiency and performance of *natural* wetland systems (e.g. Gao et al. 1998 a, b; Bouldin et al. 2009; Kidmose et al. 2010), whereas less studies focused on processes taking place in artificial or constructed wetland systems. Even if the construction of wetlands as effective and financially feasible sinks for agriculturally derived contaminants became an interesting approach for environmental engineering, only about 11 % of the work published between 1957 and 2007 was dedicated to performance and processes in *constructed* wetlands (e.g. Rodgers & Dunn, 1992; Haarstat et al. 2003; Schulz et al., 2003; Stearman et al. 2003; Gaultier et al. 2009; Gregoire et al. 2008; Imfeld et al., 2008; Lange et al., 2011; Maillard et al. 2011; Stehle et al., 2011). However, understanding contaminant mitigation in constructed wetland systems is particularly challenging (Imfeld et al., 2009), but necessary for optimizing prospective wetland performance and operations with respect to pesticide mitigation.

***Pesticides Mitigation in Wetlands.*** Volatilization, photochemical oxidation, sedimentation, sorption and biodegradation are the major processes involved in pesticide mitigation in wetland systems (Kadlec et al., 1992). Depending on specific plant metabolism and organic compound chemical characteristics, plant uptake and metabolic transformations of the compounds also may be of importance (Susarla, 2002; Gregoire et al., 2008). Several studies however proved sorption processes to be of crucial importance for the pesticides retention efficiency of wetland systems (Gao et al. 1998 a,b; De Wilde et al., 2009a,b; Si et al., 2010, Rodríguez-Cruz et al., 2011). There is a correlation between the efficiency of sorption as a specific mitigation pathway and the hydrophobicity of a target compound (Stehle et al., 2011). However, sorption processes are not always constant over both spatial and temporal scales and subsequent desorption such as observed for Metalaxyl may occur (Haarstad & Braskerud, 2003). Pesticides sorption behaviour is dependent on 1) physico-chemical properties of the compound itself, such as hydrophobicity (Margoum et al. 2006), as well as 2) on substrate characteristics, such as organic carbon content (Gao et al., 1998 a, b, De Wilde

et al., 2009b; Si et al., 2010) and particle diameter distribution (Gao et al. 1998 a, b, De Sutter et al., 2003). Even if adsorption coefficients ($K_{oc}$, $K_d$) and retention rates of common pesticides have already been assessed in several homogenous media, under lab and *in situ* conditions (Si et al., 2010), these results cannot be directly transferred from one system to the other due to deviations in soil and water physico-chemical properties. There is global recognition that not only OC (organic carbon) content, but also OC quality or electrochemical characteristics have severe effects on pesticides retention potential of a substrate (Zhou et al., 1995; De Wilde et al., 2009 b). Zhou et al. (1995) showed that pesticides $K_{oc}$ (organic carbon adsorption coefficient) are not constant with all types of organic carbon substrates, but depend on type and extend of organic coatings (primarily depending on hydrophobicity). Besides, a positive correlation for substrate calcium oxide (CaO) content and pesticides sorption capacity has been documented by former and recent studies (Zhou et al. 1995; De Wilde et al. 2009 b). This effect was related to formation of CaO complexes with the herbicide Paraquat (Amondham et al., 2006) and for a pesticide mixture containing the herbicide Isoproturon and the fungicide Metalaxyl (De Wilde et al., 2009 b). Considering these multiple effects, it is obvious that detailed characterization of substrates through-flow matrix media and compound physico-chemical properties is needed to characterize the retention potential and transport behavior for distinct target compounds in distinct wetland sediments. Further variables affecting pesticide retention in wetlands are hydrological variables like hydrologic residence time (HRT) (Stearman et al. 2003). As HRT increases, contact between pollutants and reactive compartments (e.g. sorptive particle surface, algal and microbial biofilms, plant roots) is potentially enhanced. Hence, degradation, retardation as well as retention processes are more likely to occur. Generally, best retention efficiencies are obtained under the presence of macrophyte vegetation, subsurface flow conditions (intense contact between liquid and solid phases), with increasing HRT and OC content of the wetland sediment (higher sorption site availability) (Gao et al., 1998 a, b, Stearman et al., 2003; Bouldin et al., 2005, De Wilde et al. 2009b). Depending on physico-chemical properties of the contaminants and site specific biogeochemical conditions, biodegradation of pesticides can vary (Imfeld et al., 2009). For the present study the herbicide Isoproturon and the fungicide Metalaxyl were selected as target compounds. These contaminants are frequently applied and detected in agricultural areas in Europe (Besien et al., 2000; Sorensen et al., 2003;

Alletto et al., 2006; Maillard et al., 2011) and represent members of two different pesticide groups showing notable differences with respect to physico - chemical properties, biodegradability and persistence (Haarstad & Braskerud, 2003; Sorensen et al., 2003; De Wilde et al. 2009 a,b;).

***Target Pesticide Compounds – Isproturon (IPU) and Metalxyl (MTX).*** Two commonly used pesticides of differing biodegradability, photo-sensivity and sorption tendencies were chosen as model organic contaminants. The herbicide Isoproturon ([N-(4-isopropylphenyl)-N´,N´-dimethylurea]) is part of the phenylurea pesticide group and one of the most frequently detected organic contaminants in the EU (Sorensen et al., 2003, Alletto et al. 2006). This pesticide group is characterized by an aromatic ring structure (***Figure 4A***) that impedes mineralization and makes the compound resistant against chemical degradation under moderate pH and temperature conditions (Sorensen et al. 2003). While biodegradation of IPU in aerobic top soils and unsaturated chalk cores has been observed (Besien et al., 2000; Larsen & Aamand, 2001; Bending et al., 2003; Alletto et al. 2006), there is no evidence of biological degradation of the herbicide under anoxic conditions so far (Larsen & Aamand, 2001; Alletto et al., 2006; Sorensen et al. 2003). This may indicate that IPU removal is mainly based on chemical degradation processes in anaerobic enrironments. When the compound reaches ground water its degradation is strongly slowed down and half live can reach values exceeding one year (Sorensen & Aamand, 2003). A recent study suggested that enhanced aerobic biodegradation of IPU may occur in agricultural soils due to successive IPU treatment (Sorensen & Aamand, 2003). These results may indicate that successive treatment forces microbial adaptation and/or selection processes under aerobic conditions favouring species and strains capable of IPU utilisation as a carbon source in energy metabolism. In contrast, anoxic microbial degradation of the second target compound, the fungicide Metalaxyl (Methyl N-(2,6-dimethylpehnyl)-N-(methoxyacethyl)DL-alaninate) (***Figure 4B***) was observed under field conditions in a small CW (Haarstad & Braskerud, 2003). The observed biodegradation process was recently characterized under lab conditions and in the presence of *Pseudomonas ssp.* by Massoud et al. (2008). De Wilde et al. (2009a) observed Metalaxyl BTC in column displacement experiments on naturally inoculated matrix media, which also gave evidence of anoxic microbial degradation to be the major mitigation pathway involved. Depending on the OC content

of soil matrix material, sorptive retention may play a role on MTX fate in subsurface flow systems (Rodríguez-Cruz et al. 2011). Both pesticides used in the presented study belong to the so-called non-persistent immobile pesticide category defined by De Wilde et al. (2007; De Wilde et al, 2009a,b). This definition briefly describes contaminant transport characteristics and environmental threat caused by the substances based on persistence ($DT50_{soil}$) and mobility ($K_{OC}$) (De Wilde et al., 2009b). Even belonging to this rather mobile pesticide category, both compounds show a tendency to sorption due to positive $LogP_{OW}$ values, which is stronger for IPU ($LogP_{OW}$ IPU: 2.50, $LogP_{OW}$ MTX: 1.65). The contaminants are not volatile and may therefore be used in lab experiments without causing threats to human health by air contamination (vapour pressure IPU: 2.8 – 8.1 x $10^{-6}$ Pa; MTX: 7.5 x $10^{-4}$ Pa). While liquid/solid partitioning is not affected by individual or mixture pesticide application of IPU, MTX sorption may decrease when applied as part of a pesticide mixture, especially in combination with IPU (De Wilde et al., 2009b). Even if MTX is more likely to undergo chemical degradation processes such as photolysis and hydrolysis (hydrolytic stability $DT_{50}$ IPU: 1210 days; MTX: > 200 days; photostability in water $DT_{50}$ IPU: 48 – 88 days; MTX: 156 hours), a "sorptive competition" situation such as observed by De Wilde et al. (2009b) may increase compound mobility resulting in shorter residence times and lowered chemical and biological degradation efficiency. Regarding the complexity of possible contaminant interactions in SSF wetland systems, there is a notable gap of knowledge concerning compound specific transport and transfer. In order to characterize reactive solutes transport however, the tracking of a non-reactive compound, a so-called conservative tracer is needed to assess general system hydraulics and flux pathways as a system benchmark (Rodríguez-Cruz et al., 2011).

***Tracer Hydrology.*** An ideal conservative tracer is defined by transport behaviour in water and soils that is similar to that of the water molecule (Käss, 2004). Such substance is characterized by non-reactive behaviour in terms of sorption to soil matrix, organic matter and plant uptake. Furthermore, photolytic, biological and hydrolytic degradation losses should be negligible and the applied substance is not meant to cause toxicological threats to the environment (Leibundgut et al. 2009). Frequently used tracers in hydrology are salts and organic fluorescent dyes (FT) (Sabatini, 2000; Käss, 2004; Leibundgut et al., 2009). The anion bromide and the fluorescent dye Uranine were

successfully employed as conservative tracers in studies on SF wetland hydraulics and contaminant retention (Passeport et al., 2010, Lange et al. 2011). Bromide is a favourable salt tracer due to low background concentrations. Chloride – bromide ratios in ground waters were found to be 300:1 up to 877:1 (Davis et al., 1980; Schöller, 1983 in Kass, 2004). While detection limits for salts are located in mg/L dimensions, FT concentrations are detected in µg/L (Leibundgut et al. 2009). Even tracers assumed to be conservative may show reactive behaviour under certain conditions. High contents of clay and organic matter may lead to sorption effects of Bromide for example (Leibundgut et al., 2009). Bromide recovery losses were reported by Xu et al. (2004) in the presence of wetland macrophytes (*Thypha latifolia* and *Phragmites australis*) under low $Cl^-/Br^-$ ratios. Furthermore, bromide may be retarded compared to the more ideal non-reactive tracer Tritium by retardation factors up to $Rd = 2.15$, when injected into SSF systems (Seaman et al., 1996; Seaman et al., 2007). Sorption to matrix material may be enhanced by the presence of divalid kations like $Mg^{2+}$, but also by potassium and iron oxide (Seaman et al., 1995; 1996). The FT Uranine is known to be resistant to sorption under alkaline ($> 7$) pH conditions (Sabatini, 2000), but is rapidly degraded by photolysis ($DT_{50} = 11$ h, Leibundgut et al., 2009). Therefore it can only serve as a conservative tracer in the absence of daylight. Besides these so called conservative tracer substances, there are also non-conservative hydrological tracers like the FT Sulphorhdamine B (SRB) being applied. SRB, like other Rhodamine dyes, is known to show sorption losses during transport on hydrological pathways (Smart & Laidlaw, 1977; Kasnavia et al., 1999; Sabatini, 2000). While other Rhodamine dyes show a positive correlation between sorption and sediment OC fraction, SRB sorption is known to be much more dependent on the mineral composition and overall charge of soil and sediment matrices (Smart & Laidlaw, 1977; Kasnavia et al., 1999). This behaviour is due to the presence of two highly electronegatively charged sulphonic acid groups versus carboxylic groups (Kasnavia et al. 1999). The highly anionic sulfonic groups of SRB were found interact intensely with positively charged surfaces, while the permanently kationic charge makes it sorb to a lesser extend to negatively charged surfaces (Kasnavia et al., 1999; Sabatini et al., 2000). Sorption of SRB was proven to increase with decreasing soil or sediment particle diameters (Ø range: pulverized – 6 mm) (Sabatini, 2000). Sophisticated knowledge about tracer specific interactions with sediments, plants and biofilms is crucial, since such interactions may complicate and challenge

quantitative interpretation of dye tracer studies (Sabatini, 2000). Though the biodegradability of fluorescent dyes has not been explicitly studied so far, it may occur. Both, UR and SRB molecular structures show linear singular C-C bonding, which may be easily cleaved by microorganisms. There is only one report of UR losses related to biodegradation in literature so far (Haider, 1991). To close this scientific gap, specific biodegradation assays are just being conducted at the University of Lüneburg (GER) in the framework of the INTERREG Project PhytoRet. Regarding its tendency to sorption losses and low ecotoxicological threat, SRB was suggested to be used as a proxy in pesticides fate investigations in surface-flow (SF) constructed wetlands by Lange et al. (2011). UR was suggested as a model for photo sensitive pesticides (Lange et al., 2011). To establish dye tracer studies as commonly used cost-effective and environmentally harmless proxies in pesticide fate studies in constructed wetlands, there is a need for further investigations on this approach including subsurface-flow (SSF) systems as well.

# 2. Study Objectives

The overall objective of the presented study is to evaluate and compare the transport of the dye tracers UR and SRB and two selected pesticides, IPU and MTX in lab-scale SSF wetland mesocosms. Investigations focused on:

***1) Transport parameters and sorption tendencies***
***2) Phase partitioning***
***3) Plant effects***
***4) Evaluation of dyes for pesticide fate prediction in SSF systems***

Naturally inoculated wetland sediments and on site water from a constructed stormwater wetland in Eichstetten, Kaiserstuhl region (Southwestern Germany) were used to simulate site specific biogeochemical and hydrochemical experimental conditions. We assume that site specific biology may be adapted to tracer and pesticide input and that enhanced biodegradation of tracers and pesticides may occur. Macrophyte effect on the performance of tracers and pesticides was assessed by comparative observations on a vegetated setup containing *Phragmites australis* (VEG) and a non-vegetated control (NV). Plant dependent impacts on system hydrology and plant uptake of tracers and pesticides are expected. SRB, IPU and MTX are assumed to show partitioning between dissolved and particle associated fractions in mesocosm outlet. To improve process driven understanding on leaching pathways of tracers and pesticides, mesocosm outlet was analyzed on such partitioning. Hydraulic parameters of two different types of wetland mesocosm setups (similar dimensions, differing matrix media) were assessed and compared by BTC tracking of the anion salt tracer bromide. Depending on mesocosm design, different hydrological system parameters were expected. Based on these observations, the feasibility of the fluorescent dyes UR and SRB for pesticide transport estimations in SSF wetlands was evaluated.

# 3. Materials and Methods

## 3.1. Study site and Field Sampling

***Study Site.*** The investigated constructed wetland is located within the Löchernbach catchment, at the eastern edge of the Kaiserstuhl region, South Western Germany (Lange et al., 2011). The surface catchment area is 1.61 $km^2$, subsurface catchment amounts 1.79 $km^2$, respectively (Gassmann, 2007). The artificial SF wetland was initially built in 2006. A 65 $m^2$ of the former detention pond surface area was converted to a new wetland prototype for mitigation of agricultural nonpoint source contamination in the context of the European Life Project ArtWet (Artwet Technical Guide, 2010). The wetland was extended in 2010 to a length of 10 m and a maximum width of 8 m, containing a water volume of 95.5 $m^3$ in 2010 (Lange et al., 2011)., The Löchernbach shows large variability in discharge, ranging from 3 L/s under mean flow to 1500 L/s under flood conditions (ArtWet Technical Guide 2010). Regional rainfall is 778 mm/y (ArtWet Technical Guide 2010). The catchment is characterized by intense agricultural land use, mainly composed of viniculture (61.2 %) besides others (18.5 %). Forests cover 3.5 % of the catchment area (Gassmann, 2007) (***Figure 3.1***).


**Figure 3.1:** Land use in the Löchernbach catchment; dark red: vineyards, light green: grassland, darkgreen: forest, yellow: cereals, brown: root crops, violet: vegetables, orange: fruit trees; source: Hachmann, 2008.

Catchment geology is dominated by Loess formations (80 % silt, 10 % sand and clay) and alluvial sediments (Gassmann, 2007). The system biology (indigenous microorganisms, algae and macrophytes) has been successively in contact with salt and fluorescent tracers and pesticides since 2007 until today. During sediment sampling in June 2011 the wetland was densely covered by the macrophytes *Thypha latifolia* and *Phragmites australis* (***Figure 3.2***). Some individuals of *Juncus effusus* were present and where *T. latifolia* was missing an herbaceous Brassicacea had established in groups. *P. australis* (common reed) is part of the Poaceae (grass) family. It is fast growing and rhizomatous and does not have any special demands for substrate fractionation (USDA, 2011). *P. australis* is perennial and shows high tolerance against pH fluctuations, salinity and anaerobic conditions (USDA, 2011).


**Figure 3.2:** Artificial stormwater wetland in Eichstetten, Kaiserstuhl region, South Western Germany; pictures were taken in March 2011 (A) and in June 2011, when sampling was done and a dense vegetation cover had emerged (B); dotted black arrow = Löchernbach, yellow arrows = wetland flow path.

***Field sampling.*** The sampling of wetland sediment was performed on June 16, 2011. For sampling two metal stove pipes (15 cm in diameter, same as the mesocosm diameter) were used. The sediment was sampled along the whole sediment horizon depth to ensure the presence of all reactive compartments of the *in situ* sediment in the samples. Due to very soft sediment material the pipes could be pushed down manually until the base mineral soil layer was reached. With a wooden plank and a hammer made of duroplastic, the pipes were plunged into the mineral soil to seal the sediment cores on the bottom. The filled pipes were exhumed laterally using a spade and could be extracted by hand afterwards. The sediments were kept saturated during transportation by maintaining a supernatant in the pipes to avoid changes in the oxidation stage of the material. One day after sampling, wetland sediments were transferred into the lab-scale mesocosms and connected to water flux.

Integrative samples along the wetland sediment horizon were taken to assess crucial initial sediment characteristics and tracer and target pesticide contents. Samples were stored in 100 ml HDPE bottles on - 20 °C until analysis. Mesocosm influent water was collected three times (June 16 and 22, July 18, 2011) from the wetland by an electrical pump and stored in 30 L plastic canisters. The wetland was not disturbed during collection to avoid any physico-chemical alterations by re-suspension of settled sediments. Pysico-chemical parameters were measured *in situ* by means of a portable multi probe (WTW Multi 350i SET MPP-25). At each sampling day, water samples (1L HDPE bottles) were taken to assess hydrochemical parameters (ionic composition, dissolved nutrients, total major and trace metals, organic carbon species, TSS and POC, initial tracer and target pesticide concentrations). Water samples were stored at 4 °C during transport and at -20 °C until analysis. Water samples were stored on 4 °C during transport and on -20 °C until analysis.

# 3.2. Lab scale wetlands

## *3.2.1. Mesocosm Characteristics and Operation*

***Mesocosm characteristics.*** Mesocosm studies have been successfully applied in order to assess contaminant fate and retention processes occurring in surface and subsurface flow wetland systems, such as transport and fate of nutrients, pesticides, metals from mine drainage and other anthropogenic contamination (Wintroph et al., 2002; Bouldin et al., 2005; Prochaska & Zouboulis, 2006; Prochaska et al., 2007; Zou et al., 2011). Depending on their purpose, wetland mesocosms may be planted or non-vegetated, flow direction may be bottom to top or vertically downwards or horizontal. Mesocosm dimensions in the cited studies range between 40 L and 2500 L volume, set up either as vertical flow columns or horizontal flow canisters. In the presented study, model wetland reservoirs consisted of Borosilicate glass columns.

**Table 3.1:** main characteristics of wetland mesocosms.

| ***Wetlands characteristics*** | |
|---|---|
| *Setups* | 1 planted<br>1 non-vegetated |
| *Dimensions* | height: 0.65 m<br>diameter: 0.15 m<br>sediment volume: 8.940 L |
| *Pore volume* | 4.316 L (48 %) |
| *Surface area* | 0.177 $m^2$ |
| *Flow direction* | Bottom to top |
| *Flow velocity* | 0.33 ml/min |
| *nRT* | 218 h |
| *Filling material* | Sand Ø:<br>400 – 630 µm<br>Gravel Ø:<br>1000 – 2000 µm<br>Wetland Sediment:<br>80 % silt<br>10 % clay<br>10 % sand |

Mesocosm dimensions were 15 cm in diameter and 65 cm total height (***Table 3.1***). These were filled by a sequence of 1) a 5 cm layer of gravel (Ø 1 – 2 mm) on the columns bottom, 2) a 27.5 cm layer of medium sand (Ø 400 – 630 µm), 3) a 8 cm layer of natural wetland sediments from CW Eichstetten (10 % sand, 80 % silt, 10 % clay; Lange et al., 2011) and 4) a 10 cm top layer of medium sand (Ø 400 – 630 µm) to avoid sediment losses by flushing and to reduce turbidity of mesocosm effluent water (***Figure 3.2***). Sand and gravel were from Fontainebleau, France. In order to compare plant effects on solute transport and transfer a vegetated setup (VEG) as well a non-vegetated control (NV)

were set up. Mesocosms were equipped with optical dissolved oxygen measurement sensor spots, which were read by a fibre optic oxygen transmitter (Fibox 3, PreSens®) (***Figures 3.3 and 3.4 left***). Sensors were mounted along the column length according to layering (2.5 [gravel], 20, 36.5 [sand], 39, 42 [silt] and 48 cm [sand] height) ***(Figure 3.3).*** The flow direction was set from bottom to top to avoid air enclosures and to guarantee homogeneous tracer and pesticide dispersion. Water flow rates were controlled by a high precision multi channel pump (ISMATEC® IPC model ISM936D), which was calibrated weekly.

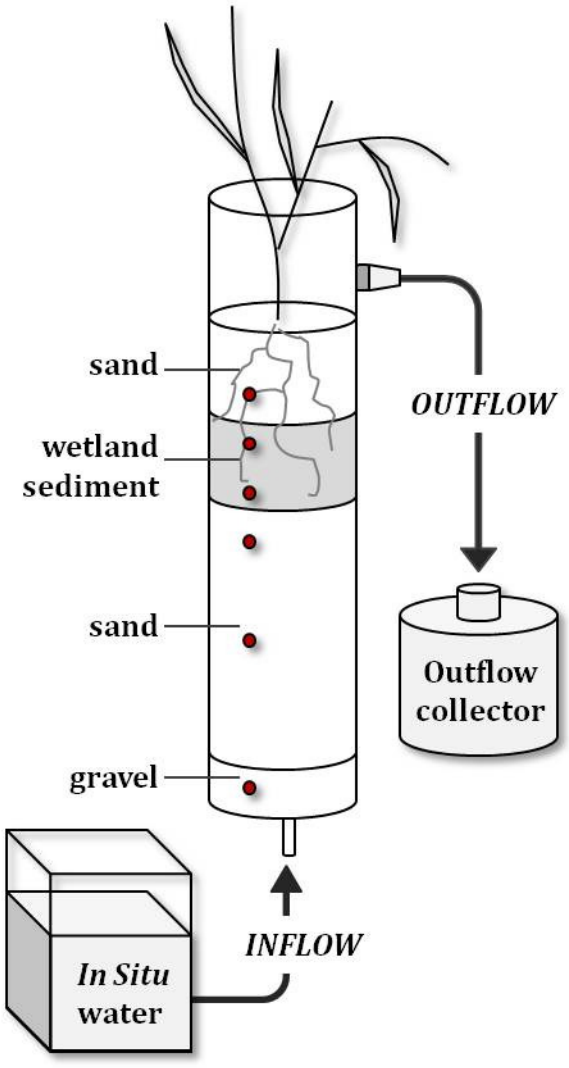


**Figure 3.3:** Planted mesocosm setup with heterogeneous layering; spots represent dissolved oxygen sensors.

Flow rate was adjusted to 0.33 ml/min. Effluent water accumulated in the column supernatant before reaching the height of the outflow port (55 cm). The port was connected to a collecting recipient (brown glass, 3L volume) via a tube (***Figure 3.3***). All tubing material used in this study was Rotilabo® - Viton® tubes. These tubes are highly resistant against ozone, weather, mineral oils and benzene and do not chemically interact with the applied contaminants. The columns were set up below a Phillipps® greenpower LED lamp (model Liagro) to control macrophyte growth and to regulate physicological plant patterns. Artificial radiation period was set to 8 hour/day. Lab air temperature was kept constant on 20 °C ± 0.5 °C by an air-conditioning system. In order to avoid photolytic degradation of the FT Uranine and pesticides, to avoid the appearance of algae and to prevent the UV sensitive *in situ* oxygen sensor spots from deterioration, the columns were covered by aluminium rescue sheets.

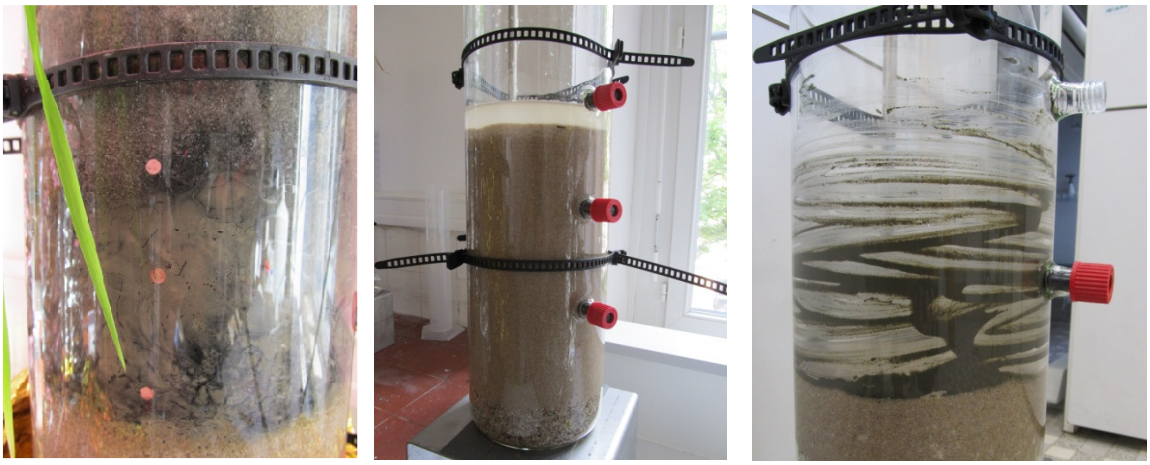

**Figure 3.4:** Dissolved oxygen measurement sensor spots (left); application of slurry packing technique on medium sand (400 – 630 µm) (middle); coating of mesocosm walls with wetland sediments (right).

***Mesocosm packing.*** When packing soil columns or lysimeters the formation of preferential flow paths needs to be avoided (Lewis & Sjöstrom, 2010). Preferential flow in soil lysimeters and columns frequently results from side-wall or so called boundary effects along walls (Sentenac et al., 2001). To avoid these flow alterations, the slurry packing technique described in Lewis & Sjöstrom (2010) was applied. Mesocosms were filled with water. Subsequently, dry gravel and sand were slowly poured into the water column and settled as thin layers (***Figure 3.4 middle***). During sedimentation the settling layer was gently stirred to avoid air bubbles. Before transfer of wetland sediments into mesocosms, the mesocosm walls were coated by saturated wetland silt to further reduce side-wall effects (Sentenac et al., 2001) (***Figure 3.4 right***). Wetland sediment cores were dropped into the mesocosms thereafter. By the dropping, cores broke and natural sediment structure was disturbed. However, the wetland sediments were homogenized using a spatula. One core was vegetated with an individual of *Phragmites australis* (***Figure 3.2***), the other one served as unplanted control setup.

***Mesocosms designed for microbial degradation studies.*** Besides investigations on the above delineated systems, hydrological functioning of four further mesocosm setups was assessed during the conducted study. Global mesocosm setup and operation corresponded to the explanations above. For mesocosm dimension, flow direction and flow rate see ***Table 3.2***. For microbial studies however, mesocosm filling was composed of a 5 cm bottom gravel layer (Ø 1000 – 2000 µm) followed by a homogeneous 52 cm medium sand horizon (Ø 400 – 630 µm). Sediment height was 57 cm in total. Total

sediment volume accounted for 10.070 L, 4.405 L representing system pore volume. Mesocosms were initially planted with *P. australis* extracted from a CW in Alteckendorf, Alsace Region, Eastern France. Influent water was extracted from CW Alteckendorf as well, resembling *in situ* physico-chemical conditions. With regard to pore volume and flow rate, nominal residence time (nRT) was calculated to be 222.5 h, slightly more than the one calculated for the Eichstetten mesocosms (218 h).

### *3.2.3. Mesocosm filling layer parameters*

To characterize the observed mesocosm wetland systems, various characteristic soil parameters were analyzed for mesocosm filling materials. Porosity, $k_f$, bulk density and particle size distribution were assessed by the School and Laboratory of Earth Sciences of Strasbourg. Porosity and $k_f$ measurements were done using dried volumetric steel cylinder samples of 250 $cm^3$. Cylinders were saturated from bottom to top under constant hydraulic head conditions. When water flow through sample cylinders had reached steady state conditions, $k_f$ was calculated according to Darcy´s Law describing saturated water percolation during a certain time period and under constant head conditions (***Eq-1***).

$$k_f = \frac{(V * l)}{(A_C * \Delta t * \Delta h)} \qquad \textbf{Eq-1}$$

with $k_f$ as the hydraulic conductivity (cm/s), $V$ as water volume ($cm^3$), $l$ as length of flow path through the cylinder (cm), $A_C$ as cylinder area ($cm^2$), $\Delta t$ as time step (s) and $\Delta h$ as difference in backwater head (cm). Subsequently, sample volumetric water content, which corresponds to the total porosity of the samples, was assessed by drying (105 °C) (***Eq-2***).

$$P = \frac{m_S - m_{105°C}}{\mathrm{V}} * 100 \qquad \textbf{Eq-2}$$

where $P$ is the total porosity (volumetric %), $m_S$ is the saturated sample weight (g), $m_{105°C}$ is the dried sample weight (g) and $V$ is the cylinder volume ($cm^3$). Particle size distribution of gravel, sand and wetland sediments was assessed by a granulometric laser technique (range 0.040 µm – 2000 µm). Dried samples (105°C) were grinded and organic matter was destroied by oxygen hydroxide ($H_2O_2$) addition before analysis. Organic carbon (OC) content was assessed by calcination of dried samples (105 °C) on 375 °C for 16 hours, minimizing losses of structural water and carbon from calcium carbonates. Weight losses after calcination were referred to as losses of organic carbon according to ***Eq-3***.

$$OC = \frac{(m_{105°C} - m_{375°C})}{m_{105°C}} * 100 \qquad \textbf{Eq-3}$$

Where OC is organic carbon fraction (mass %), $m_{105°C}$ is the mass of the dry sample (g) and $m_{375°C}$ is the mass of samples after calcination (g).

The elementary composition of filling materials was assessed by an alkaline fusion method. Dried samples (70 °C) were grinded and passed through a 100 µm mesh width sieve. After the calculation of sample water loss (105 °C), sample weight loss on 1000 °C was assessed. 100 mg of calcinated sample was homogenized with 750 mg of a fluxing agent (Lithium Tetraborate - $Li_2B_4O_7$ , Spectromelt 100A from Merck) to be fused. The alkaline fusion was conducted under neutral atmospheric conditions (Ar circulation) on 1000 °C in a muffle furnace. After dissolution in a solvent mixture (nitric acid, $HNO_3$, Merk Ultra Pure; glycerol, Merck Ultra Pure and distilled water), fusion products were analyzed for elemental fractions by means of inductively coupled plasma mass spectrometry (ICP-MS).

### *3.2.3. Hydrochemical Parameters*

Physico-chemical parameters (pH, Temperature (T), Electric Conductivity (EC) and dissolved Oxygen concentration (DO) of mesocosm effluent water were measured *in situ* by using a multi probe (WTW Multi 350i SET MPP-25). Total suspended solids (TSS), Particulate organic carbon (POC), ionic concentrations and nutrient concentrations

were analyzed at the Laboratories of ENGEES Strasbourg (National School of Water and Environmental Engineering of Strasbourg) and the LHyGeS (Laboratory of Hydrology and Geochemistry of Strasbourg) following methods described in Maillard et al. (2011) according to French laboratory standards (NF–EN–ISO). Assessed parameters and applied methods are listed in ***Table 3.2***. Column outflow water was analyzed weekly on pH, EC, Oxygen concentration, TSS and POC ionic composition and total metals.

**Table 3.1:** Hydrochemical parameters; TSS: total suspended solids; POC: particulate organic carbon; DOC: dissolved organic carbon; DIC: dissolved inorganic carbon; TOC: total organic carbon, TIC: total inorganic carbon; $NO_3^-$: nitrate; $NO_2^-$: nitrite; $NH_4^+$: ammonium; $P^-$: total phosphorpus; [1] Maillard et al. (2011).

| ***Parameters*** | ***Units*** | ***Analytical methods*** | ***Standards/Norms*** |
|---|---|---|---|
| **pH** | (-) | | |
| **EC** | µS/cm | WTW Multi 350i SET MPP-25 | |
| **T** | (°C) | | |
| **$O_2$** | (mg/L) | WTW Multi 350i SET MPP-25<br>Optical DO sensor spots | |
| **TSS/POC [1]** | mg/L | Filtration on 0.7 µm filters, drying at 105°C (SM) and calcinations at 550 °C in an oven (POC) | According to NF EN 872 (NFT 90-105 2005, June) |
| **DOC [1]** | mg/L | Organic carbon oxidation into carbon dioxide after adding of oxidising reagent. $CO_2$ is purged and detected be infrared spectrometrie (TCO analyser, 1030W – Ol Abalytical) | According to NF EN 1484 (1997, July) |
| **DIC [1]** | mg/L | | |
| **TOC [1]** | mg/L | | |
| **TIC [1]** | mg/L | | |
| **major kations/ anions** | mg/L | Ion chromatography | Internal standards |

**Table 3.2ff**

| *Parameters* | *Units* | *Analytical methods* | *Standards/Norms* |
|---|---|---|---|
| **$NO_3^-$ [1]** | mg/L | Spectophotometric analysis on continuous flux (Alliance instruments, Proxima) | NF EN ISO 13395 (1996) |
| **$NO_2^-$ [1]** | mg/L | | |
| **$NH_4^+$ [1]** | mg/L | | NF EN ISO 11732 (1997) |
| **P[1]** | mg/L | | According to T90-023 (1982, September) |
| **major/ trace metals** | mg/L<br>µg/L | ICP Spectrometry | internal laboratory standards |

# 3.3. Experimental Design

## *3.3.1. Selected Tracers and Pesticides*

The behaviour and transport of selected tracer compounds (Bromide, UR and SRB) and that of the selected pesticides Isoproturon and Metalaxyl were evaluated. General information on physico-chemical properties of the injected substances, applied tracers and pesticides, are given in ***Table 3.3***. Bromide was injected as sodium bromide (NaBr). UR served as conservative and SRB as non conservative fluorescent dyes and were treated as potential pesticide proxies in the presented study. An overview on general characteristics of the two fluorescent tracers is given in ***Table 3.4,*** molecular structures are shown in ***Figure 3.5 A and B.*** IPU and MTX (SIGMA-ALDRICH, Darmstadt, Germany) were supplied as Isoproturon PESTANAL® and Metalaxyl PESTANAL® analytical standard formulations with 99.9 % purity (water content $< 0.1$ %) and 99.6 % purity (0.4 % water content) respectively. An overview on compound characteristics of the two studied pesticides is given in ***Table 3.5*** molecular structures are shown in ***Figure 3.5 C and D***.

**Table 2.3:** Physico-chemical characteristics of investigated tracers and pesticides; Photostability is correlated with natural solar radiation; information taken from Leibundgut et al. (2009) (a), European Commission (2002, 2010) (b), http://sitem.herts.ac.uk (c), Gaspar (1987) (d).

| | ***solubility $H_2O$ (g/L) 20°C*** | ***Molar mass (g/mol)*** | ***Structural formula*** | ***Photo-stability water ($DT_{50}$)*** | ***Hydrolytic stability ($DT_{50}$)*** |
|---|---|---|---|---|---|
| **Br (NaBr)[a]** | 850 | 102.89 | NaBr | stable | stable |
| **UR** | 25[d] | 332.31[a] | $C_{20}H_{10}O_5Na_2$[a] | 11 h[a] | stable[a] |
| **SRB** | 70[d] | 580.65[a] | $C_{27}H_{29}N_2NaO_7S_2$[a] | 820 h[a] | stable[a] |
| **IPU[b/c]** | 0.072 | 206.28 | $C_{12}H_{18}N_2O$ | 48 – 88 d | 1560 d |
| **MTX[b/c]** | 8.4 | 279.33 | $C_{15}H_{21}NO_4$ | 6.5 d | 106 d |

To compare tracer and pesticide sorption parameters, the $K_{OC}$ for UR and SRB was calculated based on $K_d$ values according to Sabatini (2000) (see Table 3.3) and the mean mesocosm OC fraction of 0.00642 ($f_{OC}$, see 4.2.2) as follows (***Eq-4***):

$$K_{OC} = \frac{K_d}{f_{OC}} \qquad \textit{Eq-4}$$

**Table 3.3:** Properties of SRB and U; $K_d$ = Distribution coefficient liquid/ solid phase at equilibrium [(µg/g)/(µg/ml)]; *FI stability*: pH range of 100 % fluorescence yield; *RFI:* relative fluorescence intensity compared to UR; *Rd* = retardation coefficient; taken from Leibundgut et al. (2009).

| | ***$K_d$ (ml/g)*** | ***$K_{OC}$ (ml/g)*** | ***FI Stability (pH)*** | ***RFI (UR)*** | ***Rd*** | ***Photolytic stability ($DT_{50}$)*** |
|---|---|---|---|---|---|---|
| **UR** | 0 – 0.4 | 187 - 498 | > 9 | 100 | 0.99 – 1.22 | 11 h |
| **SRB** | 1.2 – 3.2[#] | 0 - 62 | > 2 | 7 | 2.3 – 8.8[*] | 820 h |

[*] since specific information on SRB is missing, the Rd value for Sulphorhodamine is given.
[#] $K_d$ value taken from Sabatini (2000).

**Table 3.4:** Properties of applied pesticides; $K_{oc}$ = Organic carbon adsorption coefficient; $logP_{ow}$ = octanol – water partitioning coefficient; sources are: Pesticides Properties Data Base online (2011) (a), European Commission (2002, 2010) (b) and De Wilde et al. (2007) (c).

| | ***$K_{oc}$* (ml/g) [a,b,c]** | ***log $P_{ow}$* (25°C)[b]** | ***Vapor pressure* (Pa)[b]** | ***$DT_{50}$* Photolysis (days)[b]** | ***$DT_{50\ soil}$* [b/c] aerobic (days)[b]** |
|---|---|---|---|---|---|
| **IPU** | 122 (36 – 241) | 2.50 | 2.8 – 8.1 x $10^{-6}$ (20 °C) | 48 – 88 | 23 d |
| **MTX** | 162.3 (30 – 284) | 1.65 | 7.5 x $10^{-4}$ (25 °C) | 6.5 | 46 d |

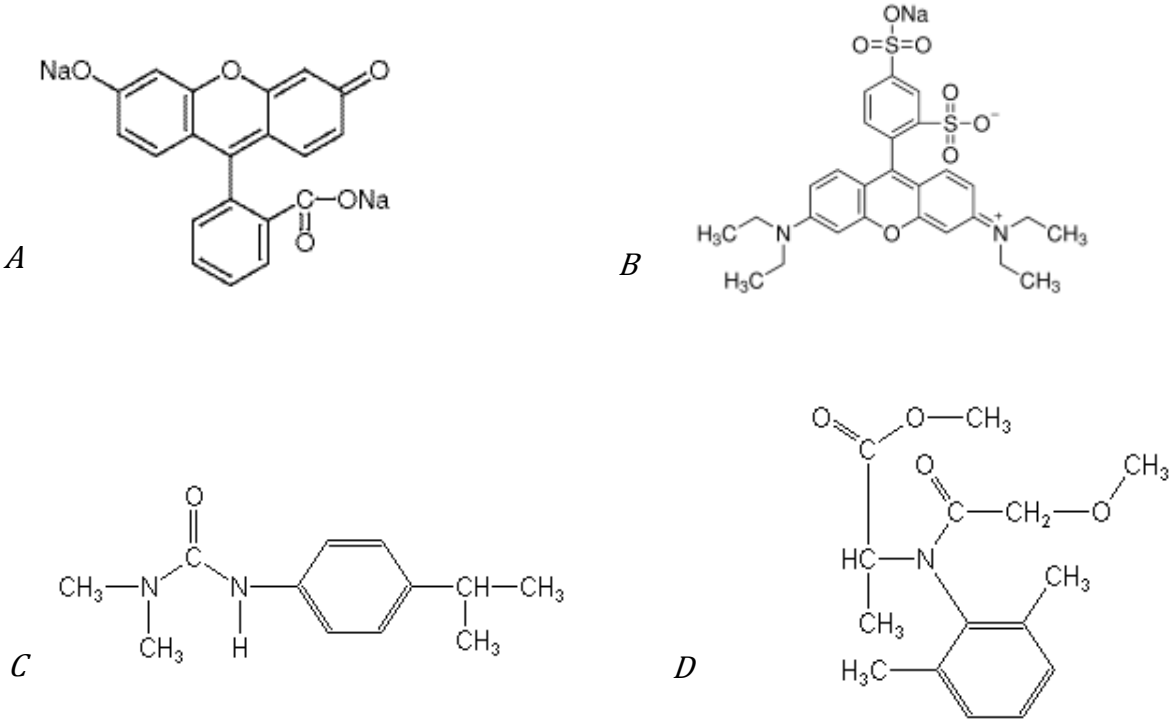


**Figure 3.5:** Molecular structures of (A) Uranine (B) Sulphorhodamine B; taken from www.tcieurope.eu, www.sigmaaldrich.com; and pesticides (C) Isoproturon and (D) Metalaxyl; taken from www.alanwood.net.

### *3.3.2. Experimental plan*

Two successive tracer experiments were designed to assess hydrological system parameters and to compare the transport behaviour of fluorescent dyes (UR and SRB) and pesticides. As a first step, the saturated mesocosms were constantly fed by *in situ* water for 28 days, which corresponds to at least 3.5 water volumes, to establish constant conditions and system equilibration. Subsequently, Bromide was injected as Dirac pulse. The injection duration needs was kept negligibly short compared to BTC duration (15 min versus 20 days, roughly) in order to fulfil the mathematical assumptions for instantaneous injection. Assuming instantaneous injection, system discharge is calculated as an integral ***(Eq-5):***

$$Q = \frac{M}{\sum_i^n (C_i - C_b) * \Delta t} \qquad \textbf{Eq-5}$$

with $Q =$ discharge, $M =$ injected tracer mass, $C_i$ and $C_b =$ measured and background tracer concentration and $\Delta t =$ time step.

As a third phase, UR, SRB, IPU and MTX were injected simultaneously as a continuous step. When applying the step injection method a favourable concentration of target substances is injected over a period of time in order to generate a concentration plateau (steady state) in the system´s outflow. Shape and position of the plateau provides evidence of transport behaviour of reactive substances and involved processes like sorption and degradation or production. Assuming continuous injection, system discharge is calculated based on a dilution effect according to ***Eq-6:***

$$Q = \frac{q_{in} * (C_{in} - C_b)}{(C_p - C_b)} \qquad \textbf{Eq-6}$$

where $q_{in}$ = tracer solution inflow rate, $C_{in}$ = tracer solution concentration, $C_p$ = measured sustained plateau concentration and $C_b$ = background concentration. ***Table 3.5*** gives an overview of experimental schedule of the documented study.

**Table 3.5:** Experimental schedule and injection functions of conducted experiments; phase 1: system equilibration phase; phase 2: hydraulic system characterization by bromide pulse injection; phase 3: comparison of transport behaviour of tracers and pesticides by continuous injection.

| *phase* | *target compound* | *injection function* | *time frame* | *aim* |
|---|---|---|---|---|
| 1 | | | 28 days | system equilibration |
| 2 | $Br^-$ | Dirac Pulse | 42 days | assessment of system hydraulics |
| 3 | UR<br>SRB<br>IPU<br>MTX | Step | 85 days | compare transport of R, SRB and pesticides |

For application of pulse and step injection methods, appropriate compound mass and concentration were calculated. An injection mass equation for pulse injection experiments in saturated column setups was published by Leibundgut et al. (2009). It takes into account the water volume to be labelled and the detection limit of the tracked compound or tracer ***(Eq-7).*** The equation was implemented for estimating bromide tracer injection mass in this study since it has been successfully applied by the authors (Leibundgut et al., 2009).

$$M = 10 * C_b * V_W \qquad \textbf{Eq-7}$$

with $M$ as estimated injection mass of the tracer or other tracked compound, $C_B$ as background concentration and $V$ as the water volume to be labelled.

Calculation of solute concentrations for simultaneous step injection of fluorescent dyes and contaminants was based on SRB as the compound of highest molecular mass. SRB injection concentration was estimated taking into account the favoured mean concentration, sorption coefficient ($K_d$) and molecular mass ***(Eq-8)***.

$$EIC = 0.6 * C_{mean} * (K_d + 1) \qquad \textbf{Eq-8}$$

where $EIC$ = injection concentration (µg/L); $C_{mean}$ = favoured SRB concentration (µg/L) at the outflow and $K_d$ = SRB sorption coefficient.
The concentration was multiplied by factor 0.6 as successive saturation of sorption sites was expected to occur over time. The calculated SRB concentration was converted into a molarity. IPU and MTX concentrations were calculated on equal molarities to simulate a sorptive competition situation between SRB, IPU and MTX ***(Eq-9)***.

$$EIC = mol_{SRB} * molmass_x * 10^6 \qquad \textbf{Eq-9}$$

where $mol_{SRB}$ is the target molality calculated for SRB (mol) and $molmass_x$ is the molecular mass of the respective contaminant (g/mol).

A helpful proxy to estimate experimental duration for a conservative tracer may be the nominal residence time, which describes the time frame that a specific saturated system needs to exchange its water content once (Lange et al., 2011) ***(Eq-10)***:

$$\mathrm{nRT} = V_W / Q_{mean} \qquad \textbf{Eq-10}$$

where $nRT$ is the nominal residence time, $V_W$ is the system water volume and $Q_{mean}$ is the average discharge (flow rate). With a defined flow rate of 0.33 ml/min and a calculated mesocosm water volume of approximately 4316 ml $t_N$ was estimated to be 218 h or 9 days, respectively. Depending on specific sorption behaviour, reactive substances (SRB, IPU, MTX) were expected to be retarded with compared to conservative ones. Due to low flow rates, solute transport was expected to show intense hydrodynamic dispersion effects (diffusion driven) resulting in peak attenuation and elongated tailings (Leibundgut et al., 2009). Sampling schedules for step injection of Bromide and for constant injection of fluorescent tracers and pesticides as well as actual injection mass and concentrations are given in ***Table 3.7***.

**Table 3.6:** Tracer and pesticide injection masses for dirac input function (Bromide) and constant injection (UR, SRB, IPU, MTX) based on Leibundgut, Maloszewski & Külls (2009) and Eq-8 and Eq-9.

| | | | ***Observation period (days)*** | | | |
|---|---|---|---|---|---|---|
| ***Pulse Injection*** | | **1 day** | **2 – 3** | **4 – 10** | **11 – 21** | **22 – 40** |
| Br | 200 mg | Injection | no sampling | sampling 3 – 6 / d | sampling 1 – 2 / d | sampling 1 / 2 days |

| ***Continuous Step*** | | | ***Observation period (days)*** | | | | |
|---|---|---|---|---|---|---|---|
| | ***C (µg/L)*** | ***E (µg)*** | **1** | **2** | **3 – 21** | **21 - 30** | **31 – 85** |
| **UR** | 10 µg/L | 168 | Injection | no sampling | sampling 1/d (tracers) 1/ 2 days (pesticides) | sampling 1/ 2 d | sampling 1/ 3 days |
| **SRB** | 100 µg/L | 1680 | | | | | |
| **IPU** | 40 µg/L | 672 | | | | | |
| **MTX** | 50 µg/L | 840 | | | | | |

Spiked inflow water for continuous injection of tracers and pesticides was prepared every 5 days to minimize changes in target compound concentrations by biological and/ or chemical degradation pathways. Actual tracer degradation under experimental conditions assessed *in situ* water from Eichstetten for five days (5 replicates, sample volume: 500 ml). Slight tracer losses were observed for both, UR and SRB fluorescent dyes. Mean concentration changes were - 0.14 % ($n = 5$, $\sigma = 2.55$ %) in case of UR and – 0.36 % ($n = 5$, $\sigma = 1.92$ %) for SRB (***Figure 3.6***). Regarding standard deviations exceeding mean values of observed degradation and degradation dimensions, target compound concentrations were treated as constant and losses were neglected. (raw data are provided in ***Table A1,*** Appendix).

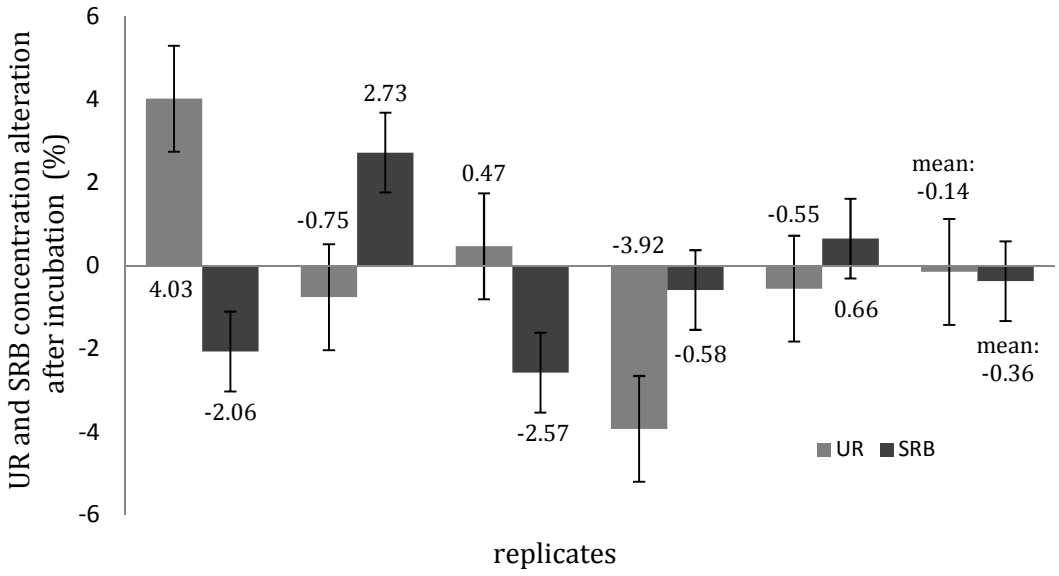


**Figure 3.6:** UR and SRB degradation in *in situ* water from CW Eichstetten within incubation time of 5 days; replicate volume: 500 ml; tracer concentrations corresponded to injection concentrations (UR: 10 µg/L, SRB: 100 µg/L).

## 3.4. Sampling procedure

Mesocosm effluent sampling was done from mesocosm supernatant. Samples were extracted using a borosilicate glass syringe (FORTUNA® OPTIMA®, 100 ml volume). The whole supernatant volume that had accumulated meanwhile the sampling intervals was sampled at each sampling time (***Figure 3.7, left***). Subsequently, the sample volume was evaluated using measuring cylinders. pH and EC were measured every five to seven days to observe mesocosm physico-chemical development. Further sample treatment for further analysis of tracers and pesticides varied according to the considered compound.

### *3.4.1. Bromide*

*In situ* measurements of bromide did not require further sample treatment. For sample analysis using ion chromatograohy (IC) sample volumes of 10 ml were filtered on 0.45 µm by hydrophobic syringe filters made of PTFE (Rotilabo®). Samples were stored in 10 ml brown glass bottles at 4°C until analysis.

### *3.4.2. Uranine and Sulphorhodamine B*

FT samples were extracted under the absence of artificial light to minimize photolytic loss of photosensitive Uranine. 200 ml of extracted mesocosm supernatant were filtered on glass fibre filters (VWR® Glass microfiber Nr. 698, Ø 47 mm, mesh width 0.7 µm) using a vacuum filtration system (1 L suction flask made of Borosilicate connected to a vacuum pump). 100 ml of filtered sample were transferred to brown glass bottles, used filters were kept in 50 ml Falcon centrifuge tubes. Both, liquid samples and filters were stored on 4 °C until analysis.

### *3.4.3. Isoproturon and Metalaxyl*

For pesticide analysis 200 ml of mesocosm supernatant were filtered on 0.7 µm filters (see 3.4.2.). 50 ml of filtrate was stored in brown glass bottles. Bottles were immediately frozen (-20 °C) until analysis. Used filters were stored in Falcon flasks (see 3.4.2.) and frozen as well (– 20 °C).

### *3.4.4. Mesocosm sediment layers*

After ending mesocosm experiments, mesocosm filling material was collected using a plastic spoon. Different layers (top sand layer, wetland sediment layer and bottom sand layer) were placed separately onto sterilized (Ethanol 98 %) plastic foil (***Figure 3.7, right***). Individual mesocosm layers were sampled in order to assess the OC fractions, loads of SRB, IPU and MTX and elementary composition at the end of the experiments. Samples were stored in 100 ml HDPE bottles on -20 °C until analysis. The VEG setup plant was separated and stored on -20 °C in a plastic bag for further analysis.

**Figure 3.7:** Liquid sample extraction from mesocosm supernatant using glass syringe (left); extracted individual mesocosm layers after ending tracer and pesticide tracking (right).

## 3.5. Sample Analysis

### *3.5.1. Bromide*

Bromide concentrations were measured during sampling and at the end of the experiment. For concentration measurements in the laboratory, an ion selective probe (WTW Br 800) connected to a hand-held equipment (WTW pH/ION 340i) was used. Samples were stirred during the measurements. The results showed that bromide concentrations largely varied at low and high concentrations ($< 5$ mg/L, $> 100$ mg/L). To enhance the reliability in mass balance estimations, *in situ* measurements obtained with the probe were compared with measurements obtained with an ion chromatography method (Dionex DX 500, detection limit = 0.018 mg/L) (for compared $Br^-$ obtained by the probe and IC see ***Figure A8***, Appendix).

### *3.5.2. Uranine and Sulphorhodamine B*

***Water samples.*** Before analysis, sample pH was raised up to $> 9$ to avoid losses of Uranine fluorescence intensity (Käss, 2004; Leibundgut et al., 2009; Wernli, 2009). Samples were alkalinized by dissolving gaseous ammonia under closed atmospheric conditions. During alkalization sample temperatures equilibrated with the environment (20 °C). Tracer concentrations were subsequently measured by focusing a fluorescence spcetrometer (Perkin Elmer LS 50 B). Measured fluorescence intensities were related to tracer concentrations via linear calibration curves that were prepared in unlabelled mesocosm effluent (filtered on 0.7 µm). Calibration ranges were adjusted to expected tracer concentrations (0.1 to 10 µg/L for Uranine and 0.1 to 50 µg/L for SRB) (see ***Figures A6*** and ***A7***, Appendix). Normalized tracer loads were calculated as follows (***Eq-11***)

$$L = \frac{\left(\frac{C}{V_T}\right)}{\Delta t} \qquad \textbf{Eq-11}$$

with $L$ = normalized tracer load (µg/h), $C$ = dissolved tracer concentration (µg/L), $V_T$ = sample volume (L) and $\Delta t$ = time step.

***Particle associated tracer loads.*** For evaluation of particle associated tracer loads, filter residues underwent a desorption process described by Wernli (2009). Therefore, used filter membranes were transferred into 100 ml brown glass bottles and covered with 50 ml of distilled water. Adsorbed tracer was mobilized using an Ammoniac – Titriplex III Solution and centrifugation. After addition of 1 ml of the solvent solution bottles were agitated in avibraxer for 3 hours. After overnight sedimentation, 10 ml of sample supernatant were centrifuged on 2000 for 20 min. Centrifuged supernatant was analyzed for tracer content using spectrometry (see dissolved concentrations). Filters were not analyzed continuously, but punctually once every 5 to 7 days. Since detectable particulate tracer loads were not expected when dissolved tracer concentrations were low, filters were analyzed during tracer plateau establishment, not during tailing phase. From fluorescence intensity signals measured in treated samples, tracer concentrations were calculated according to the calibration curves prepared in mesocosm effluent (see dissolved concentrations). Background signals exceeded the ones detected in water samples and differed significantly between one another. Therefore, sample specific background emissions were annotated and subtracted from the measured tracer signal to avoid over estimation of particulate loads. These were calculated as follows (***Eq-12***):

$$L_P = \frac{\left(C * V_F * [\frac{V_T}{V_F}]\right)}{\Delta t} \qquad \textbf{Eq-12}$$

with $L_P$ as particulate tracer load (µg/h), $C$ as measured tracer concentration (µg/L), $V_F$ as filtrate volume (L), $V_T$ as total liquid sample volume (L) and $\Delta t$ as time step.

***Mesocosm layers.*** Analysis of sediment samples followed the same protocol as described above for filter residues. In this case, 10 of sediment were suspended in 50 ml of distilled water. After addition of 1 ml of Titriplex III –Ammoniac solution samples were treated as described above. Background signals differed between samples and were high compared to the ones measured for filter residue samples. Backgrounds were documented individually and were subtracted from measured fluorescence intensity peaks. Sediment SRB loads were normalized by saturated sediment bulk density as follows (***Eq-13***):

$$L_S = ( C * V / m_S ) * \rho_{Sat} \qquad \textbf{Eq-13}$$

where $L_S$ is the sediment load (µg/cm$^3$), $C$ is the measured tracer concentration of sediment desorption solution (µg/L), $V$ is the volume of sediment suspension (L), $m_S$ is the saturated sediment mass involved in SRB desorption (g) and $\rho_{Sat}$ is the saturated bulk density of investigated sediments (g/cm$^3$).

***Uncertainty of concentration measurements.*** The accuracy of fluorescence spectrometry was defined by the accuracy of the spectrometer itself (1 %) and the reproducibility of measurement results in mesocosm effluent (UR: 0.0275 %, SRB: 0.010 %. Linear calibrations for UR and SRB revealed high accuracy with $R^2 = 1$ in both cases (***Figures A6 and A7***, Appendix). Total errors for detected UR and SRB concentration results were 1 % roughly. Accuracy was slightly higher for SRB, exact values are given below:

$$\text{UR: } z \pm 1.0275\ \%$$

$$\text{SRB: } z \pm 1.010\ \%$$

Given values may be slightly under estimated due to background signal changes in mesocosm effluent over time. Depending on coloring compounds, such as humic acids, sample turbidity probably varied between individual samples.

### *3.5.3. Isoproturon and Metalaxyl*

Pesticide liquid samples and filter residues were analyzed on concentrations and loads of the target compounds Isoproturon and Metalaxyl and two Isoproturon metabolites, 1-(4 isopropyl phenyl) urea and Desmethylisoproturon. The latter metabolite is produced in soil environments and is considered to pose a higher or comparable risk to the environment compared to that of the parent substance (PPDB, 2011). Persistence, mobility and ecotoxicity of Desmethylisoproturon are referred to as moderate (aerobic $DT_{50}$ in soils: 33 days, PPDB, 2011). Both, liquid and solid samples were analyzed by IPU commercial service of the Louis Pasteur Institute in Lille Cedex, France.

# 3.6. Data Treatment

## *3.6.1. Analysis of concentration changes over time*

***Hydraulic system parameters.*** Hydraulic characteristics of the mesocosms were assessed by pulse injection of Bromide and subsequent BTC observation. Parameters were defined according to Lange et al. (2011), based on the residence time distribution equation (RTD) originally published by Kadlec (1994). Assessed parameters are listed in ***Table 3.8***, detailed mathematical equations con be found elsewhere (Kadlec, 1994; Lange et al., 2011). Since these parameters were defined for instantaneous tracer injection, some transport parameters had to be defined differently, others could not be calculated for constant injection of tracers and pesticides (***Table 3.8***).

**Table 3.7:** Mesocosm hydraulic system parameters assessed by $Br^-$ concentration change observations (pulse injection) and transport parameters derived from continuous injection of tracers (UR, SRB) and pesticides (IPU MTX) (after [a] Kadlec, 1994 and [b] Lange et al., 2011).

| *Parameter* | *Bromide Pulse* | *UR, SRB, IPU, MTX Step* |
|---|---|---|
| $V_{max}{}^{b}$ | maximum velocity of target compound (cm/h) | |
| $V_{mean}{}^{b}$ | mean target compound velocity, 50 % of solute are detected in effluent (m/h) | mean target compound velocity, 50 % of concentration plateau is reached (m/h) |
| $t_P{}^{b}$ | Time of peak concentration in effluent (h) | |
| $t_{50}{}^{b}$ | Time after which 50 % of solute were detected in effluent (h) | |
| $C_{max}$ | Peak concentration detected in effluent (mg/L) | |
| $E\,(t)^{a,b}$ | Hydraulic residence time distribution (h) | not calculated |
| $\tau^{a,b}$ | mean residence time (h) | not calculated |
| $\sigma^{2b}$ | Hydraulic residence time distribution variation (h) | not calculated |
| $R^{b}$ | Recovered solute mass (%) | |

### *3.6.2. Modelling transport of tracers and pesticides*

To define compound specific transport parameters for both, pulse and step injection methods, a solute transport model was fitted to observations of tracer and pesticide concentrations. A common model for saturated solute transport, CXTFIT (Toride et al., 1999), was applied. Several cases of modelling tracer and pesticide concentration changes from column experiments are reported in literature (Atkinson & Bukowiecki, 2000; Kamra et al., 2001; Mao & Ren, 2004; Zhou et al., 2010). The model is able to estimate solute transport parameters from empirical observations (inverse problem) as well as for predicting solute concentrations according to fixed transport parameters (direct problem). Water and solute transport is calculated based on the convection-dispersion equation (CDE), which was developed by Lenda & Zuber (1970) ***(Eq-14)***. They assumed saturated flow conditions, transport in porous media, laminar water flow, steady state conditions, flow direction equal to *x*-axis direction and assuming no immobile water phases.

$$C\,(x,t) = \frac{M}{Q} * \frac{x}{\sqrt{4\,\pi * D_L * t^3}} * \exp\left(-\frac{(x-vt)^2}{4 *\ D_L * t}\right) \qquad \textbf{Eq-14}$$

where $C$ = solute concentration (g/m$^3$), $M$ = injection mass (g), $Q$ = discharge (m$^3$/h), $x$ = flow length (m), $D_L$ = longitudinal dispersion coefficient (m$^2$/d), $t$ = time (h) and $v$ = darcy velocity (m/h).

The CXTFIT code includes three different one-dimensional transport models: 1) the conventional CDE (equilibrium), 2) the chemical and physical non-equilibrium CDE (an extension to the simple CDE) and 3) a stochastic stream tube model including equilibrium and non-equilibrium transport (Toride et al., 1999). Solute transport empirical data was modelled applying the two first transport equations. Non-equilibrium models consider adsorption on one part (or none) of available sorption sites to be instantaneous, while adsorption on the other portion is governed by first-order kinetics Toride et al., 1999). These are the so-called two-site non-equilibrium models (Selim et al., 1976 and Cameron & Klute, 1977 in Toride et al., 1999). Physical non-

equilibrium in contrast, is modelled using a two-region formulation containing a mobile and an immobile flowing region (Coats & Smith, 1964, van Genuchten & Wierenga, 1976 in Toride et al., 1999). Parameter fitting is optimized by a non-linear least squares analysis (Marquart 1963 in Toride et al., 1999). Model quality is evaluated by the coefficient of determination ($R^2$) for regression of observed data versus prediction (Toride et al., 1999).

# 4. Results

## 4.1. Characteristics of mesocosm influent water

Mesocosms were fed by *in situ* water from CW Eichstetten. Inflow water was characterized by pH ranging from 7.65 to 7.77, DO concentrations of 4.66 mg/L and 4.72 mg/L and typical EC values for surface water bodies and streams (798 µS/cm and 895 µS/cm). TSS loads were constant between the two samplings, accounting for 11.5 and 11.1 mg/L. At the same time, POC loads were proven to be constantly low (1.6, 3.9 mg/L). No significant differences were measured between TIC and DIC, as well as between TOC and DOC, indicating that sample carbon content was mostly represented by dissolved species. While OC fractions ranged from 2.3 to 5.8 mg/L, inorganic carbon loads ranged between 31 and 67.5 mg/L. Major ion analysis gave evidence of $Mg^{2+}$ and $Ca^{2+}$ and $SO_4^{2-}$ rich geological background of the site. Nitrate concentrations may be a hint for agricultural land use and application of mineral fertilizers within the drained watershed (***Table 4.1***). None of the applied tracers was detected in the inflow water for both collection dates. Results on initial concentrations of the target pesticides IPU and MTX are not yet available at the moment, but are in progress. Raw data on hydrochemistry and physico-chemical parameters are summarized in ***Table A2***, Appendix.

**Table 4.1:** Major ion concentrations measured in *in situ* water collected from the CW Eichstetten and supplied to the mesocosm experiments.

| ***collection date*** | ***$Na^+$*** | ***$K^+$*** | ***$Mg^{2+}$*** | ***$Ca^{2+}$*** | ***$Cl^-$*** | ***$NO_3^{2-}$*** | ***$SO_4^{2-}$*** |
|---|---|---|---|---|---|---|---|
| 22.06.11 | 11.68 | 3.28 | 26.34 | 102.30 | 32.79 | 24.58 | 81.25 |
| 18.07.11 | 10.74 | 3.81 | 24.30 | 110.42 | 30.38 | 25.60 | 80.55 |

## 4.2. Observed changes in the mesocosms

### *4.2.1. Plant and biofilm development*

Studied vegetated mesocosm setups showed differences in the development of macrophytes. When bromide pulse injection was started, plant development of individual setups was documented (***Figure 4.1***). New foliation indicated good plant health in the vegetated wetland sediment setup resembling *in situ* condition of CW Eichstetten (VEG) and in the homogeneous sand filled mesocosm C2 (Alteckendorf). In setups C1 and C3 (Alteckendorf) plants seemed to have established and adapted to surrounding conditions as well, even if foliation was less intense compared to VEG and C2 (Alteckendorf). On the contrary, the plant in setup C4 did not grow any new leaves but showed severe decay (***Figure 4.1***). The non-planted setup NV served as a control to the planted wetland sediment setup VEG (resembling Eichstetten *in situ* conditions).

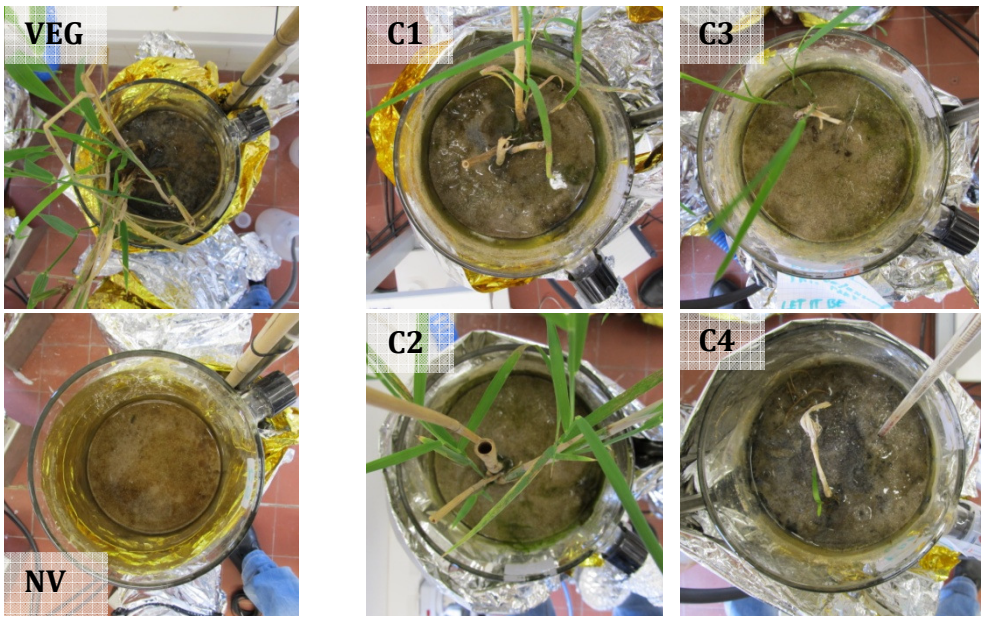


**Figure 4.1:** Mesocosm plant development on bromide pulse injection day; VEG and NV: vegetated and non-vegetated setups with hetereogeneous layering (see 3.2.1.); C1 – C4: vegetated homogeneous sand filled setups.

The plant in setup VEG stayed vital throughout bromide BTC observations and during step injection of UR, SRB, IPU and MTX and following concentration change observations. The plant root system continuously extended and was visible through the mesocosm glass walls at the end of the experiment (***Figure 4.2***). Persistent development of foliage was observed (***Figure 4.2, left***).

**Figure 4.2:** Plant and root development at the end of the experiment (November 8, 2011) in the vegetated wetland mesocosm setup (VEG).

## *4.2.2. Characteristics of the mesocosm matrix*

***Initial characteristics.*** Filling materials were initially analyzed on total porosity (P), saturated hydraulic conductivity ($k_f$), bulk density (ρ), particle size distribution, organic carbon content (OC) and elementary composition. Wetland sediment from Eichstetten was classified as sandy silt. While silt fractions (2 – 50 µm) accounted for 72.81 % of the sediment volume, sand (50 – 2000 µm) and clay (< 2 µm) particle proportions were found to be 20.80 % and 6.39 % respectively (for particle fractionation and diameter

frequency diagrams see ***Figures A4*** and ***A5***, Appendix). Initially, OC content accounted for 5.18 % weight (σ = 0.29 %, n = 3). Due to high silt and clay percentages, $k_f$ of wetland sediments could not be assessed by the applied constant head saturation method within 8 days. In literature, typical values for the hydraulic conductivity of silt, sandy silt and loess range between magnitudes of $10^{-6}$ m/s and $10^{-10}$ m/s (Clapp & Hornberger, 1978; Freeze & Cherry, 1979; Fetter, 1994). As expected, $k_f$ was highest in gravel and slightly lower in medium sand ($1.31 * 10^{-3}$ m/s versus $1.04 * 10^{-3}$ m/s). Also gravel and medium sand showed initial OC fractions (gravel: 0.15 %, sand: 0.31 %). The mean OC fraction in the mesocosm setups amounted for 0.64 % taking into account the volumetric proportions and bulk densities of individual layers. Analysis of elementary composition of different filling materials, as well granulometric analysis of gravel and sand are in progress. Available results on initial sediment pedology are given in ***Table 4.2***. Particle diameters were 1 – 2 mm for gravel and 400 – 630 µm for sand.

**Table 4.2:** Pedological characteristics of filling materials; P = total porosity; kf = saturated hydraulic conductivity; ρ = bulk density; WS = wetland sediment; OC = organic carbon; values (except granulometry) represent means of $n = 3$ measurements, standard deviations in brackets.

| | ***P (vol. %)*** | ***$k_f$ (m/s)*** | ***ρ (g/cm³)*** | ***OC (m%)*** |
|---|---|---|---|---|
| **Gravel** | 41.94 | $1.31 * 10^{-3}$ | 0.692 | 0.15 |
| | (0.14) | ($3.8 * 10^{-5}$) | (0.021) | (0.046) |
| **Sand** | 43.91 | $1.04 * 10^{-3}$ | 0.716 | 0.31 |
| | (0.82) | ($1.51 * 10^{-4}$) | (0.005) | (0.079) |
| **WS** | 72.55 | $10^{-6}$ – $10^{-10}$# | 0.948 | 5.18 |
| | (0.37) | | (0.017) | (0.299) |

* 100 % very coarse sand fractions

# derived from literature: Clapp & Hornberger, 1978; Freeze & Cherry, 1979; Fetter, 1994.

Elementary composition and OC contents of different mesocosm layers was analyzed after ending the experimental phase. Results for final OC content are given in ***Table 4.3***. Terminal elementary composition data is still in progress and cannot be demonstrated here.

**Table 4.3:** OC fractions from mesocosm layers extracted after ending tracer and pesticide observations; $t_1$ = terminal OC fraction; $t_0$ = initial OC fraction; values represent means of $n = 3$ measurements, standard deviations in brackets.

| | | ***Top sand (m %)*** | ***Wetland sediment (m %)*** | ***Bottom sand (m %)*** |
|---|---|---|---|---|
| ***VEG*** | OC ($t_1$) | 0.48 (0.09) | 5.69 (2.18) | 0.18 (0.04) |
| | Δ OC ($t_1$ - $t_0$) | *+ 0.17* | *+ 0.51* | *- 0.13* |
| ***NV*** | OC ($t_1$) | 0.37 (0.02) | 4.81 (0.09) | 0.25 (0.02) |
| | Δ OC ($t_1$ - $t_0$) | *+ 0.06* | *- 0.37* | *- 0.06* |

Within wetland sediment layers, both setups showed visible macropore development, mainly produced by benthic invertebrate tubeworm species *Tubifex spec.* (***Figure 4.3, left***). These tubeworms were transferred to the mesocosm by the natural wetland sediments from the CW in Eichstetten and resemble typical abundant species of freshwater benthic ecosystems (Collado & Schmelz, 2009). Besides, gas enclaves were observed, which probably reduced system water volume over time and indicate the presence of anaerobic metabolic pathways (fermentation) (***Figure 4.3, right***).

·s (left); gas

Black discolorations of the wetland sediment layers of both setups and within the VEG top sand layer were observed (***Figure 4.4***). Under anaerobic conditions several bacteria are capable of using sulphate as a final electron acceptor on energy production metabolic pathways. Simple organic compounds are oxidized with sulphate under the production of hydrogen sulphide and low molecular carbonates (Dvorak et al., 1992). Hydrogen sulphide in turn, reacts with several metals to form insoluble metal sulphites under neutral and low alkaline pH conditions (Dvorak et al., 1992). In presence of dissolved Fe(II), immobile iron monosulphite (mackinawite) is formed, showing typical darkening of sediments (Doyle, 1968). While mackinawite formation was restricted to the wetland sediment layer in NV, it was detected in the upper sand layer of the VEG setup as well (***Figure 4.4)***.

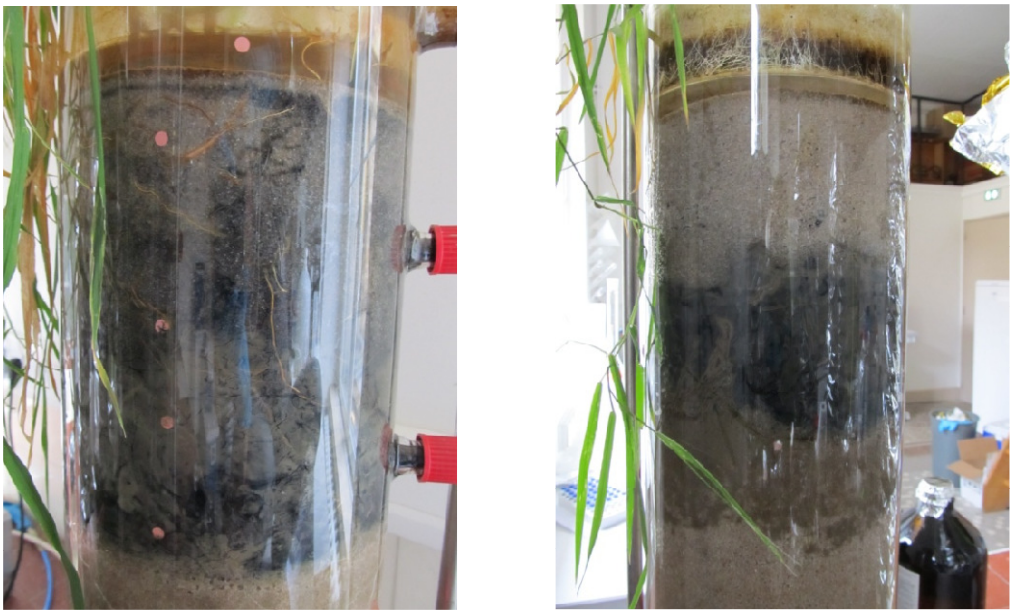

**Figure 4.4:** Differing discolorations of mesocosm setups layers in vegetated (left) and non-vegetated setup (right).

The comparison of $SO_4^{2-}$ and total Fe concentration changes over time in mesocosm effluent gives evidence of significant Fe mobilization from filling materials in the VEG setup and moderate Fe release from the control. While influent Fe concentration was 0.016 mg/L, mesocosm effluents contained mean Fe concentrations of 0.52 mg/L (VEG setup) and 0.033 mg/L (NV setup) (***Figures 4.5, 4.6***, for raw data see ***Table A4*** and ***A5,*** Appendix). At the same time, mesocosm mean sulphate concentrations lie below inflow concentration with 73.11 mg/L in the VEG setup and 57.04 mg/L in the NV control compared to 80.55 mg/L in the influent, indicating sulphate reduction to take place.

While Fe mobilization shows a slight negative trend with time, Fe mobilization in the VEG setup did not follow a linear trend. Fe concentration is declining during the 35 days of observation followed by an increase for the next 20 days. Observations end with a negative Fe concentration trend in the VEG setup. Due to the plant affecting system physico-chemical properties, the VEG setup may be subject to more complex biogeochemical interactions and changing chemical milieu than the non-vegetated one.

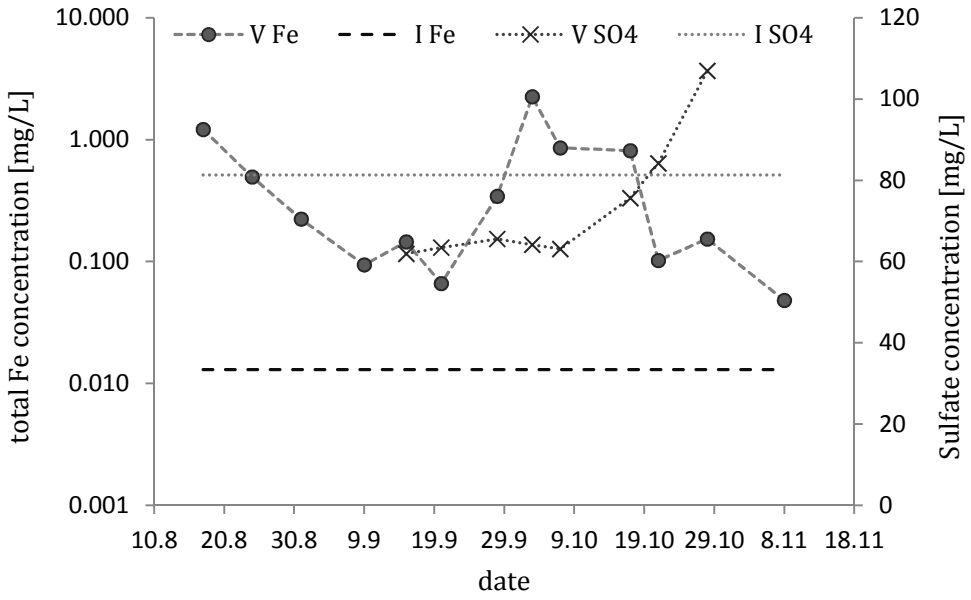


**Figure 4.5:** Total Fe and sulphate concentrations in vegetated mesocosm effluent and influent water.

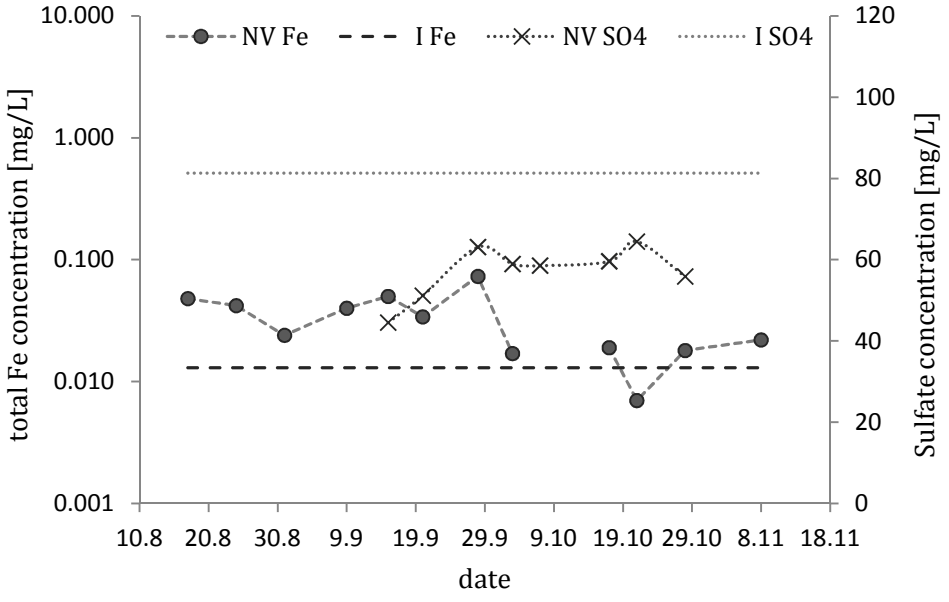


**Figure 4.6:** Total Fe and sulphate concentrations in non-vegetated mesocosm effluent and influent water.

The non-vegetated control showed brownish discolorations right below the wetland sediment layer, within the upper 5 – 8 cm of the bottom sand layer, which is not observed in the VEG mesocosm (***Figure 4.4, right***). During equilibration phase a leak in the influent tubing of the NV control setup lead to leakage of mesocosm pore water and falling water table for 24 hours. During this process, suspended clay particles from the wetland sediment layer may have precipitated within the bottom sand layer forming the observed brownish front. Another explanation may be the precipitation of insoluble ferric hydroxides, which are formed via both, biotic and abiotic reactions under the presence of oxygen (Clarke et al, 1997). These show reddish and brownish discolorations and may be responsible for the observed front formation in the NV control setup.

### *4.2.3. Hydrological characteristics and water balance*

The hydrological balance of vegetated and non-vegetated mesocosm showed notable variability. No visible plant effect on the mesocosm water balance could be observed during the salt tracer experiment, when mesocosm surfaces were not covered and supernatant was strongly exposed to evaporation ***(Table 4.4)***. When not covered, VEG mesocosm effluent loss even exceeded NV setup loss by 0.84 % ($loss_{EVT}$ VEG: 19.39 %; $loss_{EVT}$ NV: 18.55 %) (***Figure 4.7***; ***Table 4.4***).

During combined injection of tracers and pesticides however, evaporation losses from mesocosm supernatant were significantly minimized by covering column surfaces with aluminium. Losses were reduced by 9.69 % in the vegetated setup and 13.55 % in the non-vegetated control, respectively. Globally, effluent loss was significantly higher in the vegetated mesocosm setup than in the control (VEG: 8.86 %, NV: 5.84 %) ***(Figure 4.8***; ***Table 4.4)***. During the first 20 days of observation however, effluent volumes increased dramatically in the VEG setup before system discharge stabilized at about 97 % of theoretically expected effluent volume (***Figure 4.8***). After 480 hours, effluent yields in the vegetated mesocosm started decreasing continuously until observations were stopped after 70 days. Even if effluent yields in both setups showed continuous decrease with time, this effect was higher in the vegetated setup. Between 720 h and the end of

observations after 1680 System discharge reduced by 4.8 % in the VEG setup compared to only 1.5 % in the NV control (***Figure 4.8***).

**Table 4.4:** Mesocosm hydrological balance during concentration change observations; $Q_{IN}$ = influent volume; $Q_{act}$ = measured mesocosm discharge volume; $loss_{EVT}$ = discharge loss.

| *phase* | *condition* | *setup* | $Q_{IN}$ *(ml)* | $Q_{act}$ *(ml)* | $loss_{EVT}$ *(%)* |
|---|---|---|---|---|---|
| **Br$^-$** | open | VEG | 9840 | 8015 | **18.55** |
| | surface | NV | | 7932 | **19.39** |
| **UR, SRB,** | covered | VEG | 38620 | 35230 | **8.78** |
| **IPU, MTX** | suface | NV | | 36364 | **5.84** |

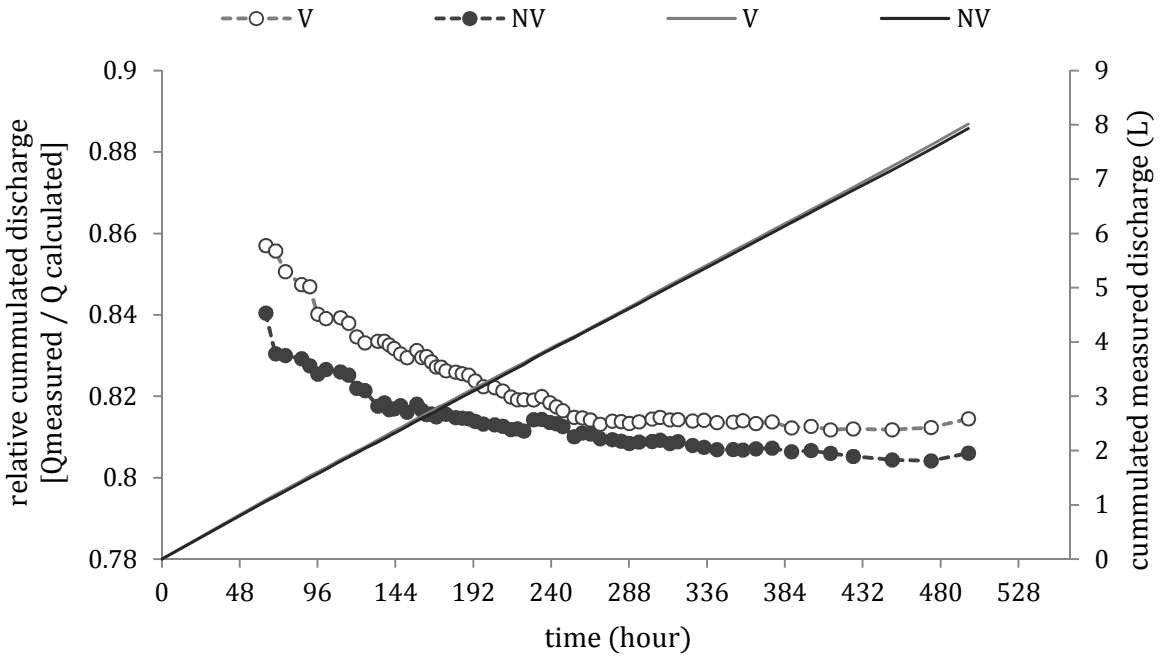


**Figure 4.7:** Hydrological balance of planted and non-vegetated wetland mesocosm setups during Bromide pulse injection and BTC observation; $Q_{measured}$ = measured effluent; $Q_{calculated}$ = calculated effluent (pump rate [L/h] * t [h]).

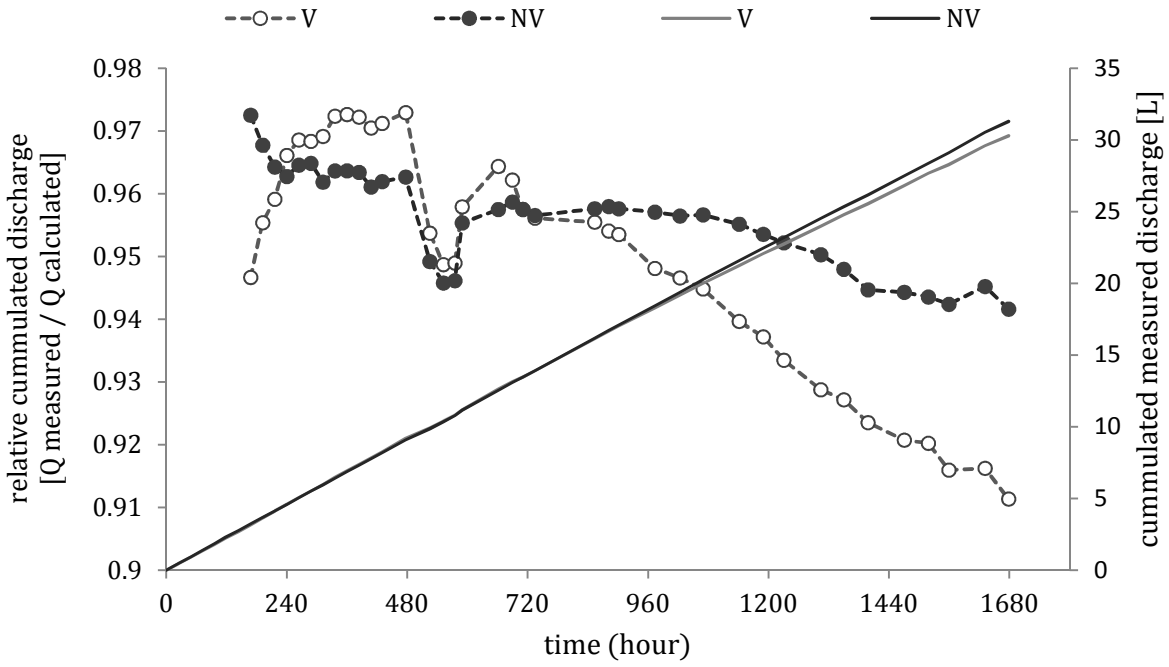


**Figure 4.8:** Hydrological balance of planted and non-vegetated wetland mesocosm setups during observation of step injection of tracers and pesticides; $Q_{measured}$ = measured effluent; $Q_{calculated}$ = calculated effluent (pump rate [L/h] * t [h]).

## *4.2.4. Hydrochemistry*

Globally, mesocosm physico-chemical conditions did not show dramatic changes during observation time. Mean pH values were 7.5 in the VEG setup and 7.82 in the NV control. Mesocosm EC values represented the one measured in the influent water. Both parameters did not show any significant trends and developments and were treated as stable conditions (***Table 4.5,*** for raw data see ***Table A3,*** Appendix). However, TSS (Total Suspended Solids) and POC (Particulate Organic Carbon) loads differed significantly between planted and non-vegetated setups. While both parameters showed low variability in the NV control ($\sigma_{TSS}$: 6.16 mg/L, $\sigma_{POC}$: 0.00 mg/L), the VEG setup showed higher loads and great temporal variability ($\sigma_{TSS}$: of 34.17 mg/L, $\sigma_{POC}$: 13.96 mg/L) ***(Table 4.5,*** see also Figure ***A3*** and ***Table A8)***.

**Table 4.5:** Mesocosm outflow physico-chemical evolution; EC [µS/cm], TSS and POC [mg/L].

| | VEGETATED | | | | NON VEGETATED | | | |
|---|---|---|---|---|---|---|---|---|
| | ***pH*** | ***EC (µS/cm)*** | ***TSS (mg/L)*** | ***POC (mg/L)*** | ***pH*** | ***EC (µS/cm)*** | ***TSS (mg/L)*** | ***POC (mg/L)*** |
| **mean** | **7.50** | **802** | **55.50** | **27.00** | **7.82** | **730** | **19.76** | **15.00** |
| min | 7.26 | 735 | 35.00 | 15.00 | 7.45 | 597 | 10.00 | 15.00 |
| max | 7.99 | 888 | 125.00 | 50.00 | 8.19 | 791 | 30.00 | 15.00 |
| σ | 0.23 | 44 | 34.17 | 13.96 | 0.21 | 50 | 6.61 | 0.00 |

***System oxidation***. Initially, both mesocosm setups showed anoxic conditions above 2.5 cm height (DO concentration $<$ 0.1 mg/L). With successive system evolution, the development of intense aerobic conditions within bottom gravel and sand layers of both setups (0 – 20 cm height) was observed. Maximal oxygen concentrations of 8.47 mg/L were recorded in the VEG setup and 8.36 mg/L in the control. However, within the upper mesocosm half, including wetland sediment layers, dissolved oxygen concentrations did significantly vary, remaining strictly anoxic with DO $<$ 0.1 mg/L. Therefore model wetland mesocosms were treated as anoxic systems. Both setups showed great similarity concerning DO evolution in the bottom gravel and sand layers (for further illustration see ***Figure A3***, Appendix).

***Major ions.*** Mesocosm effluent showed detectable concentrations of the alkaline earth metals $Mg^{2+}$ and $Ca^{2+}$. These reflected influent water concentrations measured in *in situ* water from CW Eichstetten giving evidence of geological background conditions of the site (***Table 4.1***, for raw data see ***Table A4,*** Appendix ). Concentrations of potassium and nitrate were significantly lower in the planted mesocosm effluent, suggesting their assimilative uptake by the vegetation. Sulfate concentrations however, were higher in the planted setup, which indicates less effective sulphate reduction in the planted setup due to root zone oxidation by the vegetation (Winthrop et al, 2002). Both setups went below inflow water sulfate concentrations (***Table 4.1, Figures 4.5*** and ***4.6***). Simultaneously, the production of gaseous hydrosulfide ($H_2S$) was detected by olfactory testing, which gives evidence of sulphate reduction reactions.

***Major and trace elements.*** Besides the common major alkaline earth metals $Mg^{2+}$ and $Ca^{2+}$, silicium, aluminium, iron, manganese and potassium were detected in the mesocosm effluent water. Detected elements reflected those detected in influent water. Trace metals detected were strontium, barium, nickel, tin and copper. Both, major and trace element concentrations measured in mesocoms effluent exceeded influent water concentrations detected in *in situ* water from CW Eichstetten, indicating reductive mesocosm milieus resulting in mobilization processes (for data see ***Tables A5*** and ***A6***, Appendix).

***Carbon species.*** Concentration of carbon species was evaluated on a weekly basis, starting after the first 30 days of the step injection experiment on UR, SRB, MTX and IPU. Observations of dissolved and total organic and inorganic carbon species (TIC, TOC, DIC, DOC) indicated that carbon fractions in mesocosm effluent were strictly dominated by dissolved species initially (***Figures 4.9, 4.10***). During this period DOC accounted for 5 to 10 % of DIC in the VEG setup and 5 to 13 % in the NV control, roughly. These proportions correspond to those assesses in mesocosm influent water from CW Eichstetten, where DOC amounted for 5.8 to 9 % of DIC and carbon species were solely available in the dissolved form (for further data see ***Table A7***, Appendix).

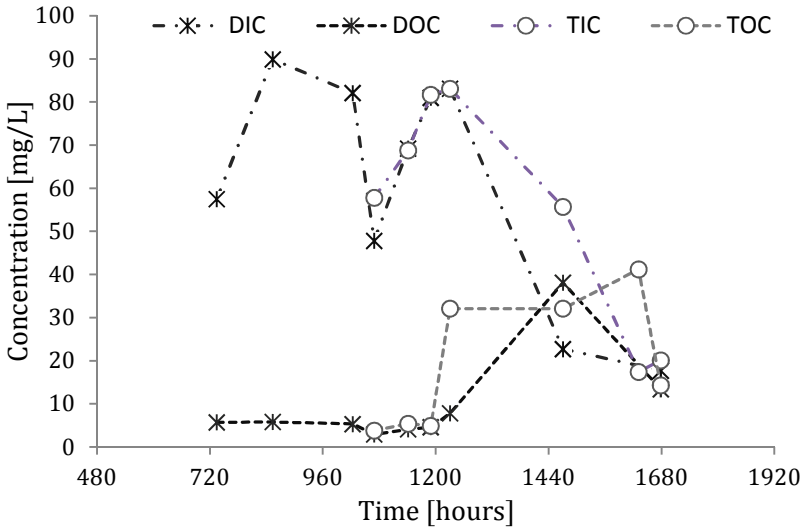


**Figure 4.9:** Carbon species fractionation over time in VEG mesocosm setup effluent.

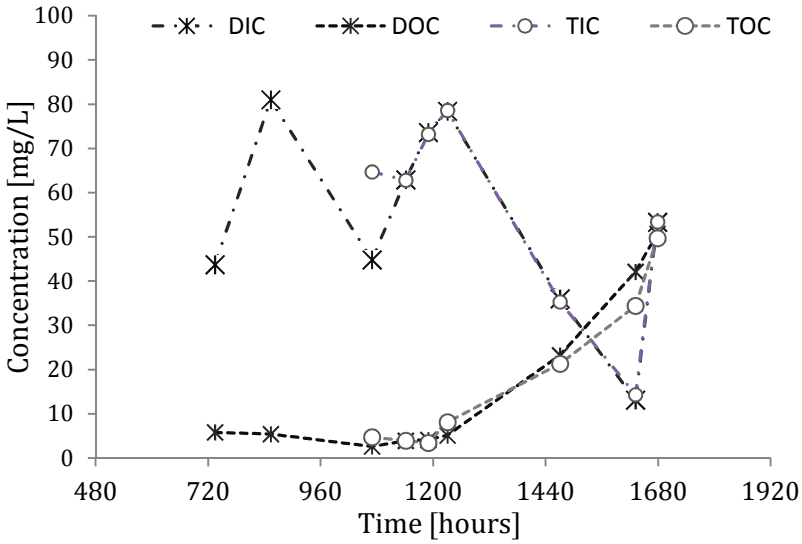


**Figure 4.10:** Carbon species fractionation over time in VEG mesocosm setup effluent.

After 1200 h there was a significant difference between dissolved and total organic and inorganic fractions in both setup, which indicates the presence of particulate carbon. In the control there was no evidence of particulate carbon species throughout the observations. The presence of root channels from vegetation obviously decreased the mechanical water filtration capacity of the vegetated mesocosm matrix. Organic carbon concentrations start increasing after 1200 hours of observation in both setups, which may be due to decaying organic matter (for further data see ***Table A7***, Appendix).

***Nutrients.*** Continuous data on nutrient concentration development in mesocosm effluent is only available for nitrate ($NO_3^{2-}$). Concentrations are higher in the NV setup with a mean value of 1.76 mg/L ($\sigma = 1.36$ mg/L) versus 0.29 mg/L detected in the VEG setup ($\sigma = 0.17$ mg/L). No significant concentration changes were measured over time. Nitrate concentrations however, went far below the ones detected in influent water (25.60 mg/L). Punctual nitrite measurements did not reveal any detectable $NO_2^-$ in the VEG system and were low in the NV control (0.25 – 0.62 mg/L). Similar observations were made for ammonium, which was detected in low concentrations in the NV control (0.34 – 1.52 mg/L), but was not present in detectable concentrations in the VEG system (for raw data see ***Table A7,*** Appendix).

## 4.3. Tracer concentration tracking and transport parameters

Pesticide liquid samples and filter residues could not be analyzed within the given time frame of this study, but are currently analyzed. Results of Isoproturon and Metalaxyl concentration changes cannot be displayed or modelled in this work.

### *4.3.1. Bromide pulse injection*

Results obtained by the ion selective probe (WTW Br 800) showed intense fluctuations and over estimation of bromide concentrations and recovery rates (up to $R = 184$ %). Due to large concentration fluctuations between measurements, results could not be correlated to the ones obtained by ion chromatography. Therefore, the following results of bomide tracking and transport parameters are based on ion chromatography measurements solely. A comparison between probe and IC data is demonstrated in ***Figure A8***, Appendix.

BTC observations proved that hydraulic performance of wetland mesocosms resembling conditions of CW Eichstetten did not differ dramatically between the VEG and NV setups and hydraulic parameters represented similar dimensions (***Table 4.6, Figure 4.11***). Even though, 50 % of injected tracer mass was recovered slightly faster in the VEG system effluent than in the control (***Table 4.6***). Calculated HRT was lower with 349.46 h versus 365.7 hours in the vegetated setup, respectively. Moreover, maximum and mean bromide velocities were higher and reached faster in the planted system, resulting in lower peak attenuation capacities ($C_{max}$ VEG: 50.2 mg/L, $C_{max}$ NV: 47.5 mg/L). At the same time, Bromide recovery (R) in the VEG setup went below the one of the NV control (94.18 % versus 98.81 %). RTD variances indicated larger variance of the mean system retention time in the NV control compared to the VEG setup (***Table 4.6***). Both systems simultaneously returned to background concentrations after 35 days. NV bromide BTC showed a little shoulder formation in concentration decrease, which is not observed in the vegetated system.

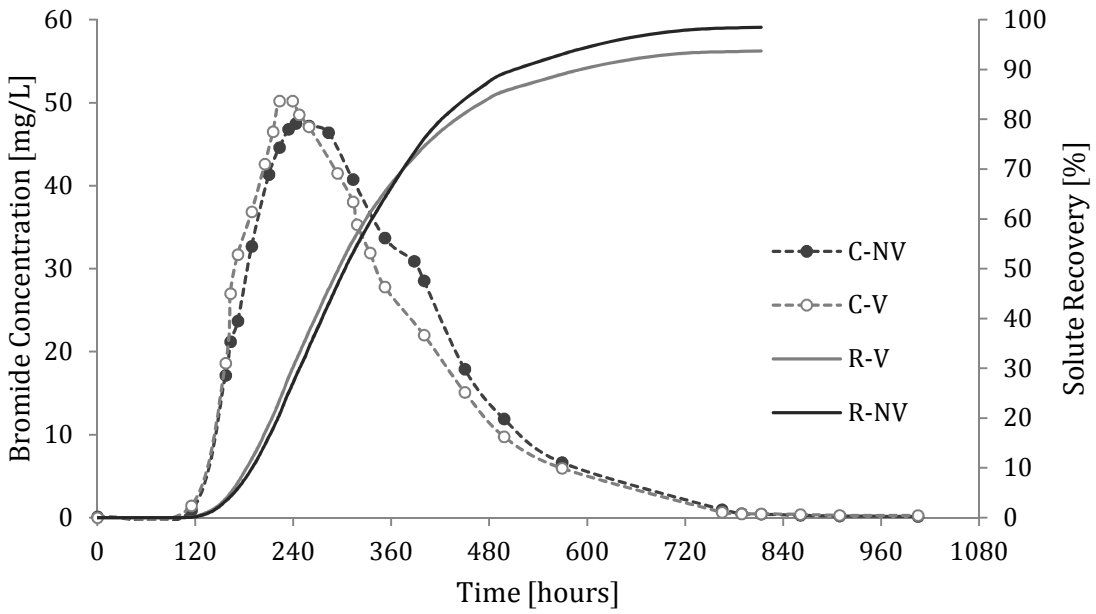


**Figure 4.11:** BTCs and solute recovery for Bromide pulse injection experiment in vegetated (VEG) and non-vegetated (NV) wetland mesocosm setups.

On the contrary, the homogeneous medium sand filled mesocosms receiving influent water from the CW in Alteckendorf showed more heterogeneous hydraulic behaviour between individual setups (***Figure 4.12 and 4.12 ff***).

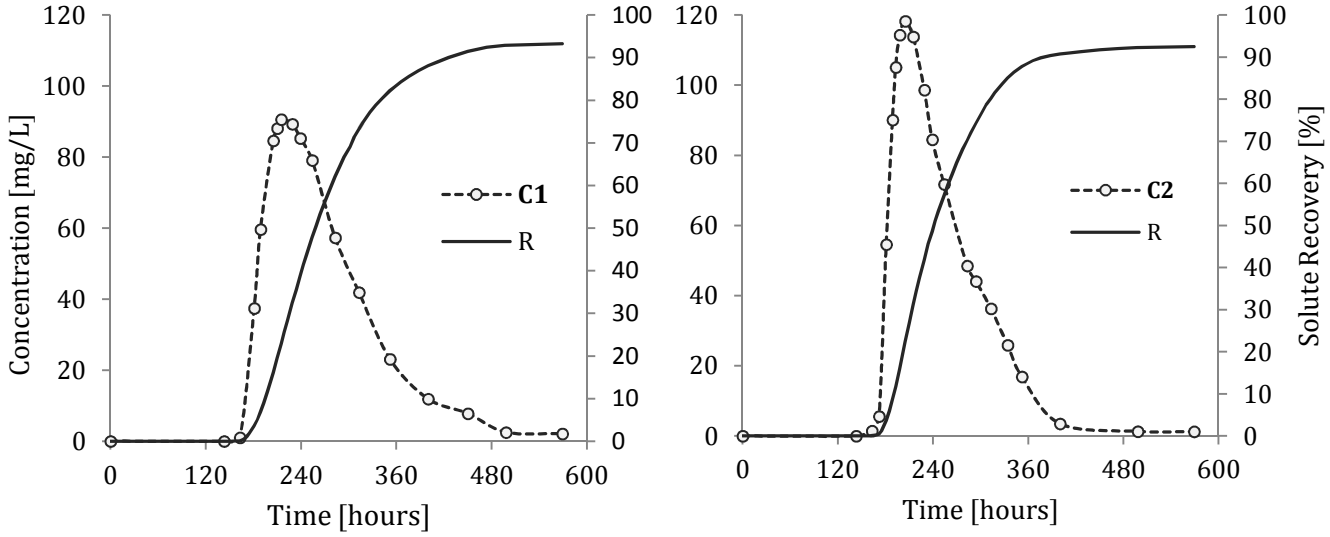


**Figure 4.12:** BTCs and solute recovery rates for planted wetland mesocosms containing homogeneous medium sand media; C1 (left) and C2 (right) = Concentration observations in planted sand filled mesocosms.

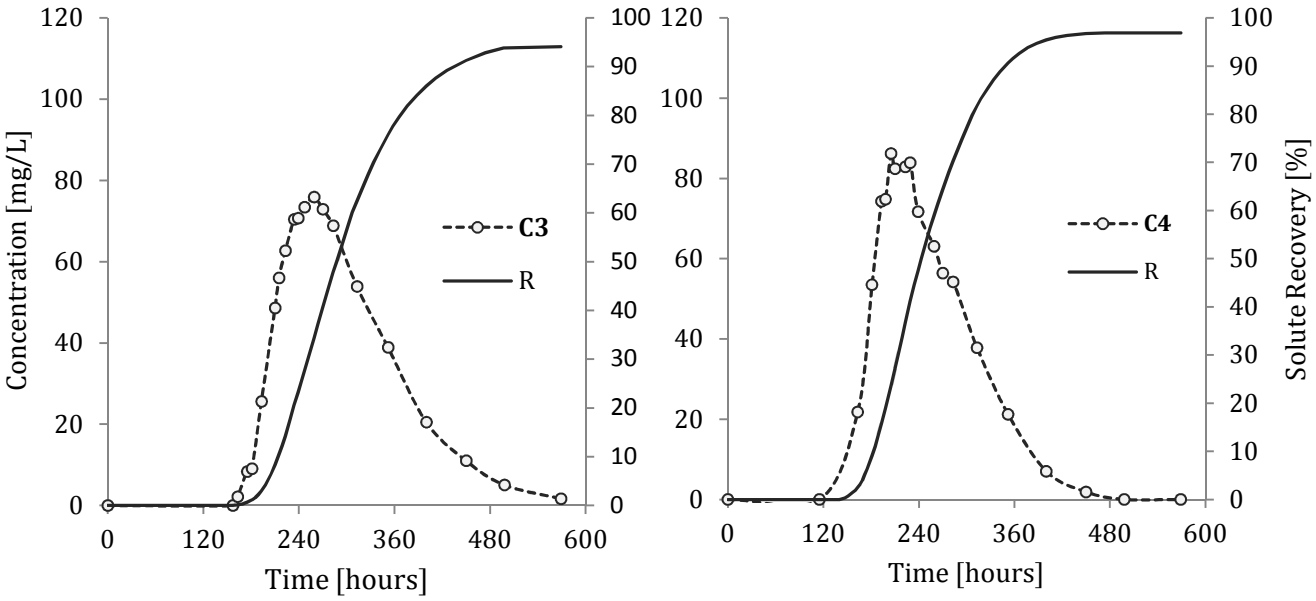


**Figure 4.12ff:** BTCs and solute recovery rates for planted wetland mesocosms containing homogeneous medium sand media; C3 (left) and C4 (right) = Concentration observations in planted sand filled mesocosms

C4 showed fastest reaction with first bromide being detected after 157 hours ($t_1$), followed by setups C1 and C2 with 163 hours. In setup C3 the first bromide signal appeared after 175 hours. Setup specific mean hydraulic retention times are wide spread. HRT was highest in setup C3 with 296 hours and lowest in C2 with 253 hours, followed by C4 (254 hours) respectively. C2 and C4 BTCs are characterized by a relatively short tailing compared to C1 and C2. In accordance to these findings, C3 showed highest peak attenuation potential showing maximum effluent Br concentrations of 75.90 mg/L, while highest maximum concentration was measured in C2 with 118.26 mg/L. Highest mean pore water velocities are reached in C2 followed by C4. Highest Br recovery was measured in C4 (96.91 %), the replicate containing a decaying plant. Lowest recovery was found in setup C2 (92.52 %), showing most vital plant development (see 4.2.1.). Replicates C2 and C3 however, showed mean recovery rates and were characterized by moderate plant development. Hydraulic parameters of the investigated mesocosm setups are summarized in ***Table 4.6***.

**Table 4.6:** Hydraulic parameters of VEG and NV setups derived from Br pulse injection observation; $t_1$ = first detection of solute in effluent; $t_P$ = time of peak concentration detection; $t_{50}$ = time of detection of 50 % injection mass in effluent; $v_{max}$ = maximum solute; $v_{mean}$ = mean solute velocity; $C_{max}$ = maximum concentration; $\tau$ = mean detention time; R = recovery; $\sigma^2$ = variation of tracer BTC.

| *setup* | $t_1$ *(h)* | $t_p$ *(h)* | $t_{50}$ *(h)* | $v_{max}$ *(m/h)* | $v_{mean}$ *(m/h)* |
|---|---|---|---|---|---|
| **VEG** | 101 | 223 | 298 | $5.00 * 10^{-3}$ | $1.69 * 10^{-3}$ |
| **NV** | 110 | 243 | 304 | $4.59 * 10^{-3}$ | $1.67 * 10^{-3}$ |
| **C1** | 163 | 215 | 254 | $3.53 * 10^{-3}$ | $2.67 * 10^{-3}$ |
| **C2** | 163 | 205 | 243 | $3.53 * 10^{-3}$ | $2.80 * 10^{-3}$ |
| **C3** | 175 | 259 | 279 | $3.29 * 10^{-3}$ | $2.51 * 10^{-3}$ |
| **C4** | 157 | 205 | 234 | $3.67 * 10^{-3}$ | $3.04 * 10^{-3}$ |

| *setup* | $C_{max}$ *(mg/L)* | $\tau$ *(h)* | *R (%)* | $\sigma^2$ *(h)* |
|---|---|---|---|---|
| **VEG** | 50.2 | 351.4 | 94.18 | $1.98 * 10^4$ |
| **NV** | 47.5 | 367.3 | 98.81 | $2.02 * 10^4$ |
| **C1*** | 90.60 | 271.7 | 93.28 | $4.99 * 10^3$ |
| **C2*** | 118.26 | 252.8 | 92.52 | $3.43 * 10^3$ |
| **C3*** | 75.90 | 295.8 | 94.13 | $4.92 * 10^3$ |
| **C4** | 86.21 | 253.8 | 96.91 | $3.60 * 10^3$ |

* Observations were ended before background bromide concentrations had returned to background (last measured Br concentrations: C1 = 2.1 mg/L; C2 = 1.25 mg/L; C3 = 1.65 mg/L); therefore R may be slightly underestimated in setups C1 – C3.

Higher $v_{max}$ but lower $v_{mean}$ in the setups VEG and NV co pared to C1 to C4 indicate the presence of channelled flow pathways besides highly dispersive matrix flow. The assumption is underlined by significantly higher residence times in VEG and NV compared the homogeneous sand filled setups.

### *4.3.2. Combined step injection of tracers and pesticides*

Constant step injection of the tracers UR and SRB and the two pesticides IPU and MTX was conducted in two mesocosm setups (VEG and NV). Injection was stopped after 35 days. Steady state conditions for UR were reached at least 10 days before ending the injection (***Figure 4.13***). Due to retardation processes, SRB concentrations did not reach steady state conditions throughout the observations. The spiked inflow water volume injected was 4.7 pore volumes in total. UR shows most rapid solute (pore water) movement trough the mesocosms, which is comparable to the ones calculated from $Br^-$ tracking. UR transport velocity was faster in the VEG setup than in the NV control ($v_{max}$ VEG $= 5.26 * 10^{-3}$ m/h, $v_{max}$ NV $= 4.28 * 10^{-3}$ m/h; $t_1$ VEG $= 96$ h; $t_1$ NV $= 118$ h). $v_{max}$ is likely to be under estimated in NV due lower sampling frequency compared to $Br^-$ tracking (5h versus 24 h). Even on steady state conditions, UR outflow concentrations of both mesocosm setups did not display inflow concentrations (10 µg/L). Relative maximum concentrations did not exceed 0.82 (***Table 15***), which indicates UR losses on transport pathways. First detection of SRB took approximately 200 hours, which is about double the time needed for UR first arrival. SRB transport in the VEG setup was slightly faster than in the NV control ($t_1$ VEG $= 192$ h, $t_1$ NV $= 204$ h). Though there is a significant difference between SRB maximum concentrations in VEG and NV setups, both systems returned to similar concentrations during tailing, once the injection was stopped. Peak attenuation potential for SRB underlines the important role of matrix-solute interactions in the NV setup. Without macropore flow, sorptive retardation of SRB is significantly higher than in the VEG setup. Characteristic parameters of tracer transport were calculated for each target compound comparing VEG setup and NV control after Lange et al. (2011) (***Table 4.7***). A method for residence time estimations for solutes from constant injection experiments was not found. Therefore, such parameters cannot be demonstrated here.

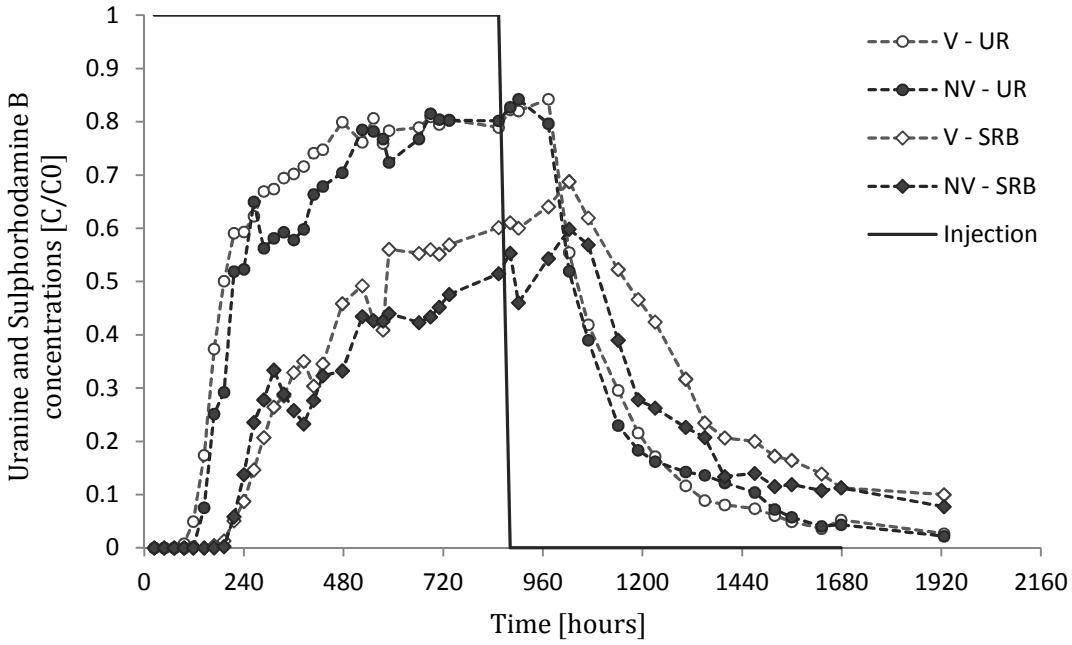


**Figure 4.13:** Uranine (UR) and Sulphorhodamine (SRB) BTCs for vegetated (V) and non-vegetated (NV) mesocosm setups (dotted lines) and injection time (solid blue line), σ (UR) = z *1.025 * $10^{-3}$ [C/C0], σ (SRB) = z * 1.010 * $10^{-3}$ [C/C0].

**Table 4.7:** Transport parameters for tracers and pesticides derived from combined step injection observations. $t_1$ = first detection of solute in effluent; $t_{C50}$ = time after 50 % of maximum solute concentration is detected in effluent; $v_{max}$ = maximum solute velocity; $C_{max}$ = maximum concentration; R = solute recovery.

**URANINE**

| *setup* | $t_1$ *(h)* | $t_{C50}$ *(h)* | $v_{max}$ *(m/h)* | $C_{max}$ *(C/C0)* | *R (%)* |
|---|---|---|---|---|---|
| **VEG** | 96 | 180 | 5.26 * $10^{-3}$ | 0.855 | 81.70 |
| **NV** | 118 | 204 | 4.28 * $10^{-3}$ | 0.845 | 78.55 |

**SULPHORHODAMINE B**

| *setup* | $t_1$ *(h)* | $t_{C50}$ *(h)* | $v_{max}$ *(m/h)* | $C_{max}$ *(C/C0)* | *R (%)** |
|---|---|---|---|---|---|
| **VEG** | 168 | 582 | 3.01 * $10^{-3}$ | 0.688 | 65.55 |
| **NV** | 192 | 750 | 2.63 * $10^{-3}$ | 0.598 | 55.91 |

R*: SRB BTCs were not observed entirely (see Figure 4.13).

Tracer concentrations detected in mesocosm effluent were converted into loads normalized by time. In the VEG setup higher load fluctuations of UR and SRB were observed than in the control (***Figures 4.14 and 4.15***). Recovered tracer masses of UR and SRB were higher in the vegetated system. Regarding UR, this effect is moderate, while SRB recovery in VEG setup exceeded the one of the control system by 10 % of injected mass. UR load recovery plots show differences in UR transport velocities during the first 15 days, roughly. When reaching the plateau establishment phase (240 h) the recovery offset between the two setups stays constant throughout the following 60 days of observation. (***Figure 4.14***). The differences in UR transport between planted and non-planted mesocosm setups obviously derive from fast flow components. In contrast, SRB recovery does not start individual development in the two mesocosms before the first 20 days of observation (480 h). During the following 60 days however, the difference between VEG and NV recovery constantly increases, pointing at intense sorptive SRB interactions in the NV setup, where macropore flow was not observed (***Figure 4.15***).

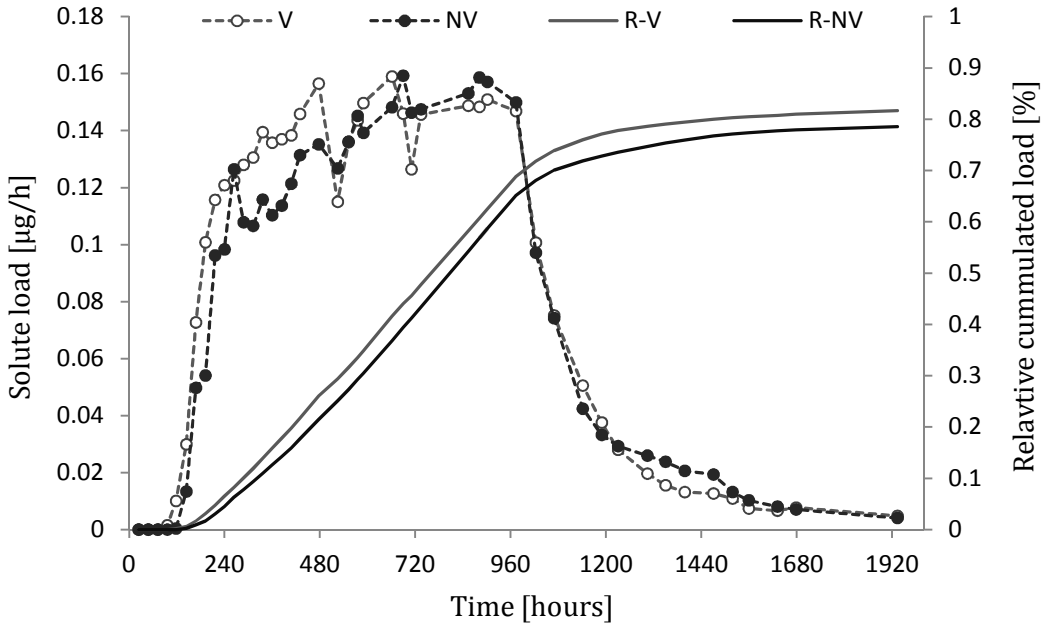


**Figure 4.14:** UR loads in VEG and NV mesocosm setups; dotted lines: relative solute load (load/Δt [µg/h]); solid lines: cumulated solute loads, errors negligible.

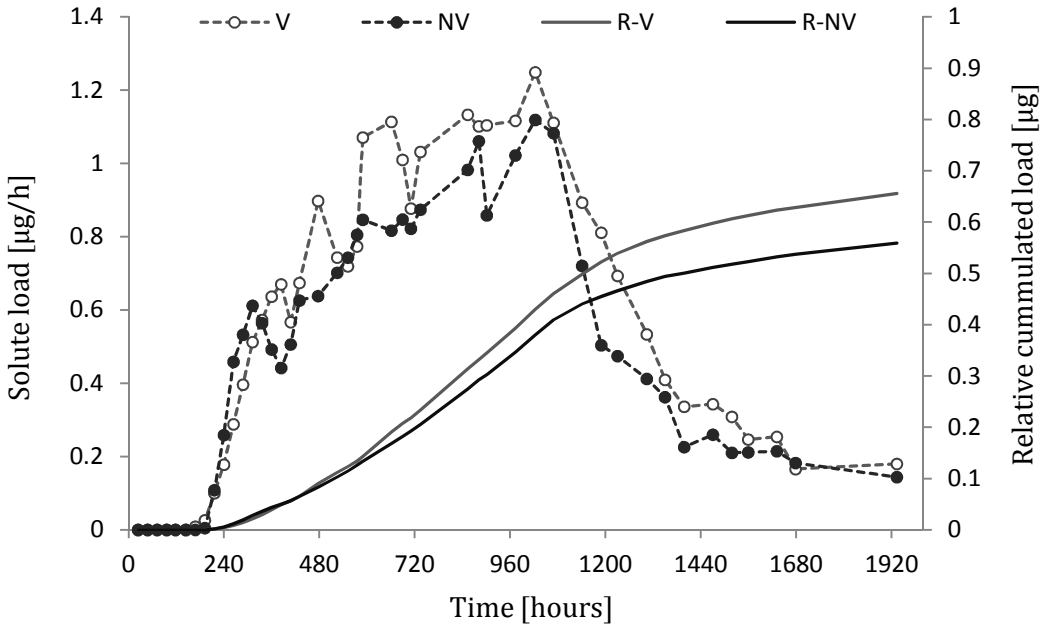


**Figure 4.15:** SRB loads in VEG and NV mesocosm setups; dotted lines: relative solute load (load/Δt [µg/h]); solid lines: cumulated solute loads, errors negligible.

## 4.4. Modelling solute transport parameters – CXTFIT

***Bromide.*** Tracer BTCs were modelled using the Convection Dispersion Equation Model implemented in the saturated solute transport software CXTFIT (Toride et al., 1999). Bromide pulse BTC was modelled applying the Equilibrium CDE, fitting crucial hydraulic parameters $v$ (average solute velocity [cm/h]) and $D$ (hydrodynamic dispersion coefficient [$cm^2/h$]) (***Figure 4.16***). No parameters were found to reproduce both, BTC tailing and peak shape in the VEG setup. For optimized simulation of the BTC, the first-order degradation parameter $\mu$ ($h^{-1}$) was fitted. Regarding observed recovery losses, the implementation of $\mu$ is adequate in case of the VEG setup (see ***Table 4.6***). Although the overall BTC shape and tailing are simulated properly, peak concentration is not reproduced accurately in this case (***Figure 4.16, left***). On the contrary, the bromide BTC of the NV setup was simulated with high accuracy of peak and tailing reproduction via the two parameters $v$ and $D$ (***Figure 4.16, right***). Assuming conservative transport, the retardation coefficient Rd was fixed to 1. Best fits revealed crucial hydraulic system parameters (***Table 4.8***), which were treated as distinct system hydraulic characteristics and served as fixed parameters for the fitting of UR and SRB BTCs.

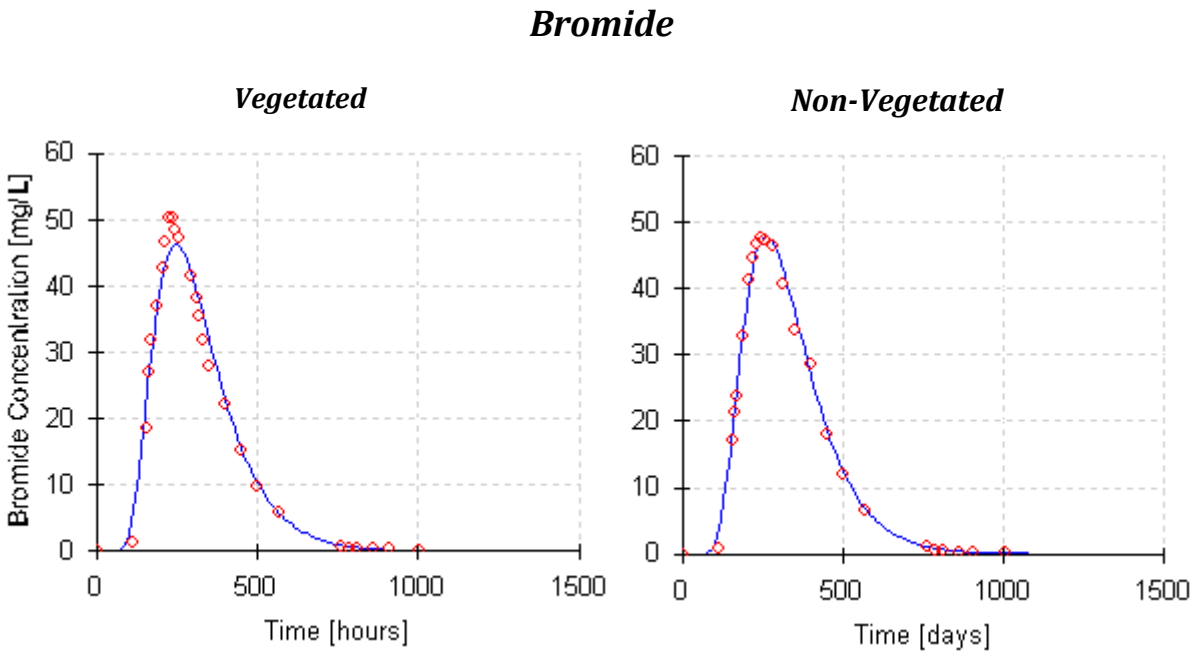


**Figure 4.16:** Observed and modelled Bromide BTCs in VEG and NV mesocosm setups applying the Equilibrium CDE in CXTFIT.

**Table 4.8:** Model parameters and model quality for Bromide BTC fitting with CXTFIT in VEG and NV setups; v = pore water velocity (m/h); D = dispersion ($m^2$/h); Rd = Retardation factor (-); μ = first-order degradation coefficient ($h^{-1}$); MSE = mean square error.

| *setup* | *model* | *v* | *D* | *Rd* | *μ* | *MSE* | $R^2$ |
|---|---|---|---|---|---|---|---|
| **VEG** | CDE | $1.61*10^{-3}$ | $6.57*10^{-5}$ | 1 | 0 | 5.197 | 0.986 |
| | Equ. | $1.61*10^{-3}$ | $6.57*10^{-5}$ | 1 | 2.56 E-4 | 4.408 | 0.987 |
| **NV** | CDE<br>Equ. | $1.53*10^{-3}$ | $5.99*10^{-5}$ | 1 | 0 | 1.677 | 0.995 |

Fitted pore water velocities corresponded well to the mean velocities calculated according to Lange et al. (2011):

| | Lange et al. (2011) | modelled |
|---|---|---|
| VEG | $1.69 * 10^{-3}$ | $1.61*10^{-3}$ |
| NV | $1.67 * 10^{-3}$ | $1.53*10^{-3}$ |

velocity [m/h]

***Uranine.*** UR concentration changes were not reproduced well applying the equilibrium CDE. Instead, the physical two-site non-equilibrium CDE was applied. This model approach implies parameters characterizing mobile an immobile liquid phase partitioning and phase specific degradation coefficients (Toride et al., 1999). Involved dimensionless parameters are the variable $\beta$, describing partitioning between mobile and immobile phases ($\theta_{im}/\theta_T$) and the parameter $\omega$, that represents mass transfer between those. UR tailings were reproduced well in both setups. (***Figure 4.17***). At the same time, modelled peak concentrations were over-estimated for the VEG setup, indicating a significant increasing concentration trend, before concentrations started decreasing. There is no evidence of such a strong trend in the observed data (***Figure***

***4.17, left***). However, the UR peak is reproduced better in the NV control mesocosm. Even if concentrations may be slightly under estimated in this case, modelled peak shape resembles observations (***Figure 4.17, right***). Concentration changes in both setups were not simulated accurately by the model without implementation of a dimensionless mobile phase degradation parameter ($\mu_1$) controlling concentration plateau levels. Assuming conservative transport and no retardation with respect to the salt tracer bromide, the variable $R$ was fixed to 1. Best fit parameters for UR concentration changes are summarized in ***Table 4.9***.

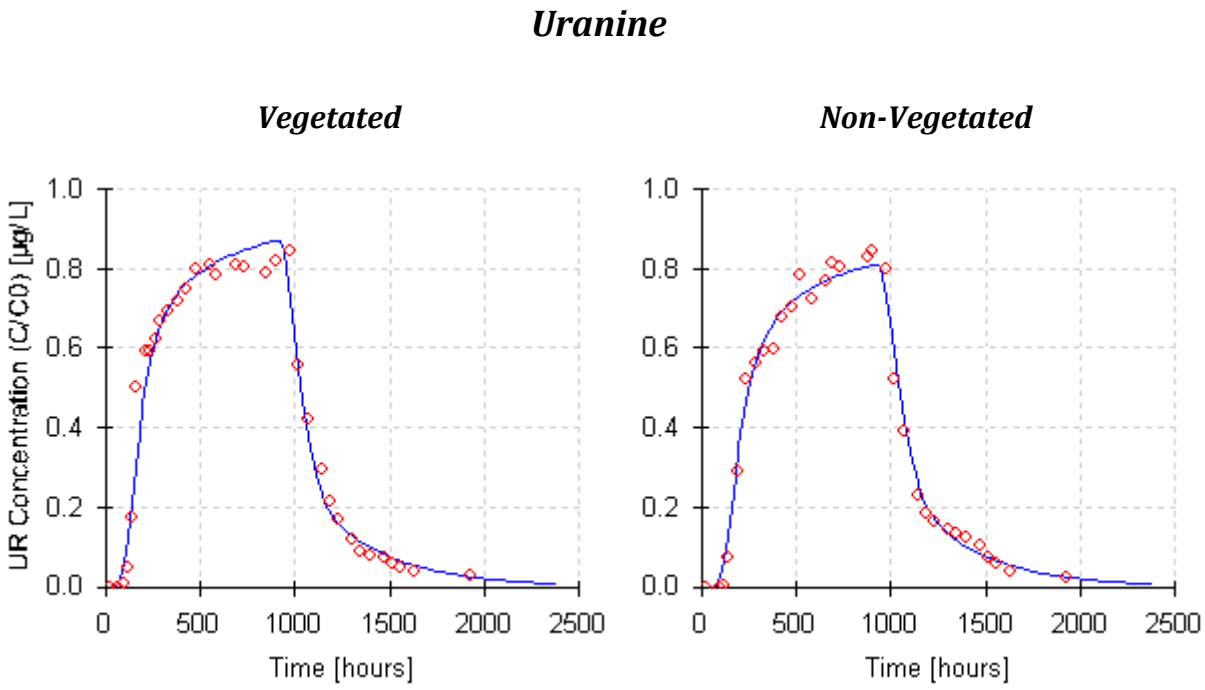


**Figure 4.17:** Observed and modelled UR concentrations in VEG and NV mesocosm setups applying the physical non-equilibrium CDE with CXTFIT.

**Table 4.9:** Model parameters and model quality for UR concentration fitting with CXTFIT in VEG and NV setups; *v* and *D* are adopted from Br fitting (Table 15); *Rd* = Retardation factor (-); $\beta$ = mobile – immobile partitioning variable ($\theta_m/\theta_T$); $\omega$ = mass transfer coefficient (-); $\mu_1$ = mobile phase degradation coefficient ($t^{-1}$); $\mu_2$ = immobile phase degradation coefficient ($t^{-1}$); *MSE* = mean square error.

| *setup* | *model* | *Rd* | $\beta$ | $\omega$ | $\mu_1$ | $\mu_2$ | *MSE* | $R^2$ |
|---|---|---|---|---|---|---|---|---|
| **VEG** | N-Eq. | 1 | 0.59 | 8.13 E$^{-3}$ | 0 | 0 | 4.00 E$^{-3}$ | 0.963 |
| | CDE | 1 | 0.62 | 6.67 E$^{-3}$ | 1.657 E$^{-3}$ | 0 | 2.30 E$^{-3}$ | 0.979 |
| **NV** | N-Eq | 1 | 0.59 | 9.79 E$^{-3}$ | 0 | 0 | 7.58 E$^{-3}$ | 0.926 |
| | CDE. | 1 | 0.59 | 9.79 E$^{-3}$ | 2.871E$^{-3}$ | 0 | 1.19 E$^{-3}$ | 0.989 |

***Sulphorhodamine B.*** Also for the simulation of SRB concentration changes, the equilibrium CDE was not adequate. SRB concentrations were best simulated applying the physical two-region non-equilibrium equation (***Figure 4.18***). Involved parameters were similar to the ones fit for UR concentration observations. To best fit the observations, a mobile phase first-order degradation coefficient was implemented. In case of SRB the retardation coefficient Rd was fit to reproduce observed retardation compared to bromide. Model quality was higher in case of the VEG system, because SRB maximum concentrations were under estimated for the NV setup by the model. (***Figure 4.18, right***). Best fit for the retardation coefficient (Rd) of SRB was nearly similar for both setups (VEG: 1.86, NV: 1.88). Modelled degradation coefficients for SRB are higher indicating stringer tracer loss effects than observed for for UR (see ***Table 4.10***). Phase partitioning variables are similar to the ones fitted for UR, mass transfer coefficients are higher. Based on the best fit for the retardation coefficient Rd, the soil-water partitioning coefficient $K_d$ for SRB was estimated according to ***Eq-15*** (Toride et al., 1999). Model parameters are summarized in ***Table 4.10***.

$$K_d = \frac{(Rd - 1) * \theta}{\rho_b} \qquad \textbf{Eq-15}$$

With $K_d$ = spoil water partitioning coefficient (ml/g), Rd = fitted retardation factor from model fitting (-), $\theta$ = reative pore volume (-) and $\rho_b$ = mean matrix bulk density (g/ml).

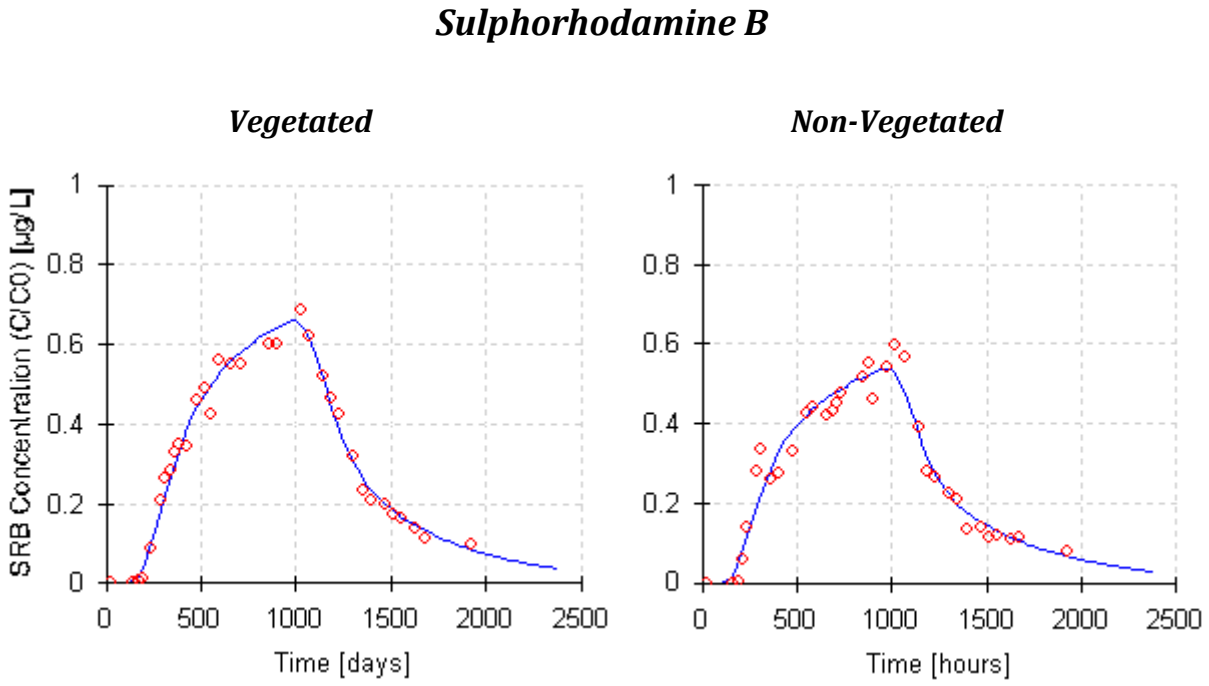


**Figure 4.18** Measured and modelled SRB concentrations in VEG and NV mesocosm setups applying the chemical non-equilibrium CDE with CXTFIT.

**Table 4.10:** Model parameters and model quality for SRB concentration fitting with CXTFIT in VEG and NV setups; $v$ and $D$ are adopted from Br fitting (Table 16); $Rd$ = Retardation factor (-); $\beta$ = partitioning variable ($\theta_m/\theta_T$); $\omega$ = mass transfer coefficient (-); $\mu_1$, $\mu_2$= mobile and immobile phase degradation coefficients ($t^{-1}$); $K_d$ = soil-water partitioning coefficient (ml/g); $MSE$ = mean square error.

| *setup* | *model* | *Rd* | *β* | *ω* | $\mu_1$ | $\mu_2$ | $K_d$ | *MSE* | $R^2$ |
|---|---|---|---|---|---|---|---|---|---|
| **VEG** | N-Eq. CDE | 1 | 1.00 E$^{-4}$ | 1.11 E$^{-1}$ | 0 | 0 | | 6.17 E$^{-2}$ | -0.409 |
| | | 1 | 1.00 E$^{-4}$ | 3.86 E$^{-1}$ | 9.948 E$^{-3}$ | 0 | | 2.07 E$^{-3}$ | 0.541 |
| | | 1.88 | 0.61 | 1.30 E$^{-2}$ | 4.964 E$^{-3}$ | 0 | 0.566 | 8.29 E$^{-4}$ | 0.982 |
| **NV** | N-Eq CDE | 1 | 1.00 E$^{-4}$ | 5.25 E$^{-2}$ | 0 | 0 | | 7.84 E$^{-2}$ | - |
| | | 1 | 8.78 E$^{-1}$ | 1.00 E$^{2}$ | 1.406 E$^{-2}$ | 0 | | 1.16 E$^{-2}$ | 0.672 |
| | | 1.86 | 0.57 | 1.42 E$^{-2}$ | 9.228 E$^{-3}$ | 0 | 0.554 | 1.94 E$^{-3}$ | 0.947 |

## 4.5. Particulate and sediment associated SRB

***SRB associated to suspended particles.*** The more sorptive dye tracer SRB was successfully desorbed from filter residues and detected by spectrometry. The more conservative dye tracer UR was not detected in any of the tested filters. While SRB signals could be identified on 10 of 11 tested filters of the vegetated setup, only 3 of 11 tested NV setup filters showed detectable SRB loads, respectively. Detected particle associated SRB loads from the VEG setup exceeded those in the control mesocosm by factor 10, roughly ($10^{-1}$ – $10^{-2}$ µg/h versus $10^{-3}$ – $10^{-4}$ µg/h) (***Figures 4.19 and 4.20***).

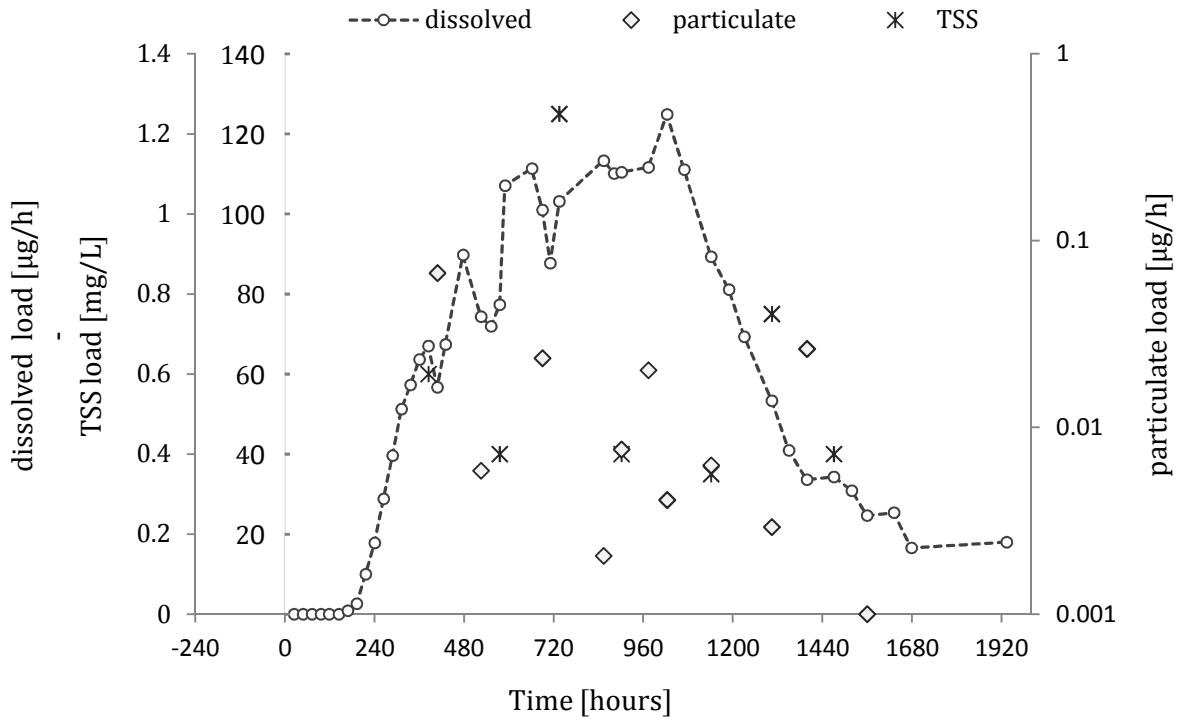


**Figure 4.19:** Punctual particle associated SRB measurements (particulate) and weekly TSS measurements compared to dissolved SRB loads in the vegetated mesocosm setup.

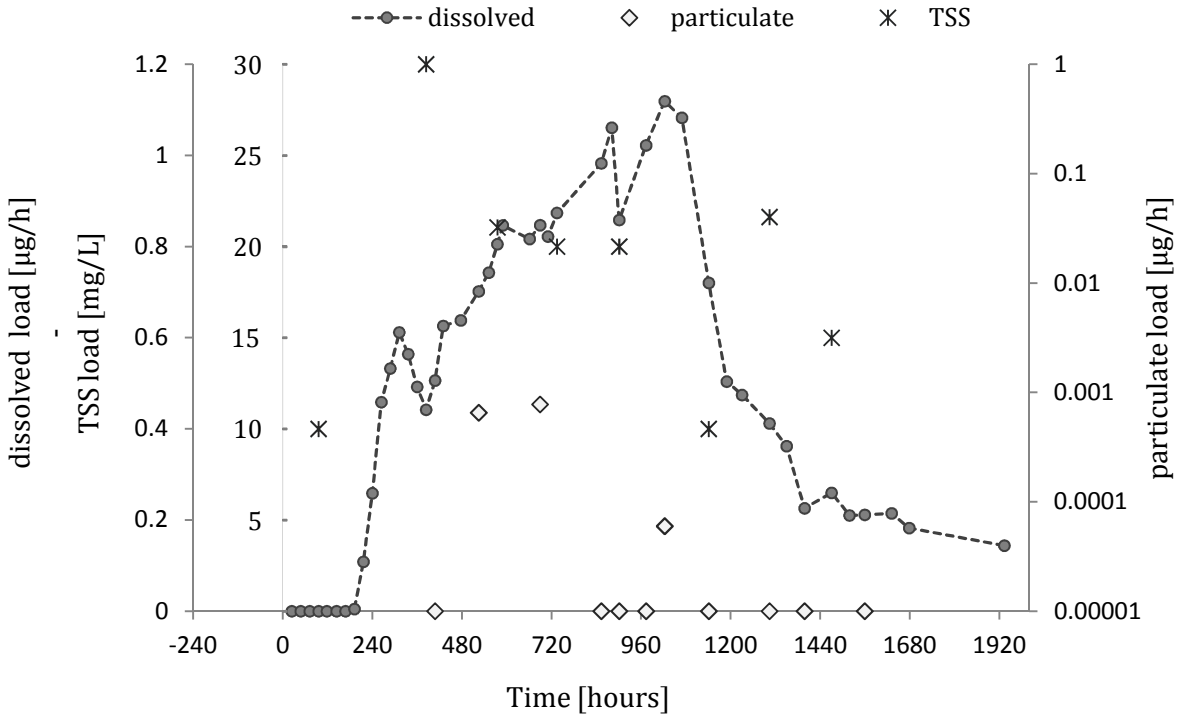


**Figure 4.20:** Punctual particle associated SRB measurements (particulate) and weekly TSS measurements compared to dissolved SRB loads in the non-vegetated mesocosm setup.

Even if the discrepancy of particle associated SRB loads between vegetated and non-vegetated setups seams to correspond to differences in TSS loads, no such mathematical correlation was found. Potentially important system variables, like dissolved SRB concentration, dissolved load, TOC, DOC and POC were tested on single linear correlation to particle associated SRB loads, but did not show any mathematical significance as well. Best results were reached for dissolved SRB load, but did not reach any level of statistical significance (VEG: $R^2 <$ -0.08; NV: $R^2 =$ -0.05). Besides, particle associated load observations could not be modeled by the application of multiple regression analysis of the mentioned independent variables. For both mesocosm setups, none of these variables showed statistical significance describing particle associated SRB load observations in any possible variable combination tested. Total particle associated fractions represented 0.18 – 11.82 % ($L_P/L_{diss}$) in the VEG setup and 0.07 – 0.09 % ($L_P/L_{diss}$) in the NV control, respectively.

***SRB associated to wetland mesocosm matrix.*** The fluorescent dye SRB was detected in wetland sediment layers of both setups. On the contrary, no SRB signals were found in upper and bottom sand layers of the two model systems. With a detected sediment associated SRB load of 0.081 µ/cm$^3$ wetland sediments in the NV setup showed more SRB trapping than the corresponding sediment of setup VEG (0.031 µg/cm$^3$). Background signals in the wetland sediment exceeded background of tested sand layer samples by factor 4. To illustrate the variability of interfering background signals depending on sediment characteristics (e.g. humic acid fractions), ***Table 4.11*** summarizes the measured backgrounds, concentrations and normalized loads of matrix layers.

**Table 4.11:** SRB loads detected in the mesocosm matrix; USa = upper sand layer; WS = wetland sediment layer; BSa = bottom sand layer; INT = spectrometric fluorescence intensity signal (-); $INT_P$ = SRB peak without background subtraction; $INT_b$ = background; $INT_{SRB}$ = ($INT_P$ – $INT_b$; $C_{SRB}$ SRB concentration; $L_{SRB}$ = SRB load.

| | ***layer*** | ***$INT_P$*** | ***$INT_b$*** | ***$INT_{SRB}$*** | ***$C_{SRB}$ (µg/L)*** | ***$L_{SRB}$ (µg/g)*** | ***$L_{SRB}$ (µg/cm³)*** |
|---|---|---|---|---|---|---|---|
| | USa | - | 10.11 | | | | |
| **VEG** | WS | 48.13 | 35 | 13.13 | 3.7872 | 0.0189 | **0.031** |
| | BSa | - | 13.9 | | | | |
| | USa | - | 12.35 | | | | |
| **NV** | WS | 72.24 | 40 | 32.24 | 9.706 | 0.049 | **0.081** |
| | BSa | - | 13.45 | | | | |

Based on a wetland sediment volume of 1420 cm$^3$ in the mesocosms and the wetland sediment bulk density, the total SRB mass adsorbed within these layers was calculated:

***VEG: 41.6 µg SRB*** ~2.5 % of injected mass

***NV: 108,7 µg SRB*** ~ 6.5 % of injected mass

# 5. Discussion

## 5.1. Biogeochemical development of the mesocoms

Eichstetten wetland mesocosm setups (VEG and NV) were characterized by strictly anaerobic conditions within naturally inoculated mesocosm layers and above (36.5 – 50.5 cm height). Sediments showed clear indicators for anaerobic microbial metabolism: 1) mackinawite formation, 2) development of gas enclosures within upper mesocosm layers, 3) production of hydrogen sulphide (detected by olfactory testing), deriving from microbial sulphate reduction. Mackinawite formation was observed only within the wetland sediment layer in the NV setup, but was diffusely spread within wetland sediment and upper sand layer in the VEG system. This observation indicates facilitated connectivity between wetland sediment layer and mesocosm surface caused by root development and root channels. The presence of Tubificidae though, caused notable macropore development (wormholes) in both setups. Wormholes were often surrounded by a thin layer of bright sediments, which gives evidence of local interference of wormholes with overall mineral redox stages. Transfer of dissolved $O_2$ via wormholes is unlikely, because no dissolved $O_2$ was measured within relevant upper sediment layers. Upper sand layers showed slight enrichment of OC fraction in both setups after the end of the experiment. Wetland sediment layer biofilms may have successively colonized upper sand layers in flow direction.

When uncovered, evaporation losses from open surface in NV unexpectedly exceeded the evapotranspiration losses in VEG. Surface shading by the plant reduced evaporation and superposed transpirative losses. After covering mesocosm surfaces however, the plant transpiration effect became clearly visible and NV effluent volume was globally higher than VEG discharge. Plant stress caused by the mesocosm cover (changing mesocosm atmospherical conditions) and by injection of the herbicide IPU correlated with high VEG system discharge at the beginning of combined tracer and pesticide observations (inhibited transpiration activity). After 25 days roughly, the plant had recovered from these stressing factors and effluent volume started decreasing successively due to increasing plant activity (transpiration).

Higher TSS loads in the VEG setup confirm the presence of macropores in the planted system. The NV system matrix very likely provides more intense mechanical pore water filtration services due to smaller pore diameters intensifying contact between solutes and matrix material. Observed mesocosm effluent nitrate losses compared to influent concentrations may be partially due to plant uptake in case of the VEG system, but may more likely be interpreted as an indicator for denitrifying bacterial metabolism (Krause et al. 2009; 2010).

## 5.2. Tracking of dissolved tracers

***Bromide tracking.*** Bromide recovery observations gave indication of notable plant uptake of bromide in vegetated wetland systems up to 6.6 % of injected mass. Such plant uptake of bromide by the common reed, *Phragmites australis,* as well as *Typha latifolia* was studied in wetland microcosms by Xu et al. (2004). Instead of chloride as an essential micronutrient, *P. australis* and *T. latifolia* were proven to take up significant quantities of $Br^-$, under $Cl^-/Br^-$ ratios of 2 (Xu et al., 2004). In this study, $Cl^-/Br^-$ ratios were even lower, ranging between 0.25 and 0.6 during peak concentrations, giving strong evidence of the connection between anion tracer recovery losses and uptake by *P. australis*. Xu et al. (2004) also revealed plant transpiration to significantly concentrate dissolved salt species in sediments of top-to-bottom flow systems. Nevertheless, plant effects seem to be restricted to interfere with recovery rates in the documented case, rather than affecting concentrations, which can be seen in similar UR concentration loads leaving VEG and NV setups. If there was significant concentration of tracers by the plant, we would expect the detection of significantly higher loads when macrophytes are present. There was evidence of fast transport pathways present in the VEG setup, which lead to higher pore water velocities and higher $Br^-$ $C_{max,}$. An explanation may be the presence of macropore flow along plant roots, which can be highly effective in channelling water and solutes (Beven & Germann, 1982; Harvey et al., 1995).

Bromide BTCs observed in the planted homogeneous sand filled mesocosms (CW Alteckendorf water and plants) revealed great variability of hydrological functioning from system to system. These variations may be interpreted as plant impacts on system macropore development on the one hand. The decaying plant in system C4 obviously

opened up high volume macropores resulting in facilitated water and solute transport. Indicators are comparably low HRT and high $C_{max}$. Bromide recovery rates show a negative correlation between plant health and $Br^-$ recovery, underlining plant assimilation effects observed in the VEG setup, as well. General sand filled mesocosm performance was characterized by higher HRT, lower $v_{max,}$ higher $v_{mean}$ and less spreading of BTCs around the mean residence time compared to setups containing wetland sediment. These observations may be due to a combined effect of macropore presence and higher dispersivity in wetland sediments of NV and VEG setups on the one hand and comparably low dispersivity effects (more coarse matrix) and heterogeneous preferential flow paths in setups C1 to C4 on the other hand. The presence of fine silty matrix material enhanced peak attenuation capacity of the tested mesocosm setups.

***Uranine.*** UR concentration plateaus did not reach influent concentration despite its assumed function as a conservative tracer substance. Maximum UR concentrations were quite similar between VEG and NV setups reaching 81.6 % of influent concentration in the VEG setup and 78.7 % in the control. Again there was indication of fast transport pathways channelling transport of water and solutes in the VEG system compared to the NV control ($v_{max}$ VEG $>$ $v_{max}$ NV, $t_1$ VEG $<$ $t_1$ NV). Higher fluctuations of UR concentrations and loads in the VEG setup indicate the presence of heterogeneous flow paths. With respect to high wetland sediment complexity in terms of sorption site availability and organic carbon availability and nature, the observations may more likely be indicators for irreversible sorption processes than biodegradation losses. Smart & Laidlaw (1977) revealed UR sorption losses to organic substrates (sawdust, humus) up to 89 % of initial dissolved concentrations ($C_{UR}$: 100 µg/L, $C_{Sediment}$: 20 g/L). Moderate UR sorption was also reported onto Bentonite substrate, which is characterized by high specific surface area and complex clay mineral composition (13 %, $C_{UR}$: 100 µg/L, $C_S$: 20 g/L; Smart & Laidlaw, 1977). There was no indication for plant uptake of UR.

***Sulphorhodamine B.*** For SRB no steady state conditions were observed within the given injection time of 35 days. Systems differed significantly in effluent concentration development with the VEG setup showing faster SRB appearance, faster increasing concentration trend and higher $C_{max}$. As expected, the tracer showed significant retardation against bromide and UR in both systems. Cumulated SRB loads showed an

offset between the two setups that increased during observation time. There is evidence of more intense contact between the tracer and mesocom matrix material in the NV setup, resulting in higher peak attenuation, lower $v_{mean}$ and higher recovery losses due to irreversible sorption processes. Unlike global pesticide sorption behaviour, SRB is more resistant to sorption onto organic substrates, but shows significant sorption losses to mineral phases of both, positive and negative overall charge (Smart & Laidlaw, 1977; Kasnavia et al., 1999; Sabatini et al., 2000). Regarding development of SRB loads recovered in mesocosm effluent, there is evidence of higher load fluctuations in the VEG setup than in the non-vegetated control mesocosm. This observation is suitable to the ones of UR transport underlining the presence of heterogeneous flow patterns in the VEG system. Significant plant uptake of SRB can be excluded from interpretation, because SRB concentrations and recovery were higher in the planted mesocosm.

***IPU and MTX.*** Concentration changes of the applied pesticides cannot be discussed here, as samples are currently being analyzed.

## 5.3. Model evaluation

The bromide concentration peak could not be simulated satisfactorily by the applied equilibrium CDE in case of the VEG setup, but was under estimated by the model. Besides slow matrix flow, there was fast macropore transport. These fast flow paths resulted in faster maximum velocity and sharper peak shape, which could not be reproduced congruently by the model. Still, model fits for pore water velocities derived from bromide BTC fitting do reproduce well the ones calculated according to Lange et al. (2011):

| | Lange et al. (2011) | modelled |
|---|---|---|
| VEG | $1.69 * 10^{-3}$ | $1.61*10^{-3}$ |
| NV | $1.67 * 10^{-3}$ | $1.53 *10^{-3}$ |

The two region physical non-equilibrium equation did satisfactorily fit UR observations for both setups, after the implementation of a mobile phase degradation coefficient $\mu_1$ ($t^{-1}$) in case of the VEG setup. Even though the model indicates degradation losses of UR, the degradation coefficient must more likely be treated as an indication for irreversible sorption. Because UR degradation has not been reported in literature so far, it is assumed to be negligible.

For reproduction of SRB concentration changes model quality was best, when fitting the physical two-region non-equilibrium equation, as well. For SRB simulation, a mobile phase first-order degradation coefficient was fitted to optimize the simulations in both, VEG and NV setup. From fitting of the retardation factor $R_d$, the soil-water partitioning coefficient could be calculated and represented analogue values of 0.566 ml/g in the VEG setup and 0.554 ml/g for the control mesocosm. Respecting mesocosm matrix OC fraction, the corresponding $K_{OC}$ values were calculated according to ***Eq-13*** (4.3.2.)and were 86.23 ml/g (NV) and 88.23 ml/g (VEG). SRB sorptive losses derived from modelling may be under estimated, when ignoring the fitted degradation coefficient $\mu_1$ ($t^{-1}$). Such as for UR, no indication for biodegradation of SRB is reported in literature so far. Model indicated degradation is interpreted as an additional sorption effect, assuming negligible biogeochemical degradation. The sorption losses indicated by μ cannot be quantified, because mean residence time of SRB is unknown.

The heterogeneous layering of the tested mesocosm setups cannot be displayed with CXTFIT, which assumes homogeneous flow in homogeneous media (Toride et al., 1999). We also know that mesocosm hydrology changed over time and did not resemble assumed stable conditions. These heterogeneities set limitations to the feasibility of CXTFIT, which revealed acceptable concentration simulations still. Different substrate specific processes influencing tracer and pesticide transport may be assessed by the application of more complex models, like HYDRUS (Simunek et al., 1998).

## 5.3. SRB associated to particles and sediments

***Particle associated SRB.*** Particle associated SRB could be detected in filter redidue samples from the wetland mesocosms. No correlation was found between relevant independent system variables and particle associated SRB loads, which could explain these observations. Tested variables were 1) dissolved concentration and 2) load, 3) TSS and 4) POC loads, 5) DOC and 6) TOC. Observations may not be explicable in the documented case, because the desorption efficiency of the applied desorption protocol according to Wernli (2009) has not been evaluated. Assuming desorption efficiencies, which go below 100 % and do not show systematic trends, particulate loads cannot be related to other milieu properties. A distinct calibration of the method should be done incorporating known particulate SRB loads and differing tracer dissolved concentrations to evaluate desorption efficiency and reproducibility of the method. Considering these uncertainties, measured absolute SRB loads need to be treated indicatively. Still, observations show that SRB partitioning between dissolved phase and particle associated fractions does occur in pore water and may be of high relevance depending on specific system properties, which cannot be identified so far. The presence of macropores is likely to facilitate particle associated SRB transport due to a reduction of mechanical filtration capacities of the overall matrix.

***SRB adsorbed to mesocosm sediments***.

Background signals of sediment desorption samples were generally higher than those measured in filter residue samples (VEG: 0.031 µg/g and NV: 0.081 µg/g). SRB was detected in wetland sediment layers of VEG and NV mesocosms only, which indicates favoured sorption to complex wetland sediment rather than sand and gravel media which are assumed to be dominated by negatively charged $SiO_2$. The fact, that higher associated loads were measured in the NV sample confirms the assumption that contact between tracers and particle surfaces was more intense in the non-planted mesocosm.

Total SRB mass adsorbed to wetland sediment was calculated as 2.5 % of total injected tracer mass in case of the VEG setup and 6.5 % in the NV control mesocosm. Even if SRB concentrations had not reached background concentrations when the observations were ended and assessed recovery rates are under estimated, the calculated adsorbed masses

are likely to be underestimated as well and cannot explain observed SRB recovery. This gives evidence of the improvement and evaluation of dye tracer desorption methods, mentioned above. When mesocosm layers were sampled on November 8, 2011 SRB dissolved concentrations in mesocosm effluent had not reached background concentrations, yet. The measured sediment SRB loads may therefore be overestimated due to interfering pore water SRB concentrations. This effect should be negligible, because SRB signals were detected in the upper sand layers at the same time however. Generally, to avoid these complications, tracer tracking observations should be conducted until system discharge has reached background concentrations again.

# 6. Conclusions and future work

Results from Bromide BTC observations in 5 planted and one non-planted wetland mesocosm setups gave evidence of plant uptake of the anion salt tracer resulting in recovery losses up to 6.56 % compared to the non-vegetated control. Recovery losses of the anionic dye tracer Uranine were more severe than the ones observed for bromide. The effect was stronger in the non-planted setup (NV: $R = 78.55$ %; VEG: $R = 81.7$ %) and UR mass losses were attributed to irreversible sorption processes onto organic matter and positively charged mineral matrix components. Assuming infinite sorption site availability, a sorptive competition between SRB and UR is unlikely because SRB is characterized by multiple functional groups. Its sorption is not restricted to positively charged surfaces only and does not show strong sorption tendencies to organic carbon, such as UR (Kasnavia, & Sabatini 1999; Sabatini, 2000).

While plant assimilation of UR and SRB by *P. australis* was not observed, the vegetation significantly facilitated SRB transport. Macropore flow along root channels resulted in lowered contact intensity between system matrix and SRB and significantly lowered the retention capacity of the system in case of the sorption-sensitive tracer.

Phase partitioning of Sulphorhodamie B was proven to occur under the tested experimental conditions, but could not be causally linked to dissolved SRB concentrations, TSS, POC or carbon species loads so far. In literature, there is a gap of sophisticated knowledge on process-driven evaluation methods including phase partitioning for sorbtive fluorescent dyes, such as the Rhodamine group. Future tracer hydrological scientific goals should include efficiency tests on existing dye tracer desorption protocols (Wernli, 2009; Lange & Leibundgut, 2007) for varying substrates, hydrochemical properties and dye concentrations. These efforts should be made with the aim to enhance process orientation of tracer hydrological science towards implementation of biogeochemical processes.

Dye tracer application as a model for pesticide fate in SSF wetlands can only serve as a model tool for pesticides and pesticide groups that show compound specific mobility and persistence in SSF systems, which are comparable to the ones of the fluorescent dye tracers. Biodegradation and plant assimilation of pesticides may occur and can have severe impact on transport behavior and mitigation. While these processes are assumed to be negligible in case of UR and SRB, they can be essential for pesticide transport, such

as anaerobic biodegradation in case of MTX (Massoud, 2008). Based on pesticide categories defined by De Wilde et al. (2007), UR ($K_{OC}$ of 0 to 62 ml/g; based on Sabatini, 2000) could serve as a proxy for the persistent mobile pesticides under light exclusion. Such contaminants are characterized by low $K_{OC}$ and high $DT_{50}$ like the herbicides Lenacil ($K_{OC}$ = 34 ml/g, $DT50_{soil}$ = 179 d) or the generally mobile insecticides, for example. In contrast, SRB ($K_{OC}$ vaules of 187 to 498 ml/g; based on Sabatini, 2000) may be applied as an indicator for immobile persistent pesticides, which are characterized by moderate $K_{OC}$ values and relatively long half life under SSF conditions. Such substance would be the applied phenylurea herbicide IPU for example, which is resistant to biodegradation in anaerobic environments and shows moderate $K_{OC}$ of 36 – 241 ml/g (European Commission, 2002). Fluorescent dyes may not be adequate to estimate the fate of the applied fungicide MTX, however, because it is subject to biodegradation under anaerobic conditions (Haarstad & Braskerud; 2003, Massoud, 2008).

Comparative tests on most frequently applied pesticide groups and crucial individual components need to be conducted to draw patterns of feasibility of the reference tracer approach in both, SF and SSF wetland systems. Strong OC sorption dependence of pesticides and rather low OC dependence of the tracers have to be taken into account under variable substrate conditions. Tested wetland systems were characterized by low flow rates, high biological activity and complex sorption site availability (heterogeneous layering, fine particles, high clay fraction, OC fraction). Regarding observed non-conservative behavior of bromide and UR, such environments resemble highly complex study sites for tracer hydrology and site specific pedological, biogeochemical and hydrochemical properties need to be taken into account for adequate evaluation and interpretation. These efforts should be made, as the reference tracer approach poses great chances for both, scientific proceeding in tracer hydrology and the development of a cost-effective and environmentally harmless tool for environmental engineering.

# URLS:

***Umweltbundesamt Germany online***, accessed 20.06.2011:
http://www.umweltdaten.de/wasser/themen/stoffhaushalt/isoproturon.pdf

***PPDB Pesticide Properties online DataBase***, University of Herfordshire (2009), accessed 20.06.2011:
http://sitem.herts.ac.uk/aeru/projects/ppdb/index/htm

***Alan Wood online***, Compedium of Pesticide Common Names, accessed 21.06.2011:
http://www.alanwood.net/pesticides/metalaxyl.html
http://www.alanwood.net/pesticides/isoproturon.html

***TCI Europe online***, accessed 21.06.2011:
http://www.tcieurope.eu/fr/catalog/F0096.html

***Sigmaaldrich online***, accessed 21.06.2011:
http://sigmaaldrich.com/catalog/ProductDetail.do?D7

***USDA United States Department of Agriculture***, Natural Resources Conservation Service, accessed 03.07.2011:
http://plants.usda.gov/java/profile?symbol=PHAU7

***Biolflor online***, database of biological-ecological characteristics of German Flora, a UFZ (Helmholtz Zentrum für Umweltforschung) and BfN (Bundesamt für Naturschutz Deutschland) project, accessed 03.07.2011:
http://www.ufz.de/biolflor/taxonomie/

***Floraweb***, floral database of Bundesamt für Naturschutz Germany, accessed 03.07.2011:
http://floraweb.de/pflanzenarten/artenhome

# Literature

Alletto, L., Coquet, Y., Benoit, P., Bergheaud, V. (2006): Effects of temperature and Water content on degradation of isoproturon in three soil profiles. Chemosphere, Vol. 64, P. 1053 – 1061.

Amondham, W., Parkpian, P., Polprasert, C., Delaune, R. D., Jugsujinda, A. (2006): Paraquat adsorption, degradation and remobilization in tropical soils of Thailand. Journal of Environmental Science and Health, Vol. 41, P. 485 – 507.

Atkinson, T. C., Bukoviecki, A. A. (2000): Sorption of fuorobenzinic acids on peat and kaolinite. In: Tracers and Modelling in Hydrogeology. IAHS Press, Wellingford, UK (2000).

ArtWet 2006 – 2010: ArtWet Technical Guide, mitigation of agricultural non-point source pesticides pollution and bioremediation in artificial wetland ecosystems – LIFE 06 ENV/F/000133.

Barth, J. A. C., Grathwohl, P., Fowler, H. J., Bellin, A., Gerzabek, M. H., Lair, G. J., Barcelo, D., Petrovic, M., Navarro, A., Négrel, Ph., Petelet-Giraud, E., Darmendrail, D., Rijnaarts, H., Langenhoff, A., De Weert, J. Slob, A., van der Zaan, B. M., Gerritse, J., Frank, E., Gutierrez, A., Kretzschmar, R., Gocht, T. Steidle, D., Garrido, F., Jones, K. C., Meijler, S., Moeckel, C., Marsman, A., Klaver, G., Vogel, T., Buerger, C., Kolditz, O., Broers, H. P., Baran, N., Jozirasse, J., Von Tuempling, W., Van Gaans, P., Merly, C., Chapman, A., Brouyère, S., Batlle Aguilar, J., Orban, Ph., Tas, N., Smidt, H. (2009): Mobility Turnover and Storage of Pollutants in Soils, Sediments and Waters: Achievements and Results of the EU Project AquaTerra – A Review. Sustainable Agriculture, Springer Scienecand Business Media B. V., 2009.

Bending, G. D., Lincoln, S. D., Sorensen, S. R., Morgan, J. A. W., Amand, J., Walker, A. (2003): In-Field Spatial Variability in the Degradation of the Phenyl-Urea Herbicide is the Result of Interactions between degradative *Sphingomonas ssp.* and pH. Applied and Environmental Microbiology, Vol. 69, Nr. 2, P. 827 – 834.

Besien, T. J., Williams, R. J., Johnson, A. C. (2000): The transport and behaviour of isoproturon in unsaturated chalk cores. Journal of Contaminant Hydrology, Vol. 43, P. 91 – 110.

Beven, K., Germann, P. (1982): Macropores and water flow in soils. Water Resources Research, Vol. 18, Nr 5, P. 1311 – 1325.

Birkholz, A. (2007): Bewertung von Verfahren der Sickerwasser- und Transportprognose von Schadstoffen. Diploma Thesis at the Institute of Hydrology, University of Freiburg.

Bouldin, J. L., Farris, J. L., Moore, M. T., Smith Jr., S., Stephens, W. W., Cooper, C. M.. (2005): Evaluated fate and effects of Athrazine and Lambda-Cyhalothrin in vegetated and unvegetated Microcosms. Wiley Periodicals, 2005.

Clapp, R. B., Hornberger, G. M. (1978): Empirical equations for some soil hydraulic properties. Water Resources Research, Vol. 14, P. 601-604.

Clark, W. A., Konhauser, K. O., Thomas, J. C., Bottrell, S. H. (1997): Ferric hydroxide and ferric hydroxysulphate precipitation by bacteria in an acid mine drainage lagoon. FEMS Microbiology Reviews, Vol. 20, P. 351 – 361.

Collado, R. Schmelz, R. M. (2001): Oligochaet distribution patterns in two German hardwater lakes of different trophic state. Limnologia, Vol. 31, P. 317 – 328.

Craft, C. B. (1997): Dynamics of nitrogen and phosphorous retention during wetland ecosystem succession. Wetlands Ecology and Management, Vol. 4, P. 177 – 187.

De Sutter, T. M., Clay, S. A., Clay, D. E. (2003): Atrazine sorption and desorption as affected by aggregate size, particle size and soil type. Weed Science, Vol. 51, P. 456 – 462.

De Wilde, T., Mertens, J., Sphanoghe, P., Ryckeboer, J., Springael, D. (2007): Sorption kinetics and its effects on retention and leaching. Chemosphere, Vol., 72, P. 29 – 32.

De Wilde, T., Mertens, J., Simunek, J., Sniegowski, K., Ryckeboer, J., Jaecken, P., Springael, D., Spanoghe, P. (2009a): Characterizing pesticide sorption and degradation in microscale biopurification systems using column displacement experiments. Environmental Pollution, Vol. 157, P. 463 – 473.

De Wilde, T., Spanoghe, P., Ryckeboer, J., Jaeken, P., Springael, D. (2009b): Sorption characteristics of pesticides on matrix substances used in biopurification systems. Chemosphere, Vol. 75, P. 100 – 108.

Doyle, R. W. (1968): Identifocation and Solubility of Iron sulfide in anaerobic lake sediment. American Journal of Science. Vol. 260, Nr. 10, P. 980 – 994.

Dvorak, D. H., Hedin, R. S., Edenborn, H. M., McIntire, P. E. (1992): Treatment of Metal Contaminated Water Using Bacterial Sulfate Reduction: Results from Pilot-Scale Reactors. Biotechnology and Bioengineering, Vol. 40, P. 609 – 616.

European Commission, Health and Consumer Protection Directorate-General (2002): Review Report for the active Substance Isoproturon, SANCO/3045/99-final.

European Commission, Health and Consumer Protection Directorate-General (2010): Review Report for the active Substance Metalaxil, SANCO/10476/2010-rev1.

Fetter, C. W. (1994).Applied Hydrogeology, 3rd edition. Upper Saddle River, NJ Prentice Hall, Inc.

Freeze, R. Allen and Cherry, John A. (1979): Groundwater. Englewood Cliffs, NJ Prentice-Hall Inc.

Gao, J. P., Maguhn, J., Spitzauer, P. Kettrup, A. (1998 a): Sorption of pesticides in the sediment of the Teufelsweiher pond (Southern Germany). I: Equilibrium Assessments, Effect of Organic Carbon Content and pH. Water Research, Vol. 32, Nr. 5, P. 1662 – 1672.

Gao, J. P., Maguhn, J., Spitzauer, P. Kettrup, A. (1998 b): Sorption of pesticides in the sediment of the Teufelsweiher pond (Southern Germany). II: Competitive Adsorption, Desorption of Aged Residues and Effect od Dissolved Organic Carbon. Water Research, Vol. 32, Nr. 7, P. 2089 – 2094.

Gaspar, E. (1987): Hydrological Tracers. In: Modern Trends in Tracer Hydrology, Vol 1, P 2 – 43. CRC Press Inc., Boca Raton, Florida.

Gassmann, M. (2007): Measuring and modeling erosion and suspended sediment. Diploma Thesis at the Institite of Hydrology, University of Freiburg.

Gaultier, J., Fahrenhorst, A., Kim, S. M., Saiyed, I., Messing, P. Cessna, A. J., Glozier, N. E. (2009): Sorption – Desorption of 2-4-Dichlorophenoxyacetic Acid by wetland sediments. Wetlands, Vol. 29, Nr. 3, P. 837 – 844.

Gregoire, C., Elsaesser, D., Huguenot, D., Lange, J., Lebeau, T., Merli, A., Mode, R., Passeport, E., Payraudeau, S., Schütz, T., Schulz, R., Tapia-Padilla, G., Tournebize, J., Trevisan, M., Wanko, A. (2008): Mitigation of agricultural non-point source pesticide pollution in in artificial wetland ecosystems. Environmental Chemistry Letters, Vol., 7, Nr 3, P. 205 – 231.

Haarstad, K., Braskerud, B. C. (2003): Pesticide retention in the watershed and in a small constructed wetland treating diffuse pollution. Poster Papers, Diffuse Pollution Conference, Dublin 2003.

Hachmann, J. (2008): Messung von Trübungs- und Sedimentdynamik in einer künstlichen Feuchtfläche, Bachelor Thesis at Institute of Hydrology, University of Freiburg.

Haider, S. (1991): Durchflussmessung in Abwasserkanälen mittels Fluoreszenztracern. Diploma Thesis, printed. University of Vienna.

Harvey, J. W., Chambers, R. M., Hoelscher, J. R. (1995): Preferencial Flow and Segregation of Pore Water Solutes in Wetland Sediments. Estuaries, Vol. 18, Nr 4, P. 568 – 578.

Imfeld, G., Aragonés, C. E., Zeiger, S., Vitzthum von Eckstädt, C., Paschke, H., Trabitzsch, R., Weiss, H., Richnow, H. H. (2008): Tracking in situ Biodegradation of 1,2-Dichloroethenes in a Model Wetland. Environmental Science and Technology, Vol. 42, P. 7924 – 7930.

Imfeld, G., Braeckevelt, M., Kuschk, P., Richow, H.-P. (2009): Monitoring and assessing processes of organic chemicals removal in constructed wetlands. Chemosphere, Vol., 74, P. 349 – 362.

Kadlec, R. H. (1992): Hydrological factors in wetland water treatment. In: Constructed Wetlands for Watewater Treatment: Municipal, Industrial and Agricultural. D.A. Hammer (Ed.), Lewis Publishers Chelsea, MI – USA.

Kadlec, R. H. (1994): Detention and mixing in free water wetlands. Ecological Engineering, Vol. 3, P. 345 – 380.

Kamra, S. K., Lennartz, B., Van Genuchten, M. T., Widmoser, P. (2001): Evaluating non-

equilibrium solute transport in small sand columns. Journal of Contaminant Hydrology, Vol. 48, P. 189 – 212.

Käss, W. (2004): Geohydrologische Markierungstechnik – Lehrbuch der Hydrologie, Band 9, 2. überarbeitete Auflage. Gebrueder Borntraeger, Berlin Stuttgart.

Kasnavia, T., Vu, D. Sabatini, A. (1999): Fluorescent Dye and Media Properties affecting Sorption and Tracer Selection. Goound Water, Vol. 37, Nr. 3, P. 376 – 381.

Kidmose, J. Dahl, M., Engesgaard, P., Nilsson, B., Christensen, B. S. B., Andersen, S., Hoffmann, C.C. (2010): Experimental and numerical study on the fate of a pesticide in a riparian wetland. Journal of Hydrology, Vol. 386, P. 67 – 79.

Kottec, M., Grieser, J., Beck, C., Rudolf, B., Rubel, F. (2006): World Map of the Köppen-Geiger classification updated. Meteorologische Zeitschrift, Vol. 15, P. 259 – 263. online version: http://koeppen-geiger.vu-wien.ac.at/present.htm.

Krause, S., Hannah, D. M., Fleckenstein, J. H., Heppel, C. M., Kaeser, D., Pickup, R., Pinay, G., Robertson, A. L., Wood, P. J. (2010): Inter-disciplinary perspectives on processes in the hyporheic zone. Ecohydrology, DOI: 10.1002/eco.176. Wiley online library 2010.

Krause, S., Haethwaite, L., Binley, A., Kennan, P. (2009): Nitrate concentration changes at the groundwater – surface water interface of small Cumbrian river. Hydrological Processes, Vol. 23, S. 2195 – 2211.

Lange J., Leibundgut, C. (1997): Floodwater Alluvium Relations. Final Report Nr. 75, Institute of Hydrology, University of Freiburg - Germany.

Lange, J., Schütz, T., Gregoire, C., Elsässer, D., Schulz, R., Passeport, E., Tournebize, J. (2011): Multi-tracer experiments to characterize contaminant mitigation capacities for different types of artificial wetlands. International Journal of Environmental Analytical Chemistry, Vol. 91, Issue 7 – 8, P. 768 – 785.

Larsen, L., Aamand, J. (2001): Degradation of Herbicides in two sandy aquifers under different redox conditions. Chemosphere, Vol. 44, P. 231 – 236.

Leibundgut, C., Maloszewski, P. Kuells, C. (2009): Tracers in Hydrology. Wiley – Blackwell, John Wiley & Sons.

Lenda, A., Zuber, A. (1970): Tracer dispersion in groundwater experiments. Isotope Hydrology, IAEA, Vienna, P. 619 – 641.

Lewis, J., Sjöstrom, J. (2010): Optimizing the experimental design of soil columns in saturated and unsaturated transport experiments. Journal of Contaminant Hydrology, Vol. 115, Issues 1 – 4, P. 1 – 13.

LfUG Sachsen (1997): Materialien zur Altlastenbewertung Nr. 4/97: Simulation von

Grundwasserströmungs- und Transportprozessenim Rahmen der Altlastenbehandlung (Lockergestein, Festgestein und ungesättigte Zone), Landesamt für Umwelt und Geologie Sachsen.

Maillard, E. Payraudeau, S., Faivre, E., Gregoire, C., Gangloff, S., Imfeld, G. (2011): Removal of pesticide mixtures in a storm water wetland collecting runoff from a vineyard catchment. Science of the Total Environment, Vol. 409, P. 20317 – 2324.

Mao, M. Ren. L. (2004): Simulating Nonequilibrium Transport of Atrazine through Saturated Soil. Ground Water, Vol. 42, No 4, P. 500 – 508.

Margoum, C., Malessard, C., Gouy, V. (2006): Investigations on various physicochemical parameter influence on pesticide sorption to ditch bed substratum by means of experimental design. Chemosphere, Vol. 63, P. 1835 – 1841.

Marius, M., Stringfellow, A., Smallman, D., Atkinson, D. (2010): Fluorescent Tracers – A Tool for Landfill Investigation and Management. In: Waste 2010 Conference, Stratford (2010).

Massoud, A. H., Derbalah, A. S., Belal, E.-S. B. (2008): Microbial detoxification of metalaxyl in aquatic system. Journal of Environmental Sciences, Vol. 20, Issue 3, P. 262 – 267.

Matson, P. A., Parton, W. J., Power, A. G., Swift, M. J. (1997): Agricultural Intensification and Ecosystem Properties. Science, Vol. 277, P. 506 – 509.

Passeport, E., Tournebize, J., Jankowski, S., Prömse, B., Chaumont, C., Coquet, Y., Lange, J. (2010): Artificial Wetland and Forest Buffer Zone: Hydraulic and Tracer Characterization. Vadose Zone Journal, Vol. 9, P. 73 – 84.

Pliwitschkies, J. (2009): Tracerhydrologische Untersuchung der Sorption an Vegetation eines künstlichen Fließgewässers. Diploma Thesis, Institute of Hydrology, University of Freiburg 2009.

Prochaska, C. A., Zouboulis (2006): Removal of phosphates by pilot-vertical flow constructed wetlands using a mixture of sand and dolomite as substrate. Ecological Engineering, Vol. 26, P. 293 – 303.

Prochaska, C. A., Zouboulis, A. I. Eskridge, K. M. (2007): Performance of pilot-scale vertical flow constructed wetlands as affected by season, substrate, hydraulic load and frequency of application of simulated urban sewage. Ecological Engineering, Vol. 31, P. 57 – 66.

Rodgers Jr., J. H., Dunn, A. (1992): Developing design guidelines for constructed wetlands to remove pesticides from agricultural runoff. Ecological Engineering, Vol. 1, P. 83 – 95.

Rodríguez-Cruz, M. S., Ordax, J. M., Arienzo, M., Sánchez-Martín, M. J. (2011): Enhanced retention of linuron, alachlor and metalaxyl in sandy soil columns intercalated with wooden barriers. Chemosphere, Vol. 82, P. 1415 – 1421.

Sabatini, D. A. & Austin, T. A. (1991): Characteristics of Rhodamine WT and Fluorescein as adsorbing ground water tracers. Ground Water, Vol. 29, Nr 3, P. 341 – 349.

Sabatini, D. A. (2000): Sorption and Intraparticle Diffusion of Fluorescent Dyes with

Consolidated Aquifer Media. Ground Water, Vol. 38, Nr. 5, P. 651 – 656.

Schulz, R., Hahn, C., Bennett, E. R., Dabrowski, J. M., Thiere, G., Peall, S. K. C. (2003): fate and effects of Azinphos-Methyl in a Flow-Through Wetland in South Africa. Environmental Science and Technologie, Vol. 37, P. 2139 – 2144.

Schulz, R. (2004): Field studies on exposure, effects and risk mitigation of aquatic nonpoint source insecticide pollution – a Review. Journal of Environmental Quality, Vol. 33, P. 419 – 448.

Seaman, J. C., Bertsch, P. M., Miller, W. P. (1995): Ionic Tracer Movement through highly weathered Sediments. Journal of Contaminant Hydrology, Vol. 20, P. 127 – 143.

Seaman, J. C., Bertsch, P. M., Korom, S. F., Miller, W. P. (1996): Physicochemical Controls on non-conservative Anion Migration in coarse textured alluvial sediments. Ground Water, Vol. 34, P. 778 – 783.

Seaman, J. C., Majs, F., Singer, Aburime, S., Dennis, S. O., Wilson, M., Bertsch, P. M. (2007): Analysis of Tracer Migration in a Diverging Radial Flow Wetland. Proceedings of the Georgia Water Resources Conference 2007, University of Georgia.

Sentenac, P., Lynch, R. J., Bolton, M. (2001): Measurement of side-wall permeability effect in soil columns using fibre-optics sensing. International Journal of Physical Modeling in Geotechnics, Vol. 1, Nr 4, P. 35 – 41.

Si, Y., Wang, M., Tian, C., Zhou, J., Zhou, D. (2011): Effect of Charcoal Amendment on Adsorption, Leaching and Degradadtion of Isoproturon in soils. Journal of Contaminant Hydrology, Vol. 123, P. 75 – 81.

Simunek, J. K., Huang, J. K., van Genuchten, M. T. (1998): The HYDRUS-code for simulation 1-dimensional movement of water, heat and multiple solutes in variably saturated media, Version 6.0. Research Report Nr. 144, US Salinity Laboratory, USDA, ARS, Riverside, California, pp. 164.

Smart, P. L. & Laidlaw, I. M. S. (1977): An evaluation of some fluorescent dyes used for water tracing. Water Resources Research, Vol. 13, No. 1, P. 15 – 33.

Sorensen, S. R., Aamand, J. (2003): Rapid Mineralization of of the herbicide Isoproturon in soil from a previously treated Danish agricultural field. Pesticide Management Science, Vol. 59, P. 1118 – 1124.

Sorensen, S. R., Bending, G. D., Jacobsen, C. S., Walker, A., Aamand, J. (2003): Microbial Degradation of Isoproturon and related Phenylurea Herbicides in and below agricultural fields. Federation of European Microbiological Societies, Microbiology Ecology, Vol. 45, P. 1 – 11.

Stearman, K. George, D. B., Carlson, K., Lansford, S. (2003): Pesticide Removal from

Container Nursery Runoff in Constructed Wetlands. Journal of Environmental Quality, Vol. 31, P. 1548 – 1556.

Stehle, S., Elsaesser, D., Gregoire, C., Imfeld, G., Niehaus, E., Passeport, E., Payraudeau, S., Schäfer,R., Tournebize, J., Schulz, R. (2011): Pesticide Risk Mitigation by Vegetated Treatment Systems: A Meta-Analysis. Journal of Environmental Quality, Vol. 40, P. 1068 – 1080.

Susarla, S., Medina,V. F., McCutcheon, S. C. (2002): Phytoremediation: An Ecological Solution to organic chemical contamination. Ecological Engineering, Vol. 18, P. 647 – 658.

Tilman, D., Fargione, J., Wolff, B., D'Antonio, C., Dobson, A., Howarth, R., Schindler, D., Schlesinger, W.H., Simberloff, D., Swackhamer, D. (2001): Forecasting agriculturally global environmental change. Science, Vol. 292, P. 281 – 284.

Toride, N., Leij, F. J., Van Genuchten, M. Th. (1999): The CXTFIT Code for Estimating Transport Parameters from Laboratory or Field Tracer Experiments, Version 2.1. Research Report, Nr. 137. U.S. Salinity Laboratory, USDA, ARS, Riverside, California.

Turgut, C. (2005): Uptake and Modeling of Pesticides by Roots and Shoots of Parrotfeather (Myriophyllum aquaticum). Environmental Science and Pollution Research, Vol. 16, Nr. 6, P. 342 – 346.

Wernli, H. R. (2009): Einführung in die Tracerhydrologie, Hydrologisches Praktikum. Geographisches Institut, Universität Bern.

Winthrop, C. A., Hook, P. B., Bierdermann, J. A., Stein, O. R. (2002): Temperature and Wetland Plant Species Effects on Wastewater Treatmant and Root Zone Oxidation. Journal of Environmental Quality, Vol. 31, P. 1010 – 1016.

Xu, S., Leri, A. C., Myneni, S. C. B., Jaffe, P. R. (2004): Uptake of Bromide by two wetland plants (*Typha latifolia* L. and *Phragmites australis* (Cav.) Trin. Ex. Steud). Environmental Science and Technology, Vol. 38, P. 5642 – 5648.

Zhou, J. L., Rowland, S. J., Mantoura, R. F. C., Harland, B. J. (1995): Influence of the nature of particulate organic-matter on the sorption of cypermethrin – implications on K-Oc correlations. Environment International, Vol. 21, P. 187 – 195.

Zhou, Y., Wang, Y., Hunkeler, D., Zwahlen, F., Boillat, J. (2010): Differential Transport of Atrazine and Glyphosate in Undisturbed Sandy Soil Column. Soil and Sediment Contamination: An International Journal, Vol. 19, P. 365 – 377.

Zou, Y., Lu, X., Yu, X., Jiang, M., Guo, Y. (2011): Migration and retention of iron in three mesocosm wetlands. Ecological Engineering, Vol. 37, P. 1630 – 1637.

# Appendix

**Table A1:** Degradation test on UR and SRB under experimental conditions (absence of light; T = 20 °C; incubation time = 5 days; n = 5); INT = Fluorescence intensity (-); C = concentrations (µg/L).

| | **Before Incubation** | | | | | |
|---|---|---|---|---|---|---|
| ***replicates*** | ***$INT_{UR}$*** | ***$INT_{SRB}$*** | ***$C_{UR}$*** | ***$C_{SRB}$*** | ***$C_{UR}$ (%)*** | ***$C_{SRB}$ (%)*** |
| 1 | 587.15 | 342.67 | 10.56 | 105.86 | 100.00 | 100.00 |
| 2 | 571.86 | 341.16 | 10.28 | 105.39 | 100.00 | 100.00 |
| 3 | 575.60 | 339.21 | 10.35 | 104.78 | 100.00 | 100.00 |
| 4 | 545.27 | 337.93 | 9.80 | 104.39 | 100.00 | 100.00 |
| 5 | 566.08 | 333.83 | 10.18 | 103.12 | 100.00 | 100.00 |
| | **After Incubation** | | | | | |
| ***replicates*** | ***INT UT*** | ***INT SRB*** | ***C UR*** | ***C SRB*** | ***Δ C UR (%)*** | ***Δ C SRB (%)*** |
| 1 | 563.78 | 335.63 | 10.14 | 103.68 | 4.03 | -2.06 |
| 2 | 576.10 | 350.45 | 10.36 | 108.27 | -0.75 | 2.73 |
| 3 | 572.90 | 330.52 | 10.30 | 102.09 | 0.47 | -2.57 |
| 4 | 566.39 | 335.98 | 10.18 | 103.78 | -3.92 | -0.58 |
| 5 | 569.14 | 336.02 | 10.23 | 103.80 | -0.55 | 0.66 |
| | | | | ***mean*** | ***-0.14*** | ***-0.36*** |
| | | | | ***σ*** | ***2.86*** | ***2.14*** |

**Table A2:** Quality parameters of mesocosm influent.

| | In Situ Measurements | | | | | Suspended Load (mg/L) | | Carbon Species (mg/L) | | | |
|---|---|---|---|---|---|---|---|---|---|---|---|
| ***sampling*** | ***T (°C)*** | ***pH*** | ***$O_2$ (mg/L)*** | ***$O_2$ (%)*** | ***EC (µS/cm)*** | ***TSS*** | ***POC*** | ***TOC*** | ***DOC*** | ***TIC*** | ***DIC*** |
| **22.06.2011** | 19 | 7.65 | 4.66 | 51.6 | 798 | 11.5 | 1.6 | 5.3 | 5.6 | 67.3 | 67.5 |
| **18.07.2011** | 15 | 7.77 | 4.72 | 43.4 | 895 | 11.1 | 3.9 | 2.8 | 2.2 | 31 | 37.7 |

| | Nutrients (mg/L) | | | | Major Kations (mg/L) | | | | Major Anions (mg/L) | |
|---|---|---|---|---|---|---|---|---|---|---|
| ***sampling*** | ***$NO_2$*** | ***$NO_3$*** | ***$NH_4$*** | ***$PO_4$*** | ***$Na^+$*** | ***$K^+$*** | ***$Mg^{2+}$*** | ***$Ca^{2+}$*** | ***$Cl^-$*** | ***$SO_4^{2-}$*** |
| **22.06.2011** | 0.24 | 24.58 | 0.120 | 0.790 | 10.0 | 3.7 | 23.9 | 130 | 32.79 | 81.25 |
| **18.07.2011** | 0.13 | 25.60 | 0.166 | 0.440 | 10.8 | 3.2 | 25.6 | 142 | 30.38 | 80.55 |

| | Major metals (mg/L) | | | | Trace metals (µg/L) | | | | | |
|---|---|---|---|---|---|---|---|---|---|---|
| ***sampling*** | ***Si*** | ***Al*** | ***Fe*** | ***Mn*** | ***Sr*** | ***Ba*** | ***Ni*** | ***Co*** | ***Zn*** | ***Cu*** |
| **22.06.2011** | 5.49 | 0.036 | 0.016 | 0.0401 | 494 | 74.1 | 18 | - | 9 | - |
| **18.07.2011** | 6.36 | 0.034 | 0.013 | 0.0187 | 547 | 102 | 25 | - | 33 | - |

**Table A3:** Dissolved oxygen concentration, electric conductivity and pH development.

| | VEGETATED | | | | | | NON VEGETATED | | | | | | | VEGETATED | | NON VEGETATED | |
|---|---|---|---|---|---|---|---|---|---|---|---|---|---|---|---|---|---|
| | *DO (mg/L)* | | | | | | *DO (mg/L)* | | | | | | | *EC (µS/cm)* | *pH* | *EC (µS/cm)* | *pH* |
| **date** | **48 cm** | **42 cm** | **39 cm** | **36 cm** | **20 cm** | **2.5 cm** | **48 cm** | **42 cm** | **39 cm** | **36 cm** | **20 cm** | **2.5 cm** | **date** | | | | |
| 08.07.2011 | 0.00 | 0.00 | 0.03 | 0.00 | 0.00 | 0.85 | 0.00 | 0.00 | 0.00 | 0.00 | 0.01 | 1.87 | 18.07.2011 | 782 | 7.86 | 678 | 8.02 |
| 11.07.2011 | 0.00 | 0.01 | 0.04 | 0.00 | 0.00 | 0.53 | 0.00 | 0.00 | 0.00 | 0.00 | 0.14 | 1.85 | 15.08.2011 | 735 | 7.99 | 597 | 8.19 |
| 18.07.2011 | 0.00 | 0.00 | 0.03 | 0.00 | 0.22 | 0.64 | 0.00 | 0.00 | 0.00 | 0.00 | 1.65 | 2.96 | 30.08.2011 | 801 | 7.26 | 760 | 7.45 |
| 08.08.2011 | 0.00 | 0.00 | 0.03 | 0.00 | 4.33 | 4.41 | 0.00 | 0.00 | 0.00 | 0.00 | 5.47 | 5.11 | 01.09.2011 | 807 | 7.29 | 761 | 7.68 |
| 17.08.2011 | 0.00 | 0.00 | 0.03 | 0.00 | 5.76 | 5.93 | 0.00 | 0.00 | 0.00 | 0.00 | 6.14 | 6.68 | 04.09.2011 | 800 | 7.38 | 742 | 7.51 |
| 31.08.2011 | 0.00 | 0.00 | 0.02 | 0.00 | 6.06 | 6.54 | 0.01 | 0.00 | 0.00 | 0.00 | 6.73 | 7.07 | 09.09.2011 | 775 | 7.69 | 736 | 7.89 |
| 12.09.2011 | 0.00 | 0.00 | 0.02 | 0.00 | 5.81 | 5.59 | 0.00 | 0.00 | 0.00 | 0.00 | 6.43 | 6.55 | 14.09.2011 | 766 | 7.77 | 732 | 7.99 |
| 20.09.2011 | 0.00 | 0.00 | 0.02 | 0.00 | 7.19 | 8.47 | 0.00 | 0.00 | 0.00 | 0.00 | 7.03 | 7.87 | 20.09.2011 | 873 | 7.37 | 766 | 7.68 |
| 26.09.2011 | 0.00 | 0.00 | 0.02 | 0.00 | 7.43 | 8.23 | 0.00 | 0.00 | 0.00 | 0.00 | 6.87 | 7.20 | 26.09.2011 | 828 | 7.36 | 791 | 7.74 |
| 03.10.2011 | 0.00 | 0.02 | 0.02 | 0.00 | 7.20 | 8.03 | 0.00 | 0.00 | 0.00 | 0.00 | 7.00 | 7.40 | 03.10.2011 | 888 | 7.36 | 783 | 7.70 |
| 07.10.2011 | 0.00 | 0.00 | 0.02 | 0.00 | 7.15 | 7.96 | 0.01 | 0.00 | 0.00 | 0.01 | 7.02 | 7.38 | 06.10.2011 | 799 | 7.46 | 756 | 7.82 |
| 17.10.2011 | 0.00 | 0.00 | 0.01 | 0.00 | 6.90 | 7.64 | 0.00 | 0.00 | 0.00 | 0.00 | 6.86 | 7.37 | 17.10.2011 | 780 | 7.42 | 715 | 8.02 |
| 24.10.2011 | 0.01 | 0.00 | 0.00 | 0.00 | 6.83 | 7.29 | 0.00 | 0.00 | 0.00 | 0.00 | 6.76 | 7.06 | 24.10.2011 | 783 | 7.41 | 702 | 7.96 |
| 28.10.2011 | 0.00 | 0.00 | 0.00 | 0.00 | 7.06 | 7.52 | 0.00 | 0.00 | 0.00 | 0.00 | 6.95 | 7.18 | 28.10.2011 | 816 | 7.45 | 699 | 7.79 |

**Table A4:** Development of major anion and kation concentrations in mesocosm outlet.

| | VEGETATED | | | | | | | NON-VEGETATED | | | | | | |
|---|---|---|---|---|---|---|---|---|---|---|---|---|---|---|
| | $Na^+$ | $K^+$ | $Mg^{2+}$ | $Ca^{2+}$ | $Cl^-$ | $NO_3^{2-}$ | $SO_4^{2-}$ | $Na^+$ | $K^+$ | $Mg^{2+}$ | $Ca^{2+}$ | $Cl^-$ | $NO_3^{2-}$ | $SO_4^{2-}$ |
| ***Detection limit*** | *0.07* | *0.2* | *0.03* | *0.04* | | | | *0.07* | *0.2* | *0.03* | *0.04* | | | |
| 17.08.2011 | 13.0 | 4.1 | 28.0 | 102 | 50.33# | 300.87* | 3.99* | 12.9 | 4.2 | 27.0 | 108 | 32.12 | 255.88* | 2.86* |
| 24.08.2011 | 12.7 | 3.0 | 26.0 | 89.5 | 127.49# | 234.24* | 1.99* | 11.8 | 3.2 | 23.1 | 63.7 | 45.71# | 587.97* | 16.76* |
| 31.08.2011 | 12.2 | 2.4 | 25.4 | 96.4 | 32.75 | 348.99* | 2.58* | 12.0 | 3.1 | 23.8 | 82.7 | 33.39 | 465.05* | 32.84* |
| 09.09.2011 | 13.1 | 2.0 | 25.3 | 122 | 149.89# | 53.83* | 59.48* | 12.1 | 3.3 | 22.7 | 98.5 | 53.46# | 33.51* | 37.53* |
| 15.09.2011 | 12.8 | 1.8 | 27.2 | 124 | 131.77# | 0.34 | 61.92 | 11.8 | 3.2 | 24.4 | 113 | 173.19# | 0.64 | 44.54 |
| 20.09.2011 | 12.6 | 1.7 | 28.4 | 130 | 34.12 | 0.19 | 63.44 | 12.0 | 3.4 | 26.0 | 115 | 32.11 | 0.67 | 51.18 |
| 28.09.2011 | 12.6 | 2.3 | 27.0 | 126 | 33.87 | 0.22 | 65.57 | 12.0 | 3.4 | 25.5 | 122 | 32.00 | 0.85 | 63.13 |
| 03.10.2011 | 12.9 | 1.8 | 26.6 | 137 | 34.81 | 0.29 | 64.17 | 11.8 | 3.2 | 25.2 | 117 | 32.16 | 0.97 | 58.96 |
| 07.10.2011 | 12.5 | 1.3 | 26.7 | 122 | 32.36 | 0.18 | 63.09 | 11.8 | 3.2 | 25.7 | 93.2 | 31.65 | 2.14 | 58.57 |
| 17.10.2011 | 11.9 | 0.8 | 24.2 | 117 | 31.56 | 0.24 | 75.61 | 11.0 | 2.6 | 22.9 | 111 | 32.00 | 4.09 | 59.62 |
| 21.10.2011 | 11.8 | 2.6 | 25.1 | 116 | 32.58 | 0.68 | 84.16 | 11.2 | 2.9 | 23.0 | 101 | 31.65 | 3.51 | 64.49 |
| 28.10.2011 | 12.7 | 1.0 | 26.4 | 123 | 31.23 | 0.22 | 106.92 | 11.0 | 2.7 | 22.8 | 99.7 | 31.74 | 1.20 | 55.87 |
| 08.11.2011 | | | | | | | | | | | | | | |
| ***mean*** | ***12.6*** | ***2.1*** | ***26.35*** | ***117*** | ***32.91*** | ***0.29*** | ***73.11*** | ***11.8*** | ***3.2*** | ***24.34*** | ***102*** | ***32.09*** | ***1.76*** | ***57.04*** |
| ***σ*** | ***0.41*** | ***0.91*** | ***1.23*** | ***14.12*** | ***1.26*** | ***0.17*** | ***15.71*** | ***0.52*** | ***0.40*** | ***1.49*** | ***16.42*** | ***0.53*** | ***1.36*** | ***6.52*** |

# over estimation of Cl concentrations due to sample contamination with hydrochloric acid (HCl) residues deriving from washing of sampling material; data not included in mean value calculations.

* data not reliable due to alkalization of samples with Ammonia and acidification with $HNO_3$; data not included in mean value calculations.´

**Table A5:** Temporal change of concentration of major metal and phosphorous in mesocosm outlet; detection limits are in brackets; Titanium was not detected in any sample.

| | **Si (mg/L)** *(0.01)* | | **Al (mg/L)** *(0.007)* | | **Fe (mg/L)** *(0.006)* | | **Mn (mg/L)** *(0.0006)* | | **P (mg/L)** *(0.09)* | |
|---|---|---|---|---|---|---|---|---|---|---|
| ***date*** | ***VEG*** | ***NV*** | ***VEG*** | ***NV*** | ***VEG*** | ***NV*** | ***VEG*** | ***NV*** | ***VEG*** | ***NV*** |
| 17.08.2011 | 9.65 | 11.7 | 0.231 | 0.065 | 1.21 | 0.048 | 1.85 | 1.42 | 0.76 | 0.17 |
| 24.08.2011 | 8.88 | 12.1 | 0.072 | 0.057 | 0.494 | 0.042 | 1.16 | 0.861 | 0.68 | - |
| 31.08.2011 | 8.82 | 11.6 | 0.063 | 0.042 | 0.223 | 0.024 | 0.703 | 0.941 | - | - |
| 09.09.2011 | 8.35 | 11.8 | 0.079 | 0.124 | 0.094 | 0.040 | 0.703 | 0.893 | 0.10 | - |
| 15.09.2011 | 8.77 | 11.0 | 0.045 | 0.047 | 0.145 | 0.050 | 0.999 | 1.42 | 0.12 | 0.10 |
| 20.09.2011 | 8.47 | 9.56 | 0.056 | 0.045 | 0.066 | 0.034 | 1.63 | 1.62 | - | - |
| 28.09.2011 | 8.46 | 10.1 | 0.070 | 0.059 | 0.343 | 0.073 | 0.839 | 0.941 | 0.12 | 0.11 |
| 03.10.2011 | 8.05 | 10.3 | 0.129 | 0.027 | 2.25 | 0.017 | 1.88 | 0.603 | - | 0.10 |
| 07.10.2011 | 8.38 | 9.52 | 0.032 | 0.032 | 0.855 | - | 0.813 | 0.422 | - | - |
| 17.10.2011 | 7.19 | 9.04 | 0.036 | 0.038 | 0.811 | 0.019 | 0.884 | 0.253 | - | - |
| 21.10.2011 | 6.69 | 10.2 | 0.032 | 0.023 | 0.102 | 0.007 | 0.506 | 0.306 | - | - |
| 28.10.2011 | 6.00 | 8.89 | 0.025 | 0.036 | 0.153 | 0.018 | 0.373 | 0.353 | - | - |
| 08.11.2011 | 8.23 | 9.09 | 0.026 | 0.033 | 0.048 | 0.022 | 1.21 | 2.14 | - | 0.14 |

**Table A6:** Temporal change of concentration of trace metals in mesocosm outlet; detection limits are in brackets; detection limits are in brackets; Vanadium and Chromium were not detected in any sample.

| | **Sr (µg/L)** *(0.4)* | | **Ba (µg/L)** *(0.3)* | | **Ni (µg/L)** *(4)* | | **Co (µg/L)** *(4)* | | **Zn (µg/L)** *(4)* | | **Cu (µg/L)** *(3)* | |
|---|---|---|---|---|---|---|---|---|---|---|---|---|
| ***date*** | ***VEG*** | ***NV*** | ***VEG*** | ***NV*** | ***VEG*** | ***NV*** | ***VEG*** | ***NV*** | ***VEG*** | ***NV*** | ***VEG*** | ***NV*** |
| 17.08.2011 | 477 | 600 | 192 | 194 | 37 | 8 | 7 | 7 | 225 | 143 | 10 | 6 |
| 24.08.2011 | 386 | 341 | 235 | 143 | 31 | 23 | - | - | 254 | 155 | 7 | 4 |
| 31.08.2011 | 413 | 411 | 189 | 167 | 16 | 18 | - | 6 | 189 | 170 | - | 4 |
| 09.09.2011 | 502 | 467 | 421 | 163 | 19 | 40 | - | - | 391 | 234 | 6 | 4 |
| 15.09.2011 | 515 | 521 | 396 | 392 | 42 | 23 | - | - | 236 | 223 | - | 4 |
| 20.09.2011 | 545 | 539 | 361 | 346 | 9 | 35 | - | - | 209 | 215 | - | 4 |
| 28.09.2011 | 539 | 547 | 236 | 232 | 32 | 31 | - | - | 226 | 216 | - | 3 |
| 03.10.2011 | 558 | 524 | 373 | 228 | 33 | 6 | - | - | 230 | 234 | 3 | - |
| 07.10.2011 | 527 | 488 | 199 | 220 | 20 | 31 | - | - | 228 | 16 | - | - |
| 17.10.2011 | 491 | 493 | 258 | 256 | 43 | 30 | - | 4 | 313 | 675 | 25 | 3 |
| 21.10.2011 | 483 | 461 | 231 | 289 | 17 | 6 | - | - | 220 | 235 | - | - |
| 28.10.2011 | 520 | 466 | 266 | 249 | 14 | 31 | - | - | 241 | 199 | - | 3 |
| 08.11.2011 | 547 | 546 | 281 | 546 | 36 | 53 | - | - | 302 | 197 | 15 | 14 |

**Table A7:** Development of nutrient concentrations and carbon species in mesocosm outlet; *TIC* = total organic carbon, *TOC* =total inorganic carbon, *DOC* = dissolved organic carbon, *DIC* = dissolved inorganic carbon; all concentrations in mg/L.

| | $NO_2^-$ | | $NO_3^{2-}$ | | $NH_4^+$ | | P | | TIC | | TOC | | DIC | | DOC | |
|---|---|---|---|---|---|---|---|---|---|---|---|---|---|---|---|---|
| ***date*** | ***VEG*** | ***NV*** | ***VEG*** | ***NV*** | ***VEG*** | ***NV*** | ***VEG*** | ***NV*** | ***VEG*** | ***NV*** | ***VEG*** | ***NV*** | ***VEG*** | ***NV*** | ***VEG*** | ***NV*** |
| 15.09.2011 | < 0.1 | 0.625 | 0.61 | 0.26 | < 0.1 | 1.59 | 0.35 | 0.39 | | | | | 57.5 | 43.7 | 5.7 | 5.8 |
| 20.09.2011 | < 0.1 | | < 0.37 | | 0.11 | | 0.34 | | | | | | 89.9 | 81 | 5.8 | 5.4 |
| 28.09.2011 | | | | | | | | | | | | | 82.1 | | 5.3 | |
| 30.09.2011 | | | | | | | | | 57.8 | 64.7 | 3.8 | 4.7 | 47.8 | 44.8 | 2.9 | 2.6 |
| 03.10.2011 | | | | | | | | | 68.8 | 62.8 | 5.4 | 3.9 | 69.2 | 62.9 | 4.1 | 3.9 |
| 05.10.2011 | | | | | | | | | 81.7 | 73.2 | 4.9 | 3.4 | 81 | 73.6 | 4.6 | 4.1 |
| 07.10.2011 | | | | | | | | | 83.1 | 78.6 | 32.1 | 8.1 | 83.1 | 78.4 | 7.8 | 5.1 |
| 17.10.2011 | < 0.1 | 0.34 | < 0.37 | 2.93 | < 0.1 | 0.34 | 0.33 | 0.37 | 55.7 | 35.3 | 32.1 | 21.3 | 22.7 | 36 | 38.1 | 23.2 |
| 21.10.2011 | < 0.1 | 0.58 | < 0.37 | 2.33 | < 0.1 | 0.61 | 0.32 | 0.35 | 17.4 | 14.3 | 41.2 | 34.4 | | 13.1 | | 42.1 |
| 24.10.2011 | < 0.1 | 0.25 | < 0.37 | 2.89 | < 0.1 | 0.42 | 0.33 | 0.38 | 20.1 | 53.4 | 14.3 | 49.7 | 17.7 | 53.3 | 13.4 | 50.7 |

**Figure A1:** Changes of dissolved oxygen concentrations at bottom gravel and bottom sand layers (2.5 cm and 20 cm height) in VEG and NV setups.

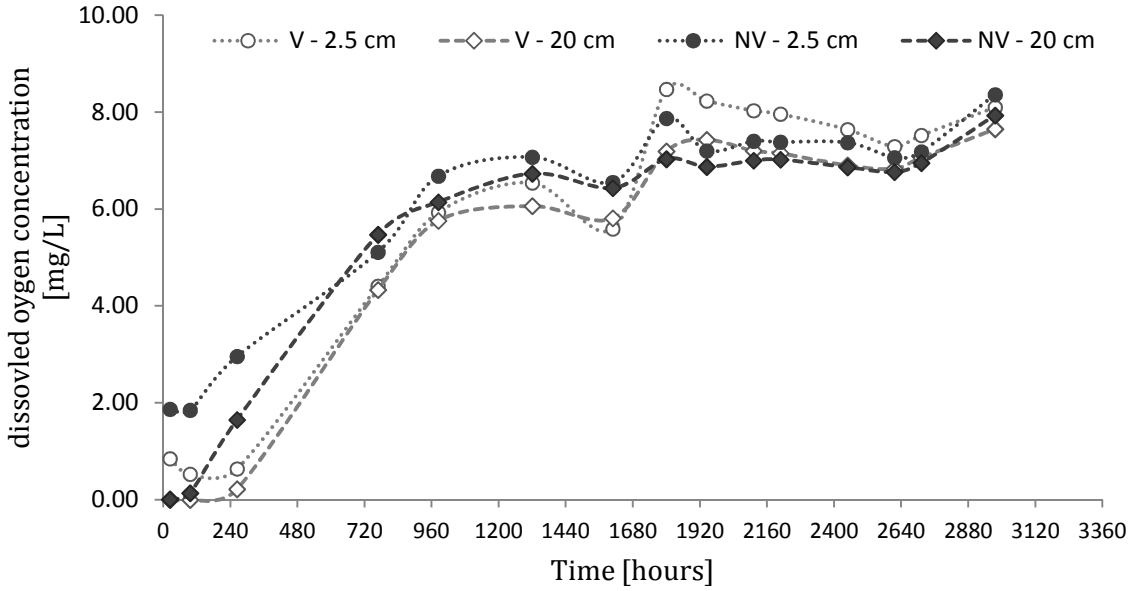


**Figure A2:** EC (electric conductivity) and pH development in VEG and NV setups over time.

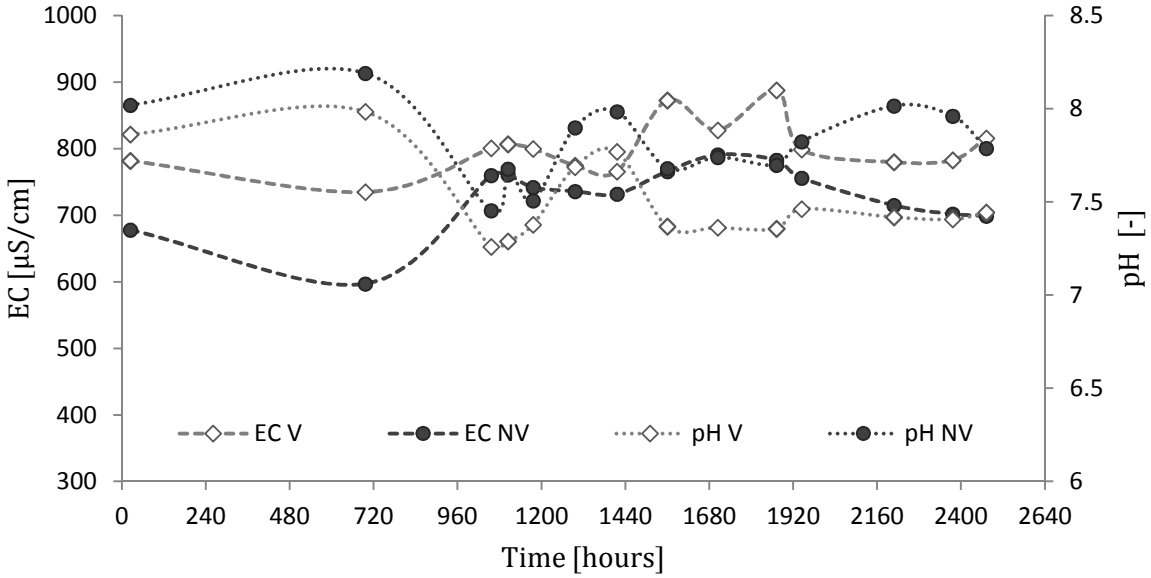

**Table A8:** Weekly TSS and POC measurements in mesocosm outlet; $VF$ = filtrate volume; $SS$ = suspended solids.

**VEGETATED**

| *week* | *date* | $V_F$ *(ml)* | *filter 105°C (g)* | *filter + SS 105°C (g)* | *filter + SS 550°C (g)* | *TSS (mg/L)* | *POC (mg/L)* | | *(mg/L)* |
|---|---|---|---|---|---|---|---|---|---|
| 1 | 22.08.2011 | | | | | | | mean | **59.29** |
| 3 | 05.09.2011 | 100 | 34.592 | 34.598 | 34.593 | 60.00 | 50.00 | TSS: | |
| 4 | 12.09.2011 | 100 | 35.664 | 35.668 | | 40.00 | | σ TSS: | **32.33** |
| 5 | 20.09.2011 | 200 | 47.644 | 47.669 | 47.663 | 125.00 | 30.00 | | |
| 6 | 28.09.2011 | 200 | 35.659 | 35.667 | 35.663 | 40.00 | 20.00 | mean | **27.00** |
| 7 | 07.10.2011 | 200 | 35.163 | 35.17 | 35.167 | 35.00 | 15.00 | POC: | |
| 8 | 14.10.2011 | 200 | 34.858 | 34.873 | 34.869 | 75.00 | 20.00 | σ POC: | **13.96** |
| 9 | 22.10.2011 | 200 | 35.751 | 35.759 | | 40.00 | | | |

**NON VEGETATED**

| *week* | *date* | *V filtrate (ml)* | *filter 105°C (g)* | *filter + SS 105°C (g)* | *filter + SS 550°C (g)* | *TSS (mg/L)* | *POC (mg/L)* | | *(mg/L)* |
|---|---|---|---|---|---|---|---|---|---|
| 1 | 22.08.2011 | 100 | 52.661 | 52.662 | | 10.00 | | mean | **18.46** |
| 3 | 05.09.2011 | 100 | 39.312 | 39.315 | | 30.00 | | TSS: | |
| 4 | 12.09.2011 | 95 | 37.488 | 37.49 | 37.485 | 21.05 | | σ TSS: | **6.65** |
| 5 | 20.09.2011 | 200 | 52.649 | 52.653 | 52.65 | 20.00 | 15.00 | | |
| 6 | 28.09.2011 | 200 | 34.586 | 34.59 | 34.587 | 20.00 | 15.00 | mean | **15.00** |
| 7 | 07.10.2011 | 200 | 35.752 | 35.754 | 35.751 | 10.00 | 15.00 | POC: | |
| 8 | 14.10.2011 | 185 | 39.306 | 39.31 | 39.307 | 21.62 | 15.00 | σ POC: | **0.00** |
| 9 | 22.10.2011 | 200 | 34.586 | 34.589 | | 15.00 | | | |

**Figure A3:** Weekly TSS and POC measurements in VEG and NV mesocosm setups.

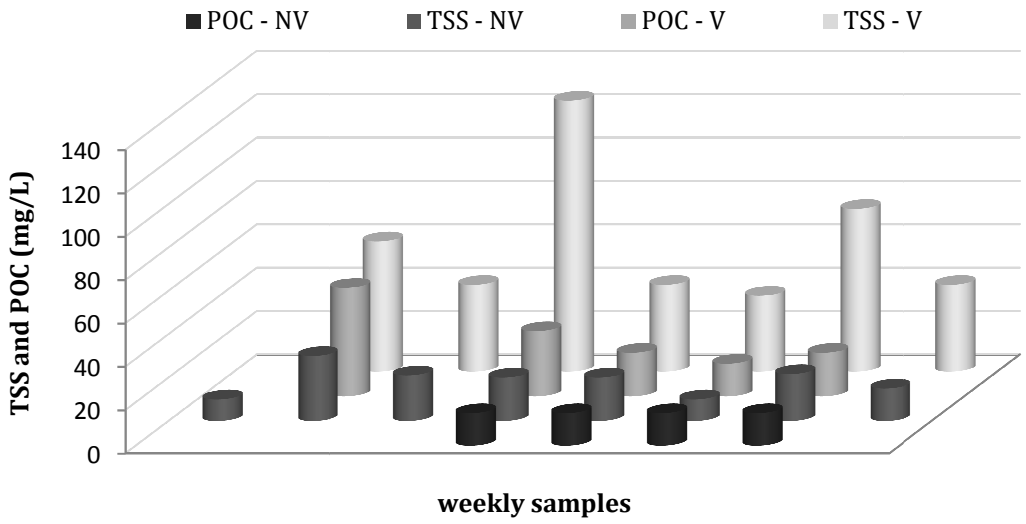
POC - NV
TSS - NV
POC - V
TSS - V
140
120
100
80
60
40
20
0
TSS and POC (mg/L)
weekly samples

**Figure A4:** Particle size distribution of wetland sediment from CW Eichstetten; analyzed fraction: 0.04 to 2000 µm.

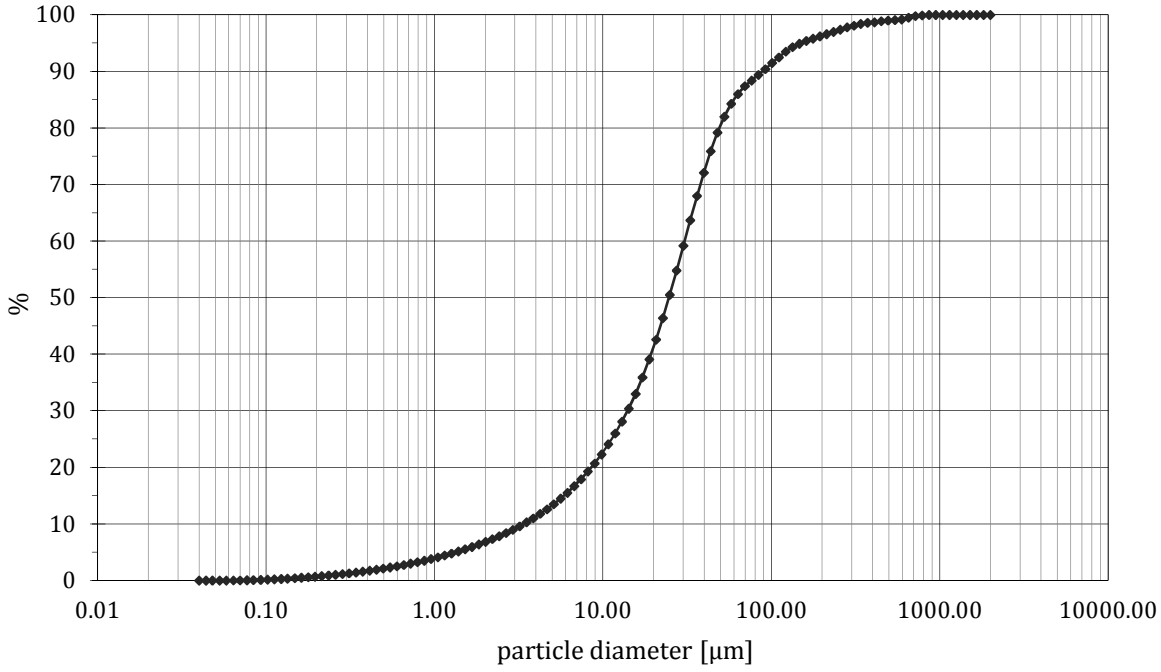


**Figure A5:** Frequency diagram of particle size distribution of wetland sediment from CW Eichstetten; analyzed fraction: 0.04 to 2000 µm.

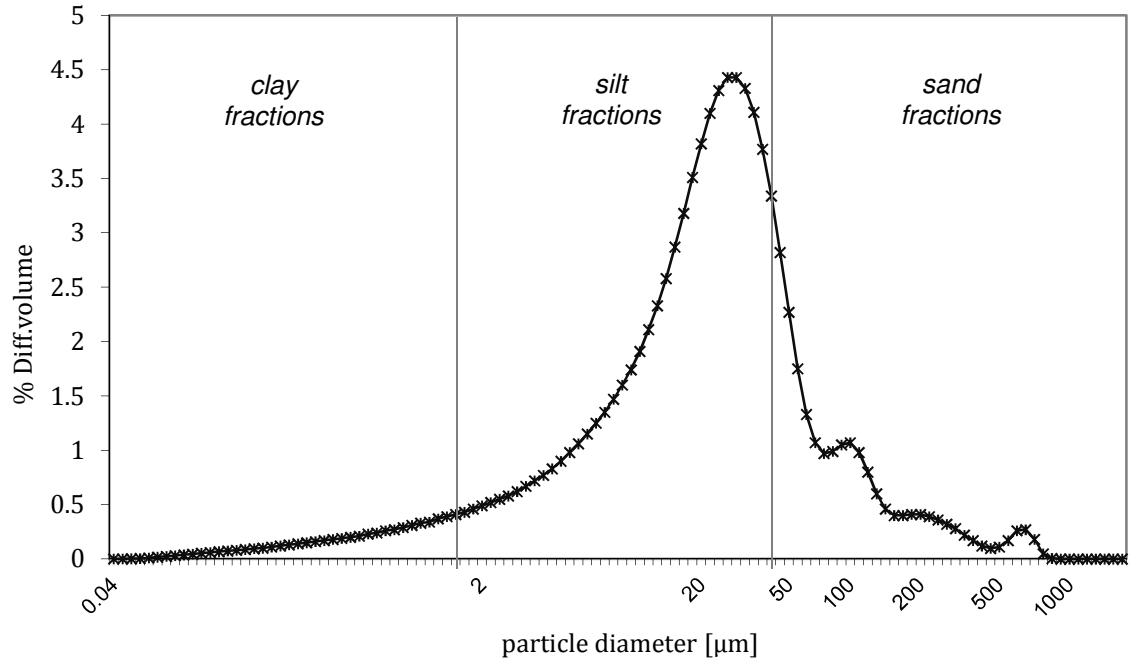

***Figure A6:*** Calibration curve for Uranine Spectrometry

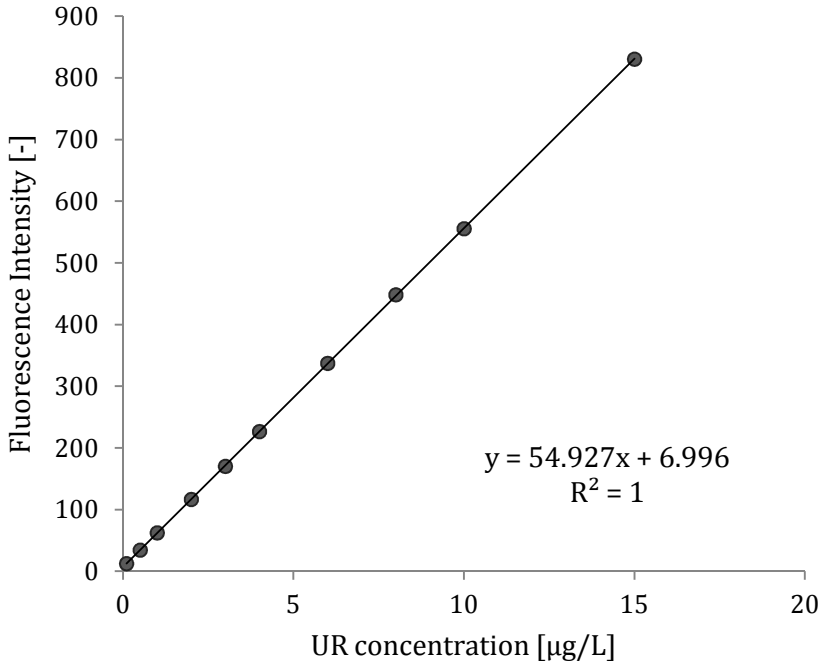


***Figure A7:*** Calibration curve for Sulphorhodamine B Spectrometry

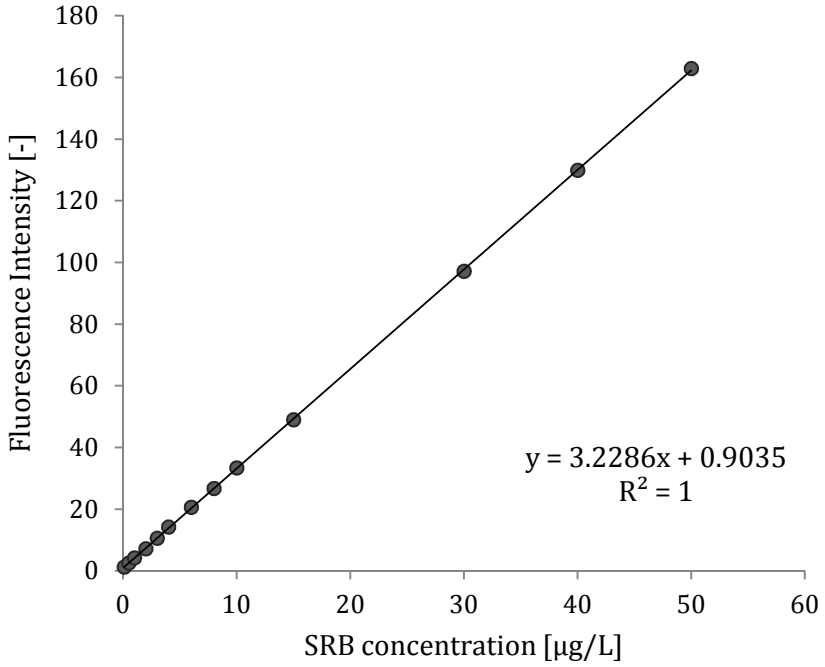

***Figure A8:*** Bromide concentration data obtained by an ion selective probe (WTW Br 800) and ion chromatography in the VEG mesocosm setup; C = concentration, R = Recovery, IC = ion chromatography.